EFFECTS OF TITANOCENE DICHLORIDE ON THE HYDROTREATMENT OF COAL LIQUIDS

By

WU SHAN CHAN

Bachelor of Science in Engineering

National Taiwan University

Taipei, Taiwan

1975

Submitted to the Faculty of the Graduate College
of the Oklahoma State University
in partial fulfillment of the requirements
for the Degree of
MASTER OF SCIENCE
July, 1982

EFFECTS OF TITANOCENE DICHLORIDE ON THE

HYDROTREATMENT OF COAL LIQUIDS

Thesis Approved:

Mayis Seapan
Thesis Adviser

Billy L Crynes

Fuhaid al-Shaieb

Robert M Henderson

Norman N Durham
Dean of the Graduate College

PREFACE

Deposition of trace elements on hydrotreatment catalyst is an important deactivation mechanism. Titanium is one of the trace elements usually presnet in coal liquids, presumably as an organometallic compound. In catalytic hydrotreatment process, it is found to penetrate and deposit deeply into the pores of catalysts, and is commonly blamed for deactivation of catalysts. In this thesis, in order to study the role of titanium in the hydrotreatment process, an SRC light oil was doctored with titanocene dichloride and hydrotreated in a trickle bed reactor over a commercial Ni-Mo/alumina catalyst and over glass beads. The effects of different concentrations of titanocene dichloride on the HDS, HDN, HDO and hydrogenation of the oil and on catalyst coking, pore size, surface area and titanium deposit content are measured and studied. Titanium is easily removed from the oil and deposits on the catalysts with the carbonaceous coking material. Both coking and titanium deposition on the catalyst appear to follow a parallel fouling model. Contrary to common expectations, titanocene dichloride did not deactivate the catalyst, but rather its presence in the feedstock improved the hydrotreatment activity of the catalyst. Titanium concentrations of 100 to 200 ppm appear to promote the catalyst, but high concentrations show lower activity and cause the reactor plugging.

I wish to express my appreciation to my thesis advisor, Dr. M. Seapan, for his guidance and help in completion of this study. My special appreciation is also expressed to Dr. Z. Al-Shaieb for his invaluable assistance in the sample analyses. I also like to thank the other committee members, Dr. B. L. Crynes and Dr. R. H. Heidersbach, Jr..

A note of thanks is given to H. J. Chang, Steve Wilkinson, Steve Smith, R. A. Rhoades, Tim Dickenson, Brad Luhrs and Shaun Pierson for providing their helpful ideas and help in conducting the experiments.

Financial support for this work was gratefully received from the School of Chemical Engineering and the United States Department of Energy.

Finally, special gratitude is expressed to my wife, my parents and brothers for their support and encouragement in making all this possible.

TABLE OF CONTENTS

LIST OF TABLES

LIST OF FIGURES

Figure Page

CHAPTER I

INTRODUCTION

In the catalytic liquefaction of coal and catalytic upgrading of coal derived liquids the catalysts suffer serious problems in maintaining high activity, high selectivity and a long life.

Recently the deactivation mechanisms of hydrotreating catalysts have received considerable attention. The main factors for the catalyst deactivation are: deposition of carbonaceous material on catalysts called coking, adsorption of basic nitrogen-containing compounds, deposition of metal impurities, and sintering of the catalyst. The coke on the catalysts can usually be burned off, whereas the metal deposition can cause permanent loss of the catalytic activities. The role of trace metals, like vanadium, nickel, iron, and arsenic in petroleum on catalyst deactivation has been documented over many years. They poison the catalyst and react with the active metals during regeneration process to cause structural changes in the catalyst surface, resulting in a permanent loss of catlyst activity.

The nature of trace metals in coal liquids is not exactly same as those in petroleum. Titanium compounds in coal liquids, one of the more abundant trace compounds, are receiving more attention because of their unique characteristics. Titanium compounds survive the severe liquefaction conditions and transfer into the product oils. They are also found to penetrate deeply into the pores of the catalysts and deposit

inside the pores. Organometallic compounds of titanium were suspected to be responsible for the unusual behaviors. Under the complex reactive conditions of coal liquefaction, Filby et al. (1) proposed the possibility of stable organometallic compounds like titanocene.

In order to study the role of titanium in the hydrotreatment process, an SRC light oil was doctored with titanocene dichloride and hydrotreated in a trickle bed reactor over a commercial NiMo/alumina catalyst and over glass beads. The effects of different concentrations of titanocene dichloride on the hydrodesulfurization (HDS), hydrodenitrogenation (HDN), hydrodeoxygenation (HDO) and hydrogenation of the oil and on the catalyst coking, pore size, surface area and titanium deposit are measured and studied.

To provide a better understanding of hydrotreatment operation, catalyst and its deactivation mechanism, and the nature of organometallic titanium in coal liquids, the pertinent literature will be reviewed in the next chapter.

CHAPTER II

LITERATURE REVIEW

Pertinent literature on the following aspects of this project will be reviewed:

1. Trickle bed reactor.
2. Operational parameters.
3. Hydrotreating operation.
4. Catalyst.
5. Catalyst deactivation.
6. Nature of titanium in coal derived liquids.

Trickle Bed Reactor

In commercial hydrotreatment of high boiling hydrocarbons, three basic reactor types, namely trickle bed reactor, up flow reactor, and ebullated bed reactor have been used. Trickle bed reactor has been the most common type and has successfully been employed in commercial plants. The advantages of this type of reactor over the other systems were discussed by Ahmed (2). In trickle bed reactors, the liquid phase flows down through a fixed catalyst bed while the gaseous phase flows either in cocurrent or counter current direction. The catalyst pellets inside the trickle bed reactor are covered with a layer of liquid which is surrounded by the continuous gas phase, whereas the pores of the

catalyst can be assumed to be filled with the oil. Hydrogen gas dissolves in the oil phase, penetrates through the catalyst pores and is adsorbed on the catalyst surface. The organic molecules of oil are similarly transported through the bulk of the liquid into the pores to reach the catalyst surface. The adsorbed molecules react on the catalyst surface to form the products which are then desorbed and transported to the bulk of the liquid. The volatile products evaporate and are transported into the gas phase (3).

The scale up of experimental results, obtained from the trickle bed reactors, into industrial reactors encounters fewer problems than other reactor types, so it is often used in laboratory studies. On the other hand, since earlier investigators at Oklahoma State University successfully used the trickle bed reactors in their hydrotreating studies, trickle bed reactor was selected for this study as well.

Factors affecting the performance of the trickle bed reactors included the gas and liquid distribution, axial backmixing and diffusion resistance. These factors will be reviewed below.

Liquid and Gas Distribution

The maldistribution of the liquid oils over the catalyst can adversely affect the performance of a trickle bed reactor (4). Liquid fluxes in the range of 6.29 - 20.96 cubic meter per square meter per hour (150-500 gallons per square foot per hour) and vapor velocities of 0.030 - 0.046 meter per second (0.1 - 0.15 ft. per second) are recommended to insure good distribution of the liquid reactants (5). The ratio of reactor diameter to the catalyst particle diameter was also shown to

have important effects on the liquid distribution (6, 7). Satterfield (8) in a review of trickle bed reactors reported that in a narrow diameter reactor, the liquid tends to migrate toward the wall and results in by-passing of some of the catalyst. At the ratio of reactor diameter to particle diameter as high as 10, the liquid flowing down the wall may be 30 - 60% of the total liquid.

To account for the above migration effect, liquid holdup has been proposed as a measure of effectiveness of contacting between the liquid and catalyst (8). Liquid hold-up is defined as the volume of the liquid present in the reactor per unit volume of empty reactor, or per unit volume of the catalyst (9). Henry and Gilbert (10) assumed that the reaction rate is proportional to liquid hold-up and this hold-up is proportional to the liquid superficial velocity to 1/3 power. They also mentioned that the liquid hold-up can be increased by decreasing the particle size. Satterfield and Way (11) stated that the liquid hold-up was a function of the viscosity of the liquid and the catalyst particle size and shape.

Mears (12) suggested that instead of liquid hold-up, effective catalyst wetting might be a better criteria to assess the effects of liquid dynamics in the reactor. The visual evidence showing that the catalyst in the packed bed is not uniformly wetted was presented by Satterfield and Ozel (13). Mears proposed that the reaction rate was proportional to the fraction of catalyst surface that was effectively and freshly wetted.

Axial Backmixing

In the analysis of trickle bed reactor data, plug flow pattern is usually assumed. The actual flow pattern can deviate significantly from the plug flow due to backmixing effect. Liquid backmixing and eddy diffusion on the axial direction can affect the residence time and conversion.

The axial backmixing has been seen to be more prevalent in shallow reactors. As the bed depth increases the effect of axial backmixing decreases. Mears (14) suggested a criteria for predicting flow pattern in trickle bed reactors based on axial dispersion model. He reported that if $h/d_p \geq (20n/Pe_L)(\ln (C_{in}/C_{out}))$ exists, where "n" is the order of reaction, Pe_L is the liquid Peclet number and h is the depth of reactor, then the assumption of plug flow can be a good approximation. This correlation can also be used to predict the minimum bed length for negligible axial dispersions. Shah and Paraskes (15) analyzed the adiabatic trickle bed reactors and reported that larger axial dispersion effects were observed at high conversions. At lower conversions, the same is true for isothermal operations.

Diffusion Resistance

In trickle bed reactors diffusion resistances occur in three phases. The diffusion resistances play an important role in the overall kinetics of the reactions. The diffusion can be encountered in the gas phase, liquid phase and inside the pores of the catalyst. Since in hydrotreating processes excessive amounts of hydrogen is supplied, the resistance in the gas phase is negligible. Therefore, the liquid phase

resistance is expected to be the rate controlling step (16).

Satterfield (17) showed that the liquid film surrounding the catalyst particles has an average thickness in the range of 0.01 - 0.1 millimeter under typical hydrotreating conditions. This is much less than the pore depth of the catalyst. Therefore, the diffusion resistance in the outside liquid film around the catalyst is expected to be much less than the pore diffusion resistance. In his review of trickle bed reactors, he reported that the diffusion resistance through the liquid film has negligible effects on hydrodesulfurization (18).

Pore diffusion resistance causes a decrease in the reactant concentrations from the outer edge to the center of the catalyst particles, which results in a decrease in the reaction rate (19). The pore diffusion resistance is accounted for by the effectiveness factor. A lower effectiveness factor signifies higher intraparticle resistance. The effectiveness factor depends on the type of reactant molecules, their diffusivity through the liquid filled pores, pore size, catalyst size and diffusion length (2).

Studies on the effectiveness factor for hydrodesulfurization (18, 19, 20, 23) and hydrodenitrogenation (18, 19) differ widely. The wide difference in the effectiveness factor may be due to the difference in the feedstocks and reaction conditions. The effectiveness factor changes as the catalyst deactivates through the coke and metal deposition on its surface.

Operational Parameters

The space time, temperature, pressure and hydrogen flow rate are four major operational parameters in hydroprocessing petroleum feedstocks and coal derived liquids. These parameters and their effects will be reviewed below.

Space Time

In hydroprocessing petroleum feedstocks for sulfur removal, the boiling range of feedstocks and the desired extent of sulfur removal determine the space time required. Typical range of the space time is between 0.1 and 2.0 hours (22). A high boiling fraction generally contains less reactive species and requires higher space time. Usually the sulfur removal increases with an increase in the space time. Studies done on the desulfurization of coal derived liquids (23) and raw anthracene oil (18, 19) have confirmed these.

For hydrodenitrogenation, the removal of nitrogen has also been observed to increase with an increase in the space time (16). The effect of space time depends on the order of reaction (18). As order increases, the dependence of sulfur and nitrogen removal on space time decreases in the higher ranges of space time. There is a general agreement in literature that the kinetics of hydrodesulfurization of petroluem feedstocks is second order in sulfur concentration. This shows that the dependence of sulfur removal on space time reduces in the higher range of space time (18).

Jones and Frieman (24) based on their studies on the denitrogenation of a COED oil, observed a first order kinetics for hydrodenitrogenation in the range of 0.77 to 3.3 weight hourly space time. However, Satchell

(18) studied hydrodenitrogenation of raw anthracene oil and observed a second order kinteics. He concluded that although the nitrogen removal increases with an increase in the space time, the effect of space time weakens in the ranges of higher space times.

Temperature

An excellent review of the hydrodesulfurization technology was prepared by Mckinley (25), and Schuman and Shalit (26). Temperature range of 260 C - 440 C (500 F - 825 F) has often been used in the hydrodesulfurization of petroleum feedstocks.

Recently Seapan and Crynes (3) reviewed the kinetics of hydrogenation of alternative crude oils. They reported that most hydrotreatment studies are conducted in temperatures varying from 320 C to 430 C.

The temperature effect on rate constant is best described by Arrhenius law $k=k_o\ e^{-E/RT}$. Where k is the frequency factor and E is the activation energy. Obviously the rate constant increases with an increase in temperature. The magnitude of activation energy also has an important role in the temperature effect. Sooter (19) in his hydrodesulfurization study of raw anthracene oil with CoMo/alumina catalyst at 1000 psig showed that the activation energy of high boiling point fractions were about 10 times of that of low boiling point fractions. The temperature effect is expected to be greater for the high boiling point fractions.

The temperature effect also depends on the rate controlling step. The temperature affects the rate of chemical reactions much more than it affects the rate of mass transfer processes (3). Therefore, it can

be expected that the temperature effect to be much more profound in a process with reaction controlling rate than that with diffusion controlling rate.

Pressure

Seapan and Crynes (3) in their review concluded that most hydrotreatment studies are conducted at pressures of 3.4 MPa (500 psi) to 17 MPa (2,500 psi). The pressure effect on the rate of desulfurization and denitrogenation reactions has been studied by several workers (18, 19, 24, 27, 28). An increase in pressure generally increases the removal of nitrogen and sulfur. However, at high pressure ranges, the pressure effect seems to be less profound than at lower pressure ranges.

Hydrogen Flow Rate

Hydrogen flow rate is expected to increase the reaction rate by two mechanisms: a) it increases hydrogen partial pressure which in turn affects the reaction rate, b) the high hydrogen flow rate makes the liquid film around the catalyst thinner, thereby reducing the mass transfer resistance. However, most researchers have observed no significant effects when hydrogen flow rate is varied.

Sooter (13) observed no significant change in the sulfur removal by increasing the hydrogen flow rate. Satchell (18) observed a similar phenomena on nitrogen removal. Wan (27) showed that hydrogen flow rate has no effect on sulfur removal but has some effects on nitrogen removal. The negligible effects of hydrogen flow rate on reaction rates might be explained by considering that under the high pressures

and elevated temperatures of reaction, hydrogen solubility in the liquid becomes quite high, therefore, the reaction rate becomes less sensitive to the hydrogen partial pressure. Also, the film diffusion resistance as discussed earlier becomes unimportant compared with the pore diffusion resistance.

Hydrotreatment Operation

Hydrodesulfurization

In catalytic hydrodesulfurization process the sulfur containing compounds react with hydrogen and produce hydrogen sulfide, resulting in the reduction of sulfur content in the oil.

Petroleum as well as coal derived liquids contain a wide variety of sulfur containing compounds, some typical compounds are mentioned in Ahmed's thesis (16). Different sulfur compounds have different reactivities and can be removed with different extents in hydrotreatment. In addition, the simultaneous occurance of various competitive reactions, like hydrodenitrogenation, hydrodeoxygenation and hydrodemetallation adds to the complexity of the hydrodesulfurization.

The difference in the extent of removal of different sulfur compounds depends on the basicity and structure of the compounds. Crynes (29) has reviewed the coal liquids hydrotreatment literature. He has reported that liquids derived from a variety of coals when hydrotreated at 343 to 454 C, 1.04×10^4 -2.08×10^4 kPa and 0.3 - 3.0 weight hourly space velocity, show sulfur removals as high as 95% depending on the processing conditions and the feed oil. SRC light oils have been hydroprocessed at 356 - 426 C, 8.27×10^3 - 1.72×10^4 kPa and 0.45 - 2.11 hours LVHSV, where more than 90% sulfur removal was observed under

some processing conditions in the presence of CoMo/alumina and NiMo/alumina catalysts (30).

Satterfield et al. (31) have reported that the hydrogen sulfide gas produced in hydrodesulfurization reactions has inhibitive effects on the hydrodenitrogenation at low temperatures, whereas it enhances the HDN rate at higher temperatures. Satterfield and Hsi (32) reveal that for hydrotreatment on a NiMo/alumina catalyst, H_2S has a slight inhibition effect on the hydrogenation step in HDN, but a strong accelerating effect on C-N bond breakage.

The recent review by Seapan (3) indicates that while most of the single compound studies show first order behavior with respect to the reactant, the mixtures of these compounds demonstrate higher than first order behavior when subjected to heteroatom removal. Theoretical discussion of Weekman (33) also shows that a mixture of several parallel first order reactions exhibits on overall kinetics order larger than unity. A simple first order kinetic model is popularly used to represent the experimental data. Second order models, though used in several cases, are not as common as the first order models are. In addition to these two models, modified models are used to account for catalyst deactivation effect, incomplete catalyst wetting and other trickle bed flow non-idealities. Another modification to the simple first order model is to divide the reactants into a fast reacting and comparatively slower reacting groups. Modified models usually give a better fit to the experimental data than simple models.

Hydrodenitrogenation

HDN is referred to the reaction of hydrogen with nitrogen containing compounds resulting in a reduction in the nitrogen content of the oils and the removal of nitrogen as ammonia (3).

Some typical nitrogen containing compounds are tabulated by Ahmed (16). These compounds include heterocyclic and non-heterocyclic compounds, the latter are composed of anilines, aliphatic amines and nitriles. Their nitrogen is relatively easier to remove than that of the heterocyclic compounds (16).

The heterocyclic nitrogen compounds include both basic and non-basic types. The basic compounds can poison the hydrotreating catalysts by strong chemisorption on the catalyst. The HDN of heterocyclic compounds proceed via the saturation of heterocyclic rings followed by the opening of the ring at the carbon-nitrogen bond and subsequent removal of nitrogen in the form of ammonia. The intermediate basic products can also poison the active sites of the catalyst (34). Generally the HDN process is relatively more difficult than HDS. This can be explained by the higher bonding energy of C-N than C-S. Gates et al. (35) found that in the catalytic hydroprocessing of phenothiazine, the C-S bond scission was 10 times more rapid than that of C-N bonds. Similar results were obtained in the comparison of HDS of dibenzothiophene and HDN of acridine.

Flinn et al. (36) have reported different reactivities for different compounds boiling in the same range, they also showed that denitrogenation tends to be more difficult with an increase in the boiling point of the feed. However, Sarbak et al. (37) in the study of HDN of

important polynuclear aromatic nitrogen compounds found in coal liquids, showed that both the rate constants and the relative reactivities of these compounds decreases when the number of rings is increased from one to four, they then increase for large compounds.

Katzer and Sivasubramanian (34) suggested that the reasons for the increased difficulty of HDN with increasing boiling range is because that the higher boiling feedstocks typically contain higher concentrations of nitrogen which can strongly inhibit other hydroprocessing reactions. Moreover, the lower hydrogen content of the feedstocks and higher tendency of coke formation for higher boiling range compounds add to the difficulties of HDN.

Hydrodeoxygenation

Hydrodeoxygenation is referred to the reaction of hydrogen with oxygen containing compounds which results in a reduction in the oxygen content of the oils, and the removal of oxygen as water (3).

The oxygen compounds present in the bitumen have been described by Moschopedis and Speight (38), they concluded that most of the oxygen existed as hydroxyl groups in asphaltenes, and as carbonyl groups in resins. Esters were identified as the principal contributor of the carboxyl form, while phenols and alcoholic groups made up the bulk of the hydroxylic oxygen.

Under thermal hydrocracking, the oxygen containing groups undergo various reactions (39). Carboxylic acids decarboxylate quickly and are not usually found in significant concentrations in liquid products. But at high temperature phenols and aromatic rings that are substituted

with ester groups are converted to products such as dibenzofuran.

The oxygen uptake from air during the storage of coal liquids contributes to a small amount of oxygen present in the coal liquids. Aliphatic peroxides, ketones and aldehydes are main products of autoxidation (40). Most of these compounds deoxygenate readily even in the absence of catalyst (39).

Furimsky (39) in his deoxygenation studies mentioned that catalytic deoxygenation followed many of the same qualitative trends as denitrogenation. A mechanism based on the opening of hetero-ring, followed by denitrogenation and deoxygenation of the fragments was proposed for both processes (41). Alumina support itself was found to be quite active in the deoxygenation. The addition of MoO_3 to the alumina support increased the oxygen removal (39). Phenols were assumed as the coke precursors as mentioned in the same paper.

Water generated in hydrodeoxygenation process could affect other hydroprocesses. Water was reported to have inhibitive effects on catalytic hydrogenation by the chemisorption on the active sites (42). The interactions of water and hydrocarbons, carbon oxides, and the steam dealkylation reactions are all possible in the hydrotreating conditions. Riley (43) claimed that water injection in a hydrodesulfurization process can improve the catalytic activity and extend the catalyst life.

Hydrodemetallation

Katzer (34) suggested that the demetallation of organonickel compounds in petroleum follow the following mechanism:

$$\text{Organo-Ni} + H_2 \xrightarrow{\text{catalyst}} \text{organic compound} + N_i$$

This reaction is accompanied by HDS, HDN and HDO reactions. The metal product in the above reaction later reacts with H_2S and is converted to metal sulfide. The evidence that the metals on spent catalyst are in the form of metal sulfides supports this mechanism (44).

In literature, with respect to the total metal concentration in the crude oils, both second order (45, 46) and first order (47, 48, 49) HDM kinetics have been reported. Cecil et al. (50) have pointed out that if the metal containing compounds could be considered as constituting of two major fractions reacting with different first order rates, the total metal disappearance would appear as second order. However, Van Dongen (51) speculated that probably the order of the individual vanadium bearing species is less than 1.0. Van Dongen in his batch autoclave studies of pure nickel and vanadium prophyrines observed fraction order kinetics. The reaction order could also depend on the concentration in the feedstock. Levy and Peterson (52) in their hydrodemetallation studies using gas oil doctored with metallic naphthenates found that the demetallation rate at high metal concentrations was nearly second order, but it decreased to about half order at metal concentrations below 50 - 60 ppm.

The chemical compound types of trace metals in synfuels have not been identified. Some metals like Fe and Ti are suggested to be in the form of organometallics. The mechanism for hydrodemetallation of these compounds could also follow the mechanism developed for nickel and vanadium. Iron in the form of iron sulfide was found deposited on the spent catalyst (34). Researchers at Pittsburgh Energy Technology

Center analyzed the titanium deposits in the pores and on the surface of the spent catalysts by X-ray diffraction and found that titanium was in a unique form of TiO_2 polymorph anatase. In their studies, model titanium containing organic compounds were hydrogenated under liquefaction conditions to yield the anatase (53).

In coal liquids, the forms of organometallics have not yet been determined, consequently, the hydrodemetallation of even the most abundent organometallics like iron and titanium has not been studied.

In the study of the kinetics of demetallation, the deposited metals could severely deactivate the catalyst or enhance the catalytic activity, such diverse interactions must be considered in the anlaysis of the kinetic data.

Catalyst

Catalysts containing Mo and Ni (or Co) supported on gamma alumina or gamma alumina stablized with minor amounts of silica are commonly used for processing petroleum feedstocks. Gamma alumina stabilized with silica have been observed to have relatively more hydrocracking activity than the alumina support alone. The activity of silica-alumina support toward different reactions varied with the ratio of silica to alumina (16).

CoMo/alumina catalyst is commonly used for HDS, while NiMo/alumina catalyst is frequently the choice for HDN. Mitchell (54) tested the activities of several kinds of commercial catalysts for a number of reactions and showed that NiMo/alumina catalysts have higher activities when compared with CoMo/alumina catalysts. Ahmed (16) concluded that

NiMo/alumina catalyst had superior HDN activity over CoMo/alumina catalyst. He also reported that NiMo/alumina catalyst has a higher resistance to the coke formation.

The ratio of Ni to Mo has significant effects on the catalyst activity. An atomic ratio of Ni to Mo of 0.6 - 1.0 was observed to have the maximum activity (55). Sultanov et al. (56) found that the order of impregnation had a strong effect on catalytic activity for HDS of petroleum oil. When Mo is added first followed by Ni, the catalyst was more active than the catalyst prepared by reverse impregnation procedure. Mone (57) reported that higher calcination temperatures produce less active catalysts. Researchers in Chevron Research Company (58) claimed that catalyst calcinated at 480 C was twice as active as the catalyst calcinated at 650 C.

Kiviat and Petrakis (59) found the infrared spectra for adsorbed pyridine on NiMo/alumina catalyst to be slightly different from that on CoMo/alumina catalyst. Both showed the evidence of Lewis and Bronsted acid sites, while NiMo/alumina catalyst had a somewhat higher Bronsted-to-Lewis acidity ratio. Similar results were reported by Mone and Moscou (60), who also concluded that the degree of interaction depends on the calcination temperature.

The effect of presulfiding on CoMo/alumina catalysts has been recognized by various investigators. Ahmed (16) observed that presulfided catalysts have higher initial activities for HDS of FMC oil and the activity is more stable. Tantarov et al. (61) observed a high activity and less coking tendency on presulfided CoMo/alumina catalyst used in the hydrorefining of thermally cracked gasoline. As for NiMo/

alumina catalysts, all studies have recognized presulfiding effects, but the interpretation of these effects has been different. Brewer et al. (62) found that if the catalyst is exposed to hot hydrogen gas the presulfiding effects of the catalyst will be lost. In contrast, Schuit et al. (63) found that hot hydrogen can activate the catalyst.

Other studies have indicated the presulfiding effects may be correlated with coke formation on the catalysts (64). Massoth (65) correlated the catalyst activity with the concentrations of various states of the supported metals.

Catalyst Deactivation

Catalyst deactivation during hydrotreating processes has been receiving considerable attention. Catalyst deactivation is believed to be due to a) coke formation, b) metal deposition, c) acid site poisoning, or d) sintering. Acid site poisoning can be because of strong chemisorption of impurities in the feed, the reaction intermediates, or the final products of reaction. The acidic property of the catalysts provides the nitrogen containing compounds of the feed a chance to be chemisorbed and become a catalyst poison. The activity decay due to sintering and mechanical failure like wear, disintegration or loss of mechanical strength are also possible, but under the most hydrotreatment conditions, these effects are less significant.

The coke formation and metal deposition were reported to be the main mechanisms of catalyst deactivation. The following literature survey will focus on these topics.

Hydroprocessing of petroluem residues shows a very characteristic deactivation curve. In industrial hydrotreatments, the average

catalyst temperature of the hydrotreater is normally raised to compensate for the deactivation of catalysts and thereby hold a particular product specifications constant. The deactivation curve can be subdivided into three distinct parts. The initial period is characterized by a rapid, but continuously decreasing deactivation rate. This deactivation has often been blamed on coke deposition on the catalysts. The final period is characterized by a rapid continuously increasing deactivation rate. This deactivation has commonly been blamed on the constriction of the catalyst pore mouth. These two periods are separated by a period in which the deactivation rate appears to be near constant (44).

The mechanism of coke formation is very complex. Modison and Roberts (66) in their pyrolysis experiments observed that nitrogen containing heterocyclic aromatic compounds have a higher coking tendency than their hydrocarbon analogs. Quinoline and acridine give more coke than naphthalene and anthracene. Also, they observed that aromatic compounds with one or more methylene groups binding the aromatic nuclei have a strong tendency toward condensation and coking. Appleby et al. (67) in their studies with commercial Silica-Zirconia-Alumina catalyst observed that the condensed rings were more susceptible to coking than their linked rings. The heterocyclic compounds were less prone to coking than their hydrocarbon analogs.

In catalytic cracking operations, Voorhies (68) and also Rudershausen and Watson (69) observed that the coking rate is a strong function of temperature as well as hydrogen partial pressure. The coking rate decreased with an increase in hydrogen partial pressure.

Lipovich et al. (70) in an experimental study with CoMo/alumina and Mo/alumina catalyst observed strong coking tendency for thiophene and indole. An increase in coking tendency for thiophene was observed at higher temperatures. The condensation of free radicals formed due to the cleavage of the heteroatom bonds is a logical explanation for coke formation. They also observed that the coking tendency of styrene, n-heptane and methylnaphthalene decreased with an increase in temperature above 420 C. In catalytic hydrodeoxygenation study, Furimsky (39) mentioned that phenols had been assumed to be coke precursors.

Coke formation and coke hydrogenation were suggested to be reversible reactions occuring on the catalyst surface (71). Ternan et al. (72) suggested that two types of coke were present on the catalyst: a reactive coke which is subsequently converted to reaction products and an unreactive coke which blocks the catalytic sites.

Hollaway and Nelson (73) observed that the amount of carbon deposition increases along the catalyst bed in a Synthoil process. Crynes (74) observed a decrease of coke content from top to bottom when hydrotreating SRC feed, but a reverse pattern for an Exxon Donor Solvent feed.

The coke formation affects the surface area and pore volume of the catalyst, reducing the rate of diffusion of reactants into catalyst pores. However, Ozawa and Bischoff (75) reported no changes in the surface area and effective diffusivity of spent catalysts due to coke formation. Ramsen and Hill (76) and Hollaway and Nelson (73) observed significant changes in the surface area of spent catalyst. Hollaway and Nelson also observed that the surface area decreased with an increase in carbon

deposition. Prasher et al. (77) in their study of residual hydrocracking found marked decrease in effectivity with the age of the catalyst which they attributed to the deposition of coke and metals.

The deposition of coke causes a decrease in catalyst activity which can be recovered by burning off the carbon, while the inorganic metals and organometallics deposited on the spent catalyst react with active metals on the catalyst during regeneration and cause a permanent loss in the catalyst activity (16). Kovach et al. (78) studied the deposition patterns of inorganic metal salts and organometallics, and found that after carbonaceous deposition reached its maximum, the deposition of oil-insoluble inorganic metal salts would be hindered by carbonaceous deposition. On the other hand, organometallics can still penetrate through the carbonaceous deposition and into the pores of the catalyst and be deposited there.

Chiou and Olson (79) analyzed the aged catalyst obtained from the H-coal process by scanning electron microscopy and electron microprobe. They showed that most inorganic metals deposit on the outer surface of the catalyst, whereas organometallics can penetrate into the catalyst pores and have the same distribution pattern as those of organo-vanadium and organo-nickel in petroleum hydrotreatments. DeRosset (80) also analyzed the aged catalysts and found that higher percentages of organometallics were deposited on the catalyst than inorganic metal salts.

Metal deposition can restrict the diffusion into the pores of the catalyst and can cover the active surface causing a permanent loss of activity even after regeneration. Some observations have suggested

that the metal deposition can accelerate the coke formation. Habil et al. (81) observed a large increase in coke content due to catalyst metals poisoning in a cracking process. Tamm et al. (44) argued that instead of coke which was commonly blamed for the initial rapid catalyst deactivation, the organometallics are the primary deactivation agents. They found that the initial deactivation period was directly related to the concentration of organometallics in the feed but not to the coke precursers as measured by Conradson carbon content.

The promoters (Ni and Co) on Mo/alumina catalyst were found to have significant effects on coke formation. Ahmed (16) found that Ni was a better promoter than Co when deposited on Mo/alumina, increasing the resistance of coke formation. However, Ternan et al. (72) studied the coke formation on the HDS catalysts and found that it is the molybdenum content of the catalyst rather than the promoter which controls the coke level.

The effects of titanium deposition on the catalyst have been investigated by few researchers. Kovach et al. (78) described that titanium and other organometallics could permanently poison the catalyst. Hollaway (73) postulated that titanium and iron did not cause significant activity decay in short-term experiments but undoubtedly caused marked activity decay as more metals deposit with longer on-stream time. In another study made by Kovach et al. (78), the $CoMo/Al_2O_3$-SiO_2 catalyst was impregnated with TiO_2 and other metal oxides, and the resulted catalysts were compared for their hydrogenation activity. TiO_2 behaved differently from other metal oxides maintaining its activity at 99% of unimpregnated catalyst even up to 8.0% TiO_2 on the catalyst. They also simulated the adsorption of metals under coal

liquefaction conditions and tested the catalyst activity. In the test, titanocene dichloride showed negligible deactivation up to the processing time of 24kg coal/kg catalyst, then the activity dropped drastically.

Beuther et al. (82) claimed that a NiMo/alumina catalyst when impregnated with titanium tetrachloride shows improved desulfurization activity. Gates et al. (35) showed that sulfided NiMo/TiO_2 was almost twice as active per unit surface area for HDN or quinoline as a comparably prepared NiMo/gamma alumina catalyst. Massoth et al. (83) evaluated the effects of catalyst support on the activity of CoMo catalysts. Alumina was found to be the best support showing high activity for HDS and hydrogenation and moderate to high activity for hydrocracking, whereas titania as support showed high hydrocracking but low HDS and hydrogenation activity.

Nature of Titanium in Coal Derived Liquids

Relative abundance of titanium in coal liquids, their possible role in the catalyst poisoning and their potential to generate atmospheric particulate pollutants upon combustion of coal liquids has generated significant interest in their research.

Filby et al. (1) suggested that titanium might occur in coal liquids as:

1. A finely divided titanium dioxide remained from the original coal that passed into the liquid during the filtration process in the plants.

2. An organotitanium, originally present in the parent coal which survived the liquefaction process and remained in the liquid products.
3. An organically associated form produced during the liquefaction process which appeared in the liquid products.

Both organically associated titanium (84) and inorganically associated titanium (85, 86) were reported to be present in coal. Eskenazy (86) found that titanium was adsorbed from aqueous solution by peat. A more stable titanium organic complex was formed on prolonged contact, compared to complexes formed initially. Miller and Given (87) found that a significant proportion of titanium in the lighter fractions of low rank coals was acid soluble. This indicates that some of the titanium present in coals was not the form of oxides which are insoluble in most acids, but possibly it was in the form of organic complexes.

Metallo-porphyrins have been found to be the main organometallic compounds in petroleum (88). It was expected that metallo-porphyrins to exist in coal liquids too. However, under the severe conditions of coal liquefaction processes, any metallo-phyrin material originally present in the coals is degraded during the hydrogenation process. Mcginnis (89) applied the non-destructive chromatographic procedure and Sanik method to analyze coal liquids, but found no evidence for the presence of metallo-porphyrins in any of the coal liquids analyzed. The lack of existence of metallo-porphyrines does not mean that other types of organometallics can not exist in the coal liquids. Mcginnis (89) did not find titanium in the form of rutile (TiO_2) or ilmenite (FeO, TiO_2) in the coal liquids. Mcginnis also claimed that titanium in the form of complexes is composed of aromatic rings connected by low

molecular weight aliphatic bridges. Research using ESR by Mcginnis obtained no signal for titanium in III state, thus indicating that titanium was in IV state, because other states of titanium were not considered sufficiently stable in coal liquids.

Weiss (90) has stated that the chemical form of titanium in coal liquids could not presently be answered by direct spectroscopic or other instrumental methods. However, from the distribution of titanium and phenols in different fractions of coal liquids, he suggested that the titanium phenoxide possibly existed in the coal liquids. Mcginnis (89) also suggested the possible existence of titanium phenoxide in coal liquids by a similar approach.

The formation of organic complexes of titanium during liquefaction requires a source of titanium which is reactive under hydrogenation conditions. Titanium oxides are extremely stable, therefore conversion of titanium oxides to titanium tetrachloride is essential in the formation of organo-titanium compounds (90).

Godnev and Pamfilov (91) and also Cottom and Wilkinson (92) found the possibility of formation of titanium tetrachloride by reacting titanium oxides with chlorine or chloride-containing compounds. Under the highly reactive conditions and the complex chemical system in the coal liquefaction, the formation of stable organometallics, like titanocene dichloride, was suggested by Filby et al. (1). However, Weiss (90), based on thermodynamic considerations and low concentration of HCl present in liquefaction processes concluded that the possibility of the formation of titanium tetrachloride during liquefaction is very slim. Weiss (90) also contended that the formation of organo-titanium through the rearrangement of original complexes was a logical assumption,

but the formation of a mobile titanium ion or the formation of an entirely different type complex is unlikely.

Literature Summary

The literature reviewed above can be summarized as follows:

1. In trickle bed reactor, the factors affecting the performance of trickle bed reactor include the gas and liquid distribution, axial backmixing and diffusion resistance.

2. The space time, temperature, pressure and hydrogen flow rate are four major operational parameters in hydroprocessing petroleum feedstocks and coal derived liquids.

3. In catalytic hydrotreatment process, the selection of operational parameters may have detrimental effects on HDS, HDN, HDO, HDM and hydrogenation reactions. The simultaneous occurance of these reactions adds to the complexity of hydrotreatment.

4. The presulfiding effects of catalysts were recognized in maintaining higher activities and reducing the coking tendency. The calcination temperature affects the catalytic activity. For the calcination of NiMo/alumina 480 C was found to result the highest activity.

5. The coke formation and metal deposition were reported to be the main mechanisms of catalyst deactivation. The deposition of coke causes a decrease in catalyst activity which can be recovered by burning off the carbon, while the inorganic metals and organometallics deposited on the spent catalyst react with active metals on the catalyst during regeneration and cause a permanent loss in catalyst activity. The deposition of inorganic metal salts can be hindered by carbonaceous deposition. However, the organometallics still can penetrate through

the carbonaceous deposition into the pores of catalyst and be deposited there.

6. The impregnation of catalysts with titanium compounds has shown both deactivation and activity enhancement.

7. Two sources of organo-titanium compounds are possible. One is the organo-titanium orginally present in coal which survives the liquefaction process and remains in the liquid products. The other is produced in the liquefaction process through the reaction of inorganic titanium and organic compounds.

8. Titanocene dichloride is suspected to be one of the organo-titanium compounds present in coal liquids.

CHAPTER III

EXPERIMENTAL SET UP AND PROCEDURES

A schematic diagram of the experimental set up used in this study is shown in Figure 1. The basic design follows the previous apparatus employed for hydrodesulfurization and hydrodenitrogenation of coal derived liquids at Oklahoma State University. Some modifications have been made in the heating, sampling and gas flow controlling systems which will be described below.

Previously, aluminum blocks with electrical heating wires placed in their grooves were used as reactor heating system. The same system was used at the beginning of this study, but several times the heating wires were burned out. Therefore, the aluminum blocks were replaced by a cylindrical copper block with three heating bands around it. The new system operated more reliably, though the outside temperature of the reactor was not as uniform as we liked it to be.

The needle valve used to adjust the gas flow rate was placed very close to the sampling bomb, which became easily contaminated with product oil resulting in the gas flow rate instability and loss of control. Relocation of the needle valve at a position away from the sampling bomb resolved the problem. The product oils contaminating the needle valve indicated that the gas leaving the sampling bomb contained some condensable oil. The addition of another sampling

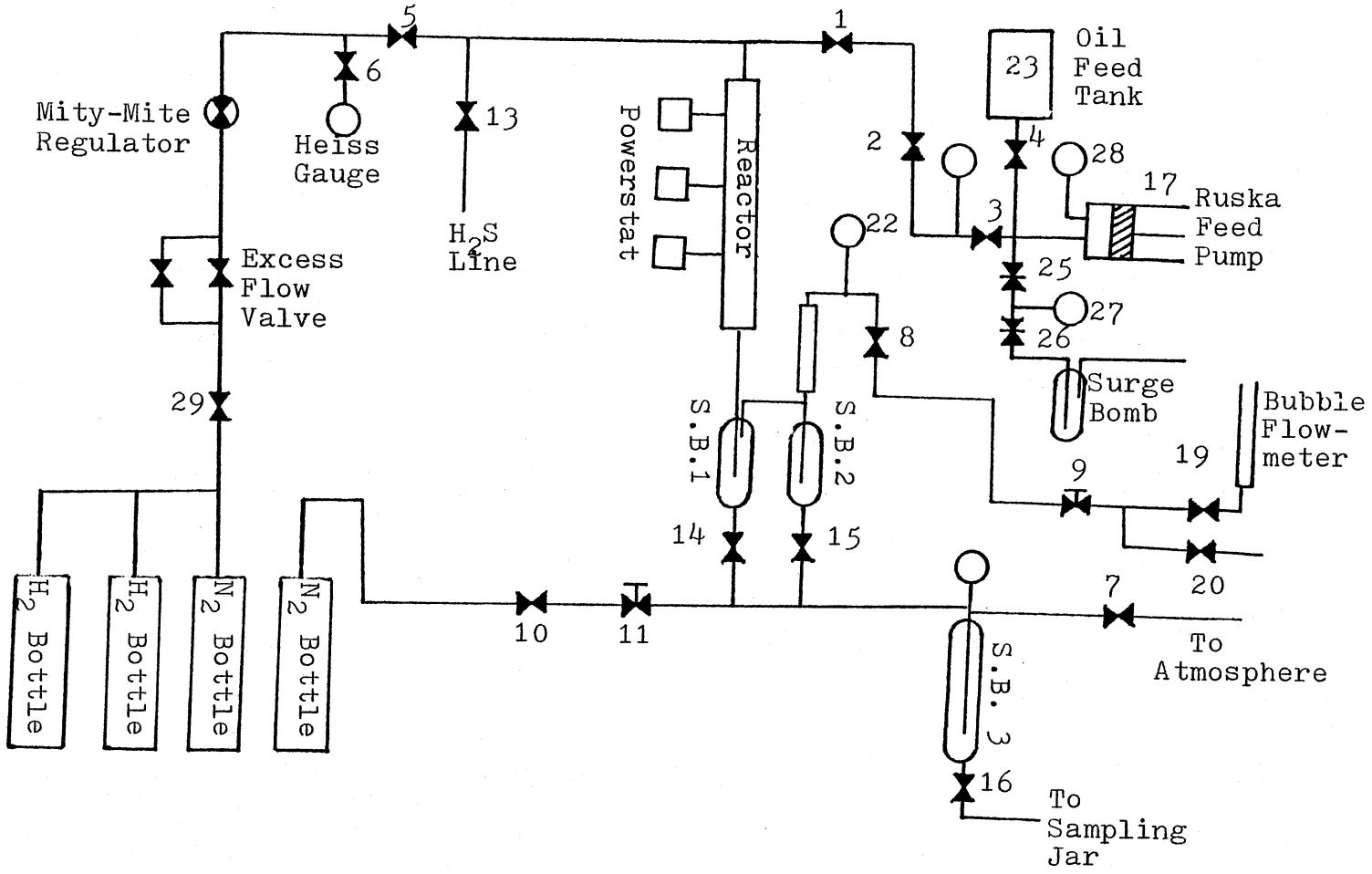

Figure 1. Experimental Set-up

bomb and a vertical half inch tube helped to condense and collect the condensable vapors.

The schematic diagram shows that the hydrogen enters the top of the reactor through valve #5, A Ruska feed pump #17 charges oil at a fixed rate to the top of the reactor. The oil and hydrogen flow concurrently through the reactor which is packed with catalyst or glass beads. Hydrogen pressure is maintained by a Mity-Mite regulator valve #18. Hydrogen flow rate is adjusted by a needle valve #9, and measured by means of a bubble flowmeter installed on the off-gas line. The product oil and gas leaving the reactor are separated in sample bomb #1. The gases leaving sample bomb #1 flow into sample bomb #2, in which the condensable gases are condensed and collected. The non-condensable gases leave the system through exit valves #8, 9 and 19 (or 20). A scrubber with NaOH solution as absorbent was located between valve #9 and 19 for removing the acidic gas. Sample bomb #3 can be isolated from bomb #1 and 2 by closing valves #14 and #15. Liquids collected in bomb #3 are purged with nitrogen gas entering through valves #10 and #11, and exiting through valve #7.

The upstream pressure of the system is monitored by a Heiss gauge #21, and the downstream pressure by pressure gauge #22. Temperature along the length of the reactor is measured by means of a movable thermocouple located inside a thermowell and is indicated on a digital read-out. A detailed description of the main components of the system is given below.

Reactor

The reactor is consisted of a 60.96 cm (24-inch) long, 1.27 cm (0.5-inch) O.D., and 0.089 cm (0.035-inch) thick stainless steel tube, fitted with a 0.5-inch Swagelock cross and union at the top and bottom respectively. The effective reactor length is 24 inches as shown in Figure 2. A 1/2-inch Swagelock cross is connected to the top of the reactor and two 1/2-inch to 1/4-inch reducers are connected to the two sides. A 1/8-inch O.D. thermowell is secured in the middle of the reactor by means of a 1/4-inch to 1/8-inch reducing union which was drilled for inserting the thermowell. Stainless steel screens of 50 mesh size and a 3/8-inch O.D. tube are used to support the catalyst bed. The bottom of the reactor is fitted with a 1/2-inch to 1/4-inch reducer to enable it to be connected to the sampling bomb #1.

Reactor Heating System

A one piece cylindrical copper block, 38.1 cm (15 inches) long, 12.7 cm (5 inches) O.D. with a 1.905 cm (3/4-inch) diameter hole in the center is the main heating block. A 3/4-inch O.D. stainless steel tube is inserted into the center of copper block to give intimate contact between the reactor and the heating block. Three heating bands, 7.62 cm (3 inches), 15.24 cm (6 inches) and 15.24 cm (6 inches) in length, are surrounding the copper block from top to bottom.

The electric power to the heaters is controlled by powerstats. Three iron-constantant thermocouples are placed in the holes of the copper blocks and used to measure the temperatures of top, middle, and bottom sections of the block. The three inch heating band is used to

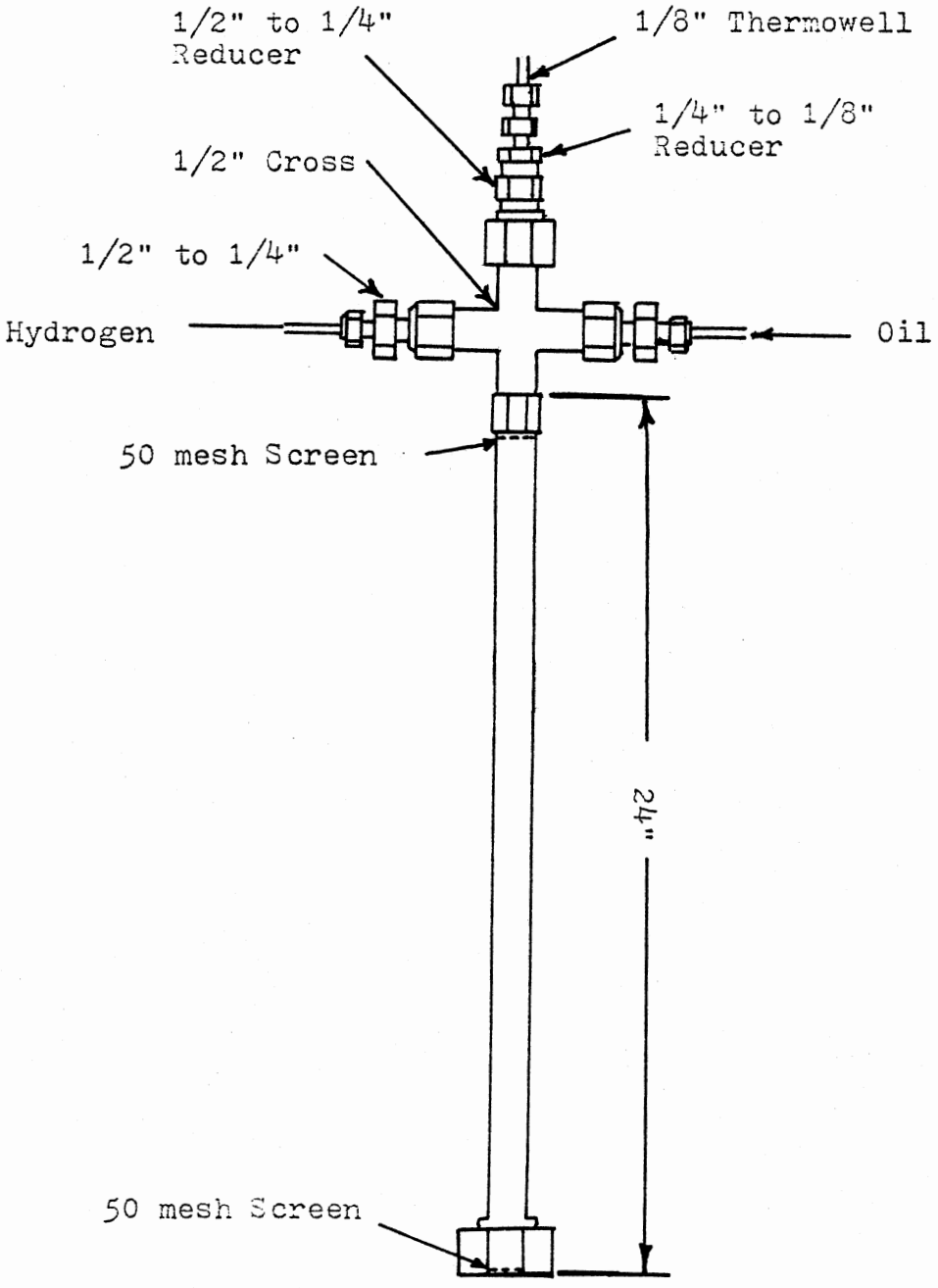

Figure 2. Reactor Design

preheat the entering oil and hydrogen gas to the desired reaction temperature. The bottom heater is used to counter the end effect heat loss. The copper block, insulated with felt fabric and asbestos tape, is secured on a support rack. Electrical connections for the heaters are made through the holes in the insulation.

Temperature Measurement

The reactor temperature profile is measured with a Conax J-type grounded tip iron constantan thermocouple. Before the measurement, the temperature selector switch was placed at the desired point and the thermocouple was slided along the thermowell. The response is shown on the OMEGA 2809 Digital Thermometer.

Pressure and Flow Control

The upstream pressure of the system is monitored on a 0-3000 psig Heiss gauge #21. The pressure indicated by this gauge is taken as the nominal reaction pressure. Pressure gauge #22 connected to sample bomb #2 shows the pressure downstream from the reactor. Under normal operations, the upstream and downstream pressures are almost the same. Once the reactor clogging happens, the restriction of gas flow through the reactor causes a decrease in the downstream pressure.

The initial pressure of new hydrogen bottle is about 2200 psig. A manifold regulator controls the outlet pressure of the hydrogen bottle. A Mity-Mite pressure regulator accurately controls and maintains the system pressure.

The gas flow rate is maintained by means of valve #8 and #9. Valve #8 is a Vee-tip type valve designed to take the major portion of pressure drop. Micro-metering needle valve #9 is used for the precise control of gas flow. A 0-100 ml bubble flowmeter is used to measure the gas flow rate. A bypass line is connected to bubble flowmeter, through valves #19 and #20, so that the effluent gas can be vented without flowing through the bubble flowmeter.

Oil and Hydrogen Feed Systems

The oil feed system consisted of a stainless steel feed tank #23, and a Ruska positive displacement pump #17. Because a light oil was used in this study, the heating system for the feed tank was removed. The oil cylinder of Ruska pump and the oil lines leading to the reactor were wrapped with flexible heating tapes which were controlled by powerstats. Under normal operation, this heating system was not used, but in case of tube clogging, the application of heat to the suspected clogged portion can be useful for the removal of clogging. Rupture disks #25 and #27, rated at 1800 and 2300 psig respectively, were installed on the feed line to prevent damage to the pump in case of oil-lines clogging or operational mistakes. A 2400 ml sample bomb was installed in the downstream of rupture disks to collect the oil if both disks ruptured. A pressure gauge #27 was connected between the rupture disks, once the first disk ruptures, the pressure would be indicated on pressure gauge #27. A pressure gauge connected to Ruska pump monitored the pressure in the oil lines.

The hydrogen was fed directly from the gas bottle through a manifold, which allowed the changing of hydrogen bottles without

interrupting the operation. An excess flow valve #30 installed between the manifold system and the Heiss gauge could shut off the hydrogen gas automatically in case of excessive flow such as a system rupture. Another quarter turn valve #29, which can function as the rapid manual cutoff of hydrogen supply in case of emergency, was installed between the manifold and excess flow valve.

Sampling System

The sampling system consists of three sample bombs #1, #2 and #3, with 300 cc, 300 cc and 600 cc capacities respectively. Figure 3 shows the design of sample bombs #1, #2 and #3. The bottom end of the reactor was connected to the sample bomb #1, with a 1/4-inch stainless steel tube. The sample bomb #2 placed in parallel with the sample bomb #1, was used to collect the condensable gases coming out of sample bomb #1. The vapor and liquid are separated in these bombs. The non-condensable gases would leave the system through the effluent gas line, and the liquid would accumulate at the bottom, flowing from bombs #1 and #2 into #3. Valve #14 and #15 are placed between these bombs and can be operated to collect liquids from sample bomb #1 and #2 separately. A pressure gauge #30 monitored the pressure of bomb #3.

Gas Detectors

A portable hydrogen sulfide detector is used during catayst pre-sulfiding and oil sampling. The detector can signal warning alarm when the concentration of hydrogen sulfide exceeds 17 - 20 ppm, also it provides a digital output of the instantaneous, average and maximum

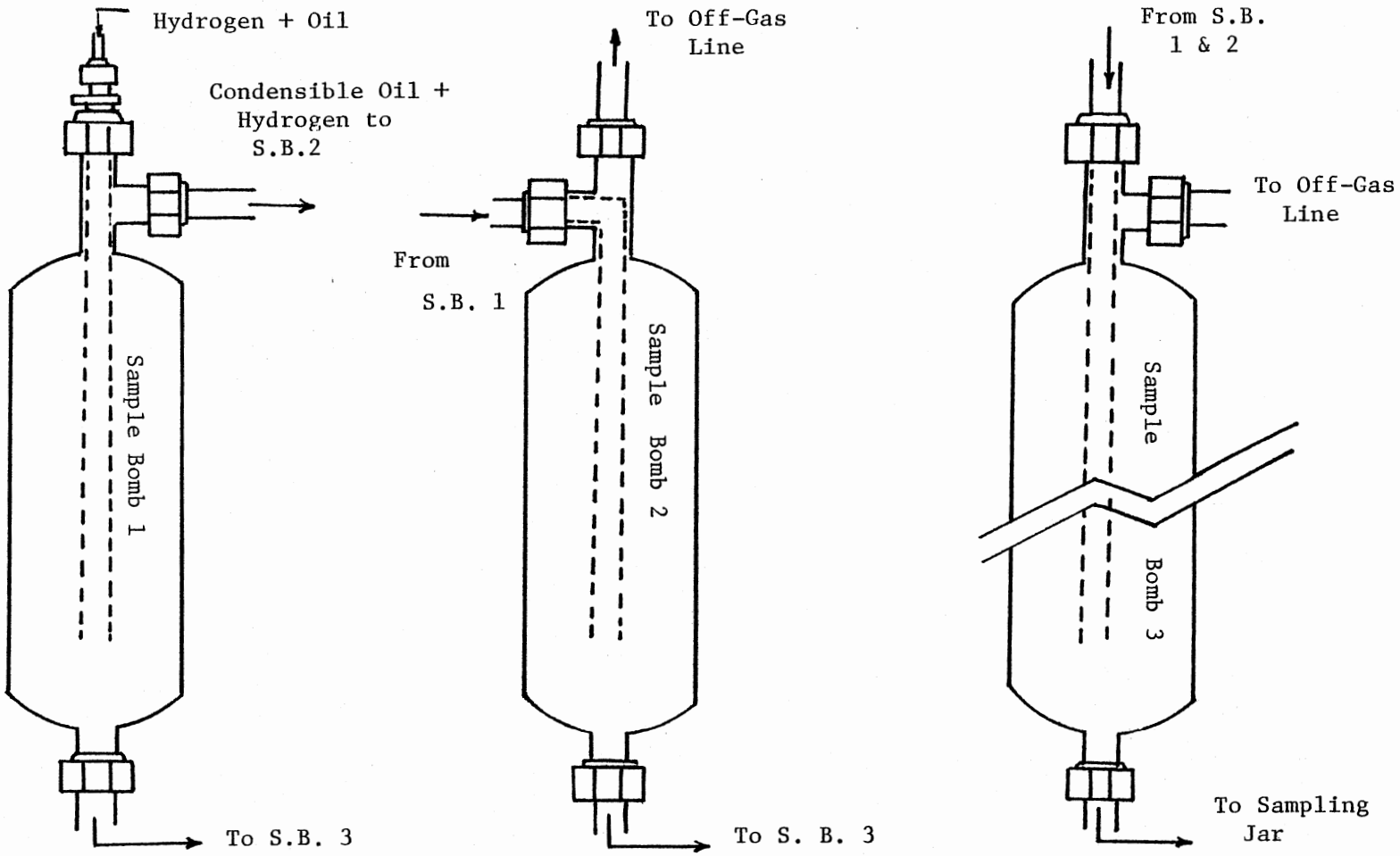

Figure 3. Sample Bomb Designs

concentrations after some period of operation.

A combustible gas detector, MSA model 501, was installed with two detector heads located over and near the reactor. The alarming red light will come on once the hydrogen concentration in the room reaches 50% of the lower explosive limit.

Inert Gas Purging Facility

After the liquid sample is collected in bomb #3, the nitrogen gas is purged through the liquid sample to remove the dissolved ammonia and hydrogen sulfide.

Nitrogen is supplied to the sample bomb #3 directly from the supply cylinder. Matheson model-8 pressure regulator is used to regulate the pressure of the purging nitrogen gas. The nitrogen flows through valves #10 and #11 into bomb #3, and vents to the atmosphere through valve #7. Check valve #31 is provided to prevent the liquid products from back-flowing into the nitrogen feed-line.

Experimental Procedure

The experimental procedure consists of the following steps: catalyst preparation and loading, catalyst calcination, catalyst presulfiding, start-up, normal operation, sampling, shut down and sample analysis. The detailed descriptions of each step will be given as follows:

Catalyst Preparation and Loading

The Shell 324 NiMo/alumina catalyst is used in this study. It is a 1/16-inch extrudate. The catalyst is packed in the middle of the

reactor to minimize the end effects. The reactor is packed at both ends with glass beads. The upper layer of glass beads provides a better liquid distribution whereas the bottom layer is used simply for supporting the catalyst bed. The reactor packing follows the procedures given below:

1. A 50 mesh size screen was wedged at the bottom of reactor.
2. The thermowell was held centrally inside the reactor.
3. The glass beads were poured into the reactor while tapping the reactor gently for uniform packing around the thermowell. The bottom glass beads layer of 11-inch was packed in the Run #1 and #2, but after these two runs, the glass beads layer was removed and replaced by a 3/8-inch O.D. stainless steel tube.
4. While gently tapping the reactor, the catalysts were poured into the reactor. In all runs, 13 grams of catalyst was packed in the reactor to a height of 8 inches.
5. A 50 mesh size screen with a 1/8-inch diameter hole in the center was slided down the thermowell, untill it touched the top of the catalyst bed.
6. The glass beads were poured into reactor while gently tapping the reactor for uniform packing. The length of the upper glass beads layer was 5 inches in TME #2, and 1-inch in TME #3. In order to eliminate the reactor plugging problem, the glass beads were not used in the other runs.
7. The packed reactor was then fitted with a 1/2-inch cross, as shown in Figure 2. The thermowell was secured by a 1/8-inch Swagelock fitting. The reactor was slided down the central hole in copper heating block. The bottom of the reactor was

fitted with a 1/2-inch to 1/4-inch reducer to enable it to be connected to the sample bomb #1.

8. After connecting the two legs of the Swagelock cross on the top of the reactor to the hydrogen gas line and oil line, the reactor becomes ready for pressure testing.
9. Each fitting in the whole reactor system is checked for the leaks by gradually pressurizing the system with nitrogen gas. The pressure test is done at 1600 psig which is 100 psig higher than the reactor operating pressure. A pressure drop of 20 psig in one hour is the maximum acceptable leak.
10. The electrical wires of heating bands are connected to the corresponding powerstats. Now the reactor is ready for operations.

Catalyst Calcination

The catalyst as obtained from supplier, has moisture and other gases adsorbed on its surface. The moisture and adsorbed gases must be removed by calcination before it can be utilized. The procedure of calcination is described as below:

1. Close valves #1, #2, #3, #4, #7, #11, #14 and #15. Open valves #5, #6, #8, #9, #19 and #20.
2. Turn the powerstats on and control the heating rate at 120 - 150 C per hour.
3. When temperature inside the reactor reaches 200 C, start nitrogen flow through the reactor to carry the described moisture and gases out of the system. The nitrogen flow is set

at 200 - 300 psig and 400 ml per minute.

4. When the temperature reaches 480 C, turn down the powerstats and maintain the temperature at 480 C for one hour. Then turn off the powerstats and let the temperature drop to 230 - 250 C. Turn on the powerstats again and maintain the temperature around 250 C.
5. The nitrogen flow may be cut off now, since the calcination is complete and the catalyst can be sulfided.

Catalyst Sulfiding

A mixture of 5.14% H_2S in H_2 was used for sulfiding in this study. The steps of catalyst sulfiding are described below:

1. Turn on the H_2S detector.
2. Close valve #5 and #6. This step is to protect the Heiss Gauge from H_2S corrosion.
3. Open valve #13, and start the flow of H_2S-H_2 gas through the reactor at 20 - 30 psig and 400 ml per minute.
4. Maintain the reactor temperature around 250 C during sulfiding. After 90 minutes of sulfiding, cut off H_2S-H_2 gas by closing the main valve on H_2S-H_2 bottle and valve #13.
5. Flush the system with nitrogen for 15 minutes by opening valves #5 and #6 and the main valve of nitrogen bottle. The nitrogen flow is set at 200 - 300 psig and 400 ml per minute.

Start-up Procedure

After the catalyst calcination and sulfiding are complete, the powerstats are turned up and the temperature is stabilized at about 10 C

lower than the desired operating temperature. At the same time, the feedstock is charged into the feed tank #23, the Ruska pump feed rate was set at the desired liquid flow rate of 30 ml per hour. Then the steps listed below are followed.

1. Charge the feedstock into Ruska pump by opening valve #4, and traverse the pump to suck the feed into pump.
2. Close valve #4 and open valves #2 and #3. Make sure valve #1 is closed.
3. Traverse the pump manually until the pressure of pump is 1500 psig.
4. Pressurize the reactor with H_2 to 1500 psig.
5. Open valve #1 and start the Ruska pump.
6. Adjust the hydrogen flow rate at 400 ml per minute by means of needle valve and bubble flow-meter.
7. Adjust the powerstats to get the desired reaction temperature.

Normal Operation

The system is considered to be under normal operation if the temperature and pressure are stable. A maximum variation of 20 psig in the pressure is tolerable. A temperature variation of 3 C along the reactor catalyst bed is deemed as normal temperature before the oil hits the catalyst.

After start-up, the temperature profile inside reactor and the temperature of heating block, pressure gauge reading, pump scale reading, off gas flow rate and hydrogen gas bottle pressure are recorded every one hour. The temperature profile inside the catalyst bed is measured at one inch intervals and recorded every hour.

Under normal operations, the reactor upstream pressure indicated by Heiss gauge should be equal to the downstream pressure monitored by pressure gauge #22. If the pressure indicated by gauge #22 keeps dropping, this would indicate a restricition in hydrogen flow, usually caused by reactor clogging. The depressurization of sample bomb #1 and #2 will generate large pressure differences between the upstream and downstream of the reactor which can sometimes open the clogging.

The system used in this study is operated manually. The throttle position of valves are important and should be checked right after start-up and after every sampling and refilling. A summary of the valve throttle positions during normal operation is given in Table I.

TABLE I

VALVE THROTTLE POSITION SUMMARY DURING NORMAL OPERATION

Position	Valve Number
Open	1, 2, 3, 5, 6, 8, 9, 19*, 20, 29, 32
Closed	4, 7, 10, 11, 12, 13, 14, 15, 16, 33

* Opened when measuring the hydrogen gas flow rate.

Sampling Procedure

After passing through the reactor, the liquid product is accumulated in bombs #1 and #2. Each bomb has a capacity of 300 ml. The product samples are taken every six hours. To minimize the possible operational disturbances due to sampling, the following procedure is followed:

1. Pressurize the sample bomb #3 with nitrogen by opening valves #10 and #11 and the main valve on nitrogen bottle. Close the valves #10 and #11 after the pressure is reached to 1200 psig.
2. Open valve #14 to let the liquid product to be transported from the bomb #1 to bomb #3. Once the pressure in bomb #3 reaches 1500 psig, close valve #14.
3. Depressurize bomb #3 by gradually opening valve #7 to vent the gases out to the atmosphere. Close valve #7 immediately when the pressure decreases to 1200 psig.
4. Open valve #15 to let the liquid product be transported from bomb #2 to bomb #3. Once the pressure in bomb #3 increases to 1500 psig, close valve #15.
5. Open valve #7 to relieve the pressure in bomb #3.
6. Purge the product with nitrogen gas. Open valves #10 and #11, adjust the nitrogen flow by means of the needle valve #11 and maintain the pressure in bomb #3 around 100 - 200 psig. Purge the sample with nitrogen for 20 minutes, then close valves #10 and #11.
7. When the pressure in bomb #3 drops to 20 psig, close valve #7. Place a sample jar under the collection port and open valve #16 to collect the sample.
8. Close valve #16 after sampling. Label and store the sample

for analysis.

Shutdown Procedure

The feed pump is switched off and valves #1 and #2 are closed. The reactor heating system is turned off and it is allowed to cool down. The hydrogen gas supply is cut off after 15 minutes, this hydrogen flow can blow the leftover oil out of the catalyst bed and prevent additional coke formation on the catalyst after shut-down. The pump is depressurized and the sampling procedure is followed to collect the last sample.

The reactor is depressurized and allowed to cool down to room temperature. Now the reactor can be removed by unscrewing the Swagelock fittings and pulling out the reactor from the heating block. The catalyst is then separated into top, middle and bottom sections and removed from the reactor. The products and spent catalysts are stored for analysis.

Sample Analysis

In this section, the catalyst characterization and product characterization will be explained. The measurements of pore volume, surface area, coke content and titanium content of spent catalyst are included in catalyst characterization. The methods for measuring the nitrogen, carbon, hydrogen, surlfur and titanium in the feedstock and the product oils, and the methods for ash content and distillation curve determination are presented under the product characterization.

Catalyst Characterization

The spent catalysts from the top, middle and bottom sections of the reactor are extracted with methyl iso-butyl ketone in a Soxhlet extraction unit for 72 hours. The complete removal of oil from the outer surface and from the catalyst pores are judged by the cleanliness of the extracted solvent. The washed catalysts are then dried and degassed at 121 C (250 F) for 6 hours. Now the catalysts are ready for measurements.

Surface Area Determination. Micromeritics Model 2100 D ORR Surface Area-Pore Volume analyzer is used for surface area measurement of the spent catalysts. The instrument is designed to obtain the nitrogen adsorption isotherm at liquid nitrogen temperatures. The surface area is then calculated from the B.E.T. plots.

The spent catalysts are first degassed at 300 C for 16 hours to ensure the removal of adsorbed gases and moisture from the catalyst surface. After samples are cooled down, the nitrogen adsorption isotherms are measured in the pressure ranges which results in a linear B.E.T. plot. The detailed procedures can be found in the Micrometeritics Instrument Corporation's instruction manual.

Pore Volume Determination. A Micromeritics Model 900/910 Series Mercury Penetration Porosimeter is used for the measurements of pore volume. The instrument indicates the quantities of a non-wetting liquid, mercury, that may be forced under various pressures into the pores of the catalysts.

The samples are placed in a glass cell in a high pressure chamber and degassed. The cell is filled with mercury. Under the increasing applied pressure, the penetration of mercury into the pores of samples results in a change of mercury level. A movable probe follows the mercury level to complete an electrical contact. The distance travelled by the probe is calculated to give the amount of mercury penetrated in the sample pores.

Coke Content Determination. The coke content in this study is defined as the weight percent of loss of carbonaceous material subjected to burning at a temperature of 500 C.

The catalyst samples are placed in glass flasks and degassed at 300 C and 0.1 μmHg for 16 hours to remove the adsorbed gases and moisture. The degassed samples are allowed to cool down to room temperature under vacuum. Helium gas is introduced into the flasks and samples are kept under a blanket helium gas at 760 mm Hg. The samples are weighed and recorded as the weight of flask and degassed sample.

The next step consists of removing the samples from the flasks and transfering them into a furnace at 500 C. The samples are kept in the furnace at 500 C for 72 hours to burn off the carbonaceous deposits. The burned samples are allowed to cool down to room temperature, and are transferred back into the same sample flasks. The same procedures for degassing, helium blanketing and weighing are followed. The weights of sample flasks under helium blanketing at 760 mm Hg are also measured. The amount of coke is calculated as follows:

$$\text{Wt\% Coke Content} = 100 \times [(W_2 - W_3)/(W_2 - W_1)]$$

where:

W_1 = Weight of sample flask,

W_2 = Weight of sample flask and degassed catlayst,

W_3 = Weight of sample flask and burned catalyst.

Titanium Content Determination. A Phillips X-ray Spectrometer PW 1410/70 equipped with XRG-3000 generator was used to measure the weight percent of titanium deposits on the spent catalysts. The principle of this method is that the analyte-line intensity $I_{A,M}$ from analyte A in a thick specimen having matrix M would be simple a function of weight fraction of A in M.

Several standards, consisting of similar ratios of alumina, molybdenum and nickel oxides as in the Shell 324 catalyst mixed with various concentrations of titanium oxide were prepared and used to prepare the calibration curve. The spent catalyst is grinded into powder and shaped into pellets. The titanium analyte-line intensity was measured in the pellets and compared with the calibration curve. This intensity can now be converted into weight percent of titanium in the spent catalyst.

Product Characterization

Nitrogen, Carbon and Hydrogen Analysis. The nitrogen, carbon and hydrogen analysis were done using a Model 240 Perkin-Elmer Elemental Analyzer. The system consists of a combustion furnace, reduction furnace and a detection system. In combustion furnace, the samples are combusted in a purified oxygen atmosphere catalyzed by magnesium oxide and silver tungstate. The produced combustion gases are carried through

the combustion tube packing by a purified helium gas, where sulfur oxides and halogens present in the combustion gases are removed by the combustion packing material. The gases are then carried through a reduction tube where nitrogen oxides are reduced to N_2. The gases coming out of the reduction tube contain water vapor, CO_2, N_2 and the carrier gas helium. These gases are then collected in a mixing volume at a constant temperature. After equilibrium is reached, the gases are swept through a series of gas traps and thermal conductivity cells.

The first gas trap containing magnesium perchlorate removes the water vapor. The difference in the thermal conductivity of sample before and after the removal of water vapor gives the concentration of water and hence the hydrogen content in the sample. Next, the dehydrated gases pass through a CO_2 trap and a similar thermal conductivity difference gives the carbon content. Finally, the remaining gases containing nitrogen and helium are passed through a conductivity cell, the thermal conductivity is compared with another cell through which only pure helium passes, the difference gives the nitrogen content.

Sulfur Analysis. A Leco Automatic Sulfur Analyzer was used to determine the sulfur content of the feed and product oils. This analysis is based on an ASTM combustion method E3065. The sulfur present in the sample is combusted in an atmosphere of purified oxygen in an inductive furnace, and is converted to SO_2. The SO_2 is then titrated with an acidic KIO_3 standard solution containing iodine with starch used as an indicator. The SO_2 decolorizes the solution resulting in the addition of KIO_3 solution from the buret. An

automatic titrator with a phototube circuit titrates automatically. The final point is indicated when no more titrant is added.

This whole system contains a Model 521-500 induction furnace, a Model 532-000 automatic titrator and an oxygen purifying train all manufactured by Leco. A detailed description of the procedure is given in the Leco manual.

Titanium Concentration Determination. A Perken-Elmer 403 double beam Atomic Absorption Spectrometer was used to measure the titanium concentration in the feeds and product oils. The sample solution is burned in a high temperature flame, where all the components present in the solution are converted to atomic vapor. A radiation from an external monochromatic line source is passed through the atomic vapor, and the attenuation of intensity by absorption of photons of the proper energy is measured.

The basic assumption of atomic absorption spectroscopic method is that the intensity of radiation emitted or absorbed is proportional to atomic concentration. Therefore, from the comparison of relative intensity values for standard solutions and unkown samples, the concentrations of unknown samples can be derived.

In determining the concentration of titanium in oils, the direct method of measurement is used. The sample is not ashed or transformed into acidic aqueous solution, but is diluted in methyl isobutyl ketone solvent, then subjected to metal measurement. A titanium-organic standard supplied by Continental Oil Company is used as organo-titanium standard, it is diluted with methyl isobutyl ketone to make standard solutions with titanium concentration below 150 ppm, in which range a

linear plot intensity versus concentration is obtained.

In determining the concentration of titanium in aqueous phase, the samples are subjected to analysis without further dilution.

Ash Content Determination. The procedure for ash content determination follows the ASTM method, as modified by Ahmed (16).

The routine procedure consists of the following steps:

1. Throughly clean the crucibles with concentrated HCL and distilled water.
2. Heat the crucibles to 775-800 C for 15 minutes in a furnace.
3. Allow the crucibles to cool down to room temperature and weight.
4. Weight the crucibles with 2-3 cc of sample oil.
5. Heat the crucibles in the furnace at the rate of about 200 C per hour.
6. Stabilize the temperature in the range of 775-800 C and maintain the temperature for one hour.
7. Allow the crucibles to cool down to room temperature and then weight.
8. Repeat steps 3 to 7 till there is no further change in the weight after repeated heating.

The ash content in the oil is calculated by:

$$\text{Wt\% Ash in Oil} = (W_f/W_i) \times 100$$

where W_f = final weight of residue left in the crucible, and

W_i = initial weight of the oil sample.

ASTM D1160 Distillation. The feed SRC light oil and a selective product oil samples from each experimental run have been fractionated following the ASTM D1160 procedure. Because of the low boiling point range of SRC light oil, all distillations were performed at atmospheric pressure. The vapor temperature at the end of the collection of every 10 ml of distillate, the volume of residue and the loss were recorded.

The distillation curves are used to characterize the oil samples, which can be a good indication for the extent of cracking during the hydrotreatment. Since ASTM D1160 is a well known standard method, the details of procedure will not be given here.

CHAPTER IV

EXPERIMENTAL RESULTS

The results of experimental runs will be presented in this chapter, while the discussion of these results will be left to the next chapter. During this project a total of twelve experimental runs were made which are labeled as TME #1 through TME #12. In all these experiments, SRC light oil was hydrotreated in a trickle bed reactor.

In reference to the literature cited in Chapter II, all experimental runs were conducted at a pressure of 10.4 MPa (1500 psig) and a nominal temperature of 375 C (707 F), a liquid volume hourly space time (LVHST) of 0.58 hour and hydrogen to oil ratio of 1425 Standard m^3H_2/m^3 oil (8,000 SCF/Bbl).

Except for the runs TME #7 and #11 which were conducted over glass beads, the rest of the runs used Shell 324 as the catalyst. Run TME #5 was the reference run using undoctored SRC light oil. The rest of the runs were SRC light oil doctored with different concentrations of titanocene dichloride. The concentrations of titanium in these doctored oils were 50, 100, 200 and 400 ppm.

The properties of SRC light oil and those of Shell 324 catalyst are given in Tables II and III. The detailed operational conditions of individual runs are described below:

TABLE II

PROPERTIES OF SRC LIGHT OIL

1. Density at 24 C (75 F): 934 kg/m^3

2. Elemental composition, wt%

C	:	79.84
H	:	9.77
N	:	0.41
S	:	0.36
O	:	9.62 (by balance)
H/C atom ratio	:	1.47
Ash content	:	0.00
H_2O content	:	1.00

3. Normal boiling point

	C		F
IBP (Vol%)	88		190
10	172		341
20	176		349
30	179		354
40	181		358
50	183		361
60	184		363
70	187		369
80	189		372
90	194		381
End Point	199		390
Recovery		98	
Residue		1	
Loss		1	

TABLE III

PROPERTIES OF SHELL 324 CATALYST

Chemical Composition wt%		
NiO		3.4
MoO_3		19.3
Physical Properties		
Geometry		1.6 mm (1/16") extrudate
Surface area, m^2/kg		146×10^3
Pore volume, m^3/kg		4.2×10^{-4}
Most frequent pore diameter, nm		11.8
Pore size distribution, % pore volume in pore diameter, nm		%
3.5 - 7.0		12
7.0 - 10.0		21
10.0 - 15.0		57
15.0 - 20.0		2
20.0 - 40.0		1
40.0 - 60.0		1
60.0		6
	Total	100

Run TME #1

The purpose of run TME #1, using SRC light oil as the feedstock, was to evaluate the HDS, HDN, HDO and hydrogenation activities of catalyst Shell 324. Also, this run was intended to serve as the reference run for comparison with the rest of the runs which used SRC light oil doctored with titanocene dichloride as feedstock. Unfortunately, right after the start-up, the feed pump failed to charge the feed oil into the reactor at the desired rate (30 ml per hour). Therefore the run was terminated after 24 hours of operation with no useful results.

Run TME #2

The feedstock in this run was SRC light oil blended with enough titanocene dichloride to form a titanium concentration of 400 ppm. The packing of reactor was a 5-inch layer of glass beads on top of an 8-inche catalyst bed. An 11-inch layer of glass beads was packed under the catalyst bed.

After 18 hours of operation, the pressure gauge #22, located downstream from the reactor, indicated a continuous pressure drop. An attempt to remove the clogging by an increase in the pressure differential was unsuccessful. The reactor got completely plugged at 29th hour of operation with pressure gauge #22 dropping to zero. At this time the system was shut down.

The reactor was removed from the system and cut into 10 sections. The clogging was found to be located at the top glass beads packing

section. It was 3.25 inches long, and located 1.75 inches above the catalyst bed. No clogging was observed inside the catalyst bed or in the bottom glass beads packing section.

The interaction of titanocene dichloride and glass beads was suspected to have caused the clogging. The removal of glass beads appeared to be a solution to the clogging problem. However, to ensure adequate distribution of oil over the catalyst, it was decided to reduce the length of the top layer of glass beads to one inch. The bottom glass beads packing was removed and replaced by an empty 3/8-inch O.D. stainless steel tube as a support for the catalyst bed.

Run TME #3

A modified reactor packing arrangement, as shown in Figure 4, was employed in this run to eliminate the possible reactor clogging. Other run conditions followed those of run TME #2.

At 15th hour of operation, the reactor downstream pressure, as indicated by pressure gauge #22, started to decrease, and within 8 hours the pressure gauge #22 reached zero, indicating a complete clogging.

The system was shut down and after cooling, the reactor was cut into 6 pieces. The clogging was observed to have occurred right in the glass beads. Again, no clogging inside the catalyst bed or in the bottom support tube was observed.

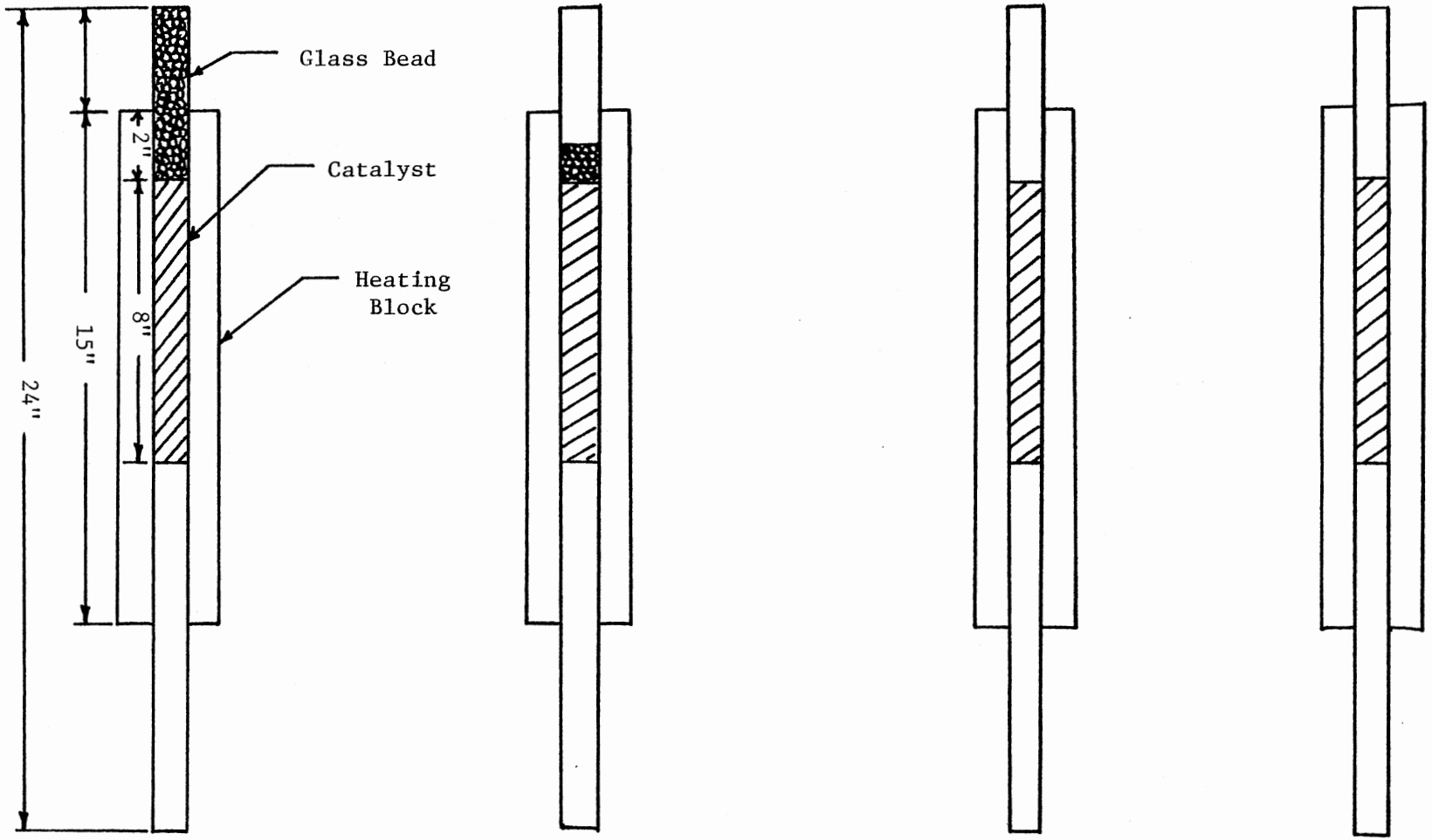

Figure 4. Reactor Packing

Run TME #4

The glass beads were completely removed from the packing arrangement of this reactor as shown in Figure 3. Other run conditions were same as in the previous two runs. After 30 hours of operation, a pressure difference across the reactor started to develop. Flushing of the reactor with hydrogen flow by generating a large pressure differential removed the clogging temporarily. By occasional flushings, the run continued for 66 hours.

The reactor tube was later cut into pieces and examined. It was observed that a 2-inch long black granular material had accumulated above the catalyst bed. This material had strongly bound the catalyst pellets together and to the reactor wall. Obviously, this material had caused the partial clogging of the reactor and had restricted the hydrogen flow.

From the comparison of the reactor packings used in TME #2, #3, and #4, the titanocene dichloride seemed to have had deterimental effects on the reactor clogging, and that the glass beads accelerated the clogging. The clogging material was later analyzed and found to contain high contents of titanium and nitrogen.

The flushing of reactor with hydrogen temporarily reduces the residence time of oil in the catalyst bed, thus downgrading the quality of product oils.

Runs TME #5, #6, #8, #9, #10, and #12

These six runs used the same reactor packings as was used in the TME #4. TME #5, using undoctored SRC ligh oil as feedstock, worked

as a reference run for comparing with other runs. TME #6, #8, #9, #10 and #12 used SRC light oil doctored with nominal concentrations of 100, 50, 200, 100 and 200 ppm of titanium respectively.

TME #6 and #10 were duplicate runs to test the experimental reproducibility. TME #9 and #12 also have the same operating conditions except that the temperature of TME #9 is 10 C lower than that of TME #12. The temperature effect may be observed from these two runs.

All runs were scheduled to have durations of 66 hours, but the failure of rupture disk during TME #8 resulted in its premature shutdown after 54 hours of operation.

Runs TME #7 and #11

The purpose of these two runs is to test the effects of titanocene dichloride on the hydrotreatment of SRC light oil in the absence of catalyst. In order to exclude the interaction between catalyst and titanocene dichloride, the catalyst Shell 324 was replaced by glass beads.

SRC light oil doctored with 100 ppm of titanium as titanocene dichloride was used as feedstock in TME #7. No titanocene dichloride was added in TME #11. The experimental conditions in these two runs were the same as they are in the other runs.

Experimental Data

The complete tabulated data for runs TME #2 through TME #12 are given in Tables IV through XVIII. The data analysis will include the hydrogenation, hydrodesulfurization, hydrodenitrogenation,

TABLE IV

RESULTS FROM RUNS TME 2, 3 WITH SHELL 324 CATALYST FEEDSTOCK:
SRC LIGHT OIL + 400 PPM TITANIUM
(AS TITANOCENE DICHLORIDE)

Sample Number	Hrs on Oil	Wt% S	%S Removal	Wt% N	%N Removal	ppm[a] Ti	%Ti Removal	H/C Atom Ratio
TME 2-1	6	0.09	75.0	0.090	77.5	0	100	1.890
TME 2-2	12	0.05	86.1	0.050	87.5	0	100	1.895
TME 2-3	18	0.04	88.9	0.040	90.0	0	100	1.867
TME 2-4	24	0.26	26.9	0.263	34.3	2.2	99.5	1.662
TME 2-5	30	0.31	11.9	0.317	20.8	0.9	99.8	1.513
TME 3-1	6	--	--	0	100	0	100	1.849
TME 3-2	12	--	--	0.010	97.1	0	100	1.860
TME 3-3	18	--	--	0.070	80.0	0	100	1.755
TME 3-4	24	--	--	0.110	68.6	0	100	1.688

a. Ti concentration is measured by atomic absorption spectrometer.

TABLE V

RESULTS FROM RUN TME 4 WITH SHELL 324 CATALYST FEEDSTOCK:
SRC LIGHT OIL + 400 PPM TITANIUM
(AS TITANOCENE DICHLORIDE)

Sample Number	Hrs[a] On Oil	Wt%[b] S	%S[c] Removal	Wt%[b] N	%N[c] Removal	ppm Ti	%Ti[c] Removal	H/C Atom Ratio	Aqueous[d] Phase (ml)
TME 4-1	6	0.23	30.3	--	--	27.0	93.3	--	11
TME 4-2	12	0.03	91.8	0.131	65.5	0	100	1.614	13
TME 4-3	18	0.01	97.0	0.098	75.8	0	100	1.800	14
TME 4-4	24	0.01	97.0	0.104	72.4	6.2	98.5	1.804	14
TME 4-5	30	0.04	87.9	0.215	56.6	9.1	97.7	1.737	10
TME 4-6	36	0.04	93.9	0.141	62.9	5.8	98.6	1.616	12
TME 4-7	42	0.04	87.9	0.182	52.1	5.8	98.6	1.647	11
TME 4-8	48	0.01	97.0	0.224	41.1	7.1	98.2	1.715	11
TME 4-9	54	0.01	97.0	0.264	30.5	5.1	98.7	1.705	8
TME 4-10	60	0.03	91.8	0.317	16.6	9.2	97.7	1.666	6
TME 4-11	66	--	--	---	--	8.4	97.9	---	5

a. Total hours which the catalyst has been contacted with oil at reaction temperature.
b. Percent of sulfur, nitrogen in liquid product.
c. % Removal = 100 x (fraction in feed less fraction in product)/(fraction in feed).
d. Volume of aqueous phase in product sample.

TABLE VI

RESULTS FROM RUN TME 5 WITH SHELL 324 CATALYST
FEEDSTOCK = SRC LIGHT OIL

Sample Number	Hrs[a] On Oil	Wt%[b] S	%S[c] Removal	Wt%[b] N	%N[c] Removal	ppm Ti	%Ti[c] Removal	H/C Atom Ratio	Aqueous[d] Phase (ml)
TME 5-1	6	0.07	81.6	0.153	59.7	0	0	1.636	9.0
TME 5-2	12	0.07	81.6	0.162	57.9	0	0	1.650	8.0
TME 5-3	18	0.08	79.0	0.164	56.8	0	0	1.615	7.0
TME 5-4	24	0.06	84.2	0.166	56.3	0	0	1.633	7.0
TME 5-5	30	0.08	79.0	0.168	55.8	0	0	1.617	7.0
TME 5-6	36	0.06	84.2	0.188	50.5	0	0	1.616	7.0
TME 5-7	42	0.10	74.0	0.227	40.3	0	0	1.622	6.0
TME 5-8	48	0.05	86.8	0.233	38.7	0	0	1.580	4.5
TME 5-9	54	0.04	89.5	0.264	30.5	0	0	1.540	4.5
TME 5-10	60	0.03	92.1	0.224	41.1	0	0	1.585	4.0
TME 5-11	66	0.05	86.8	0.263	30.8	0	0	1.612	4.0

a. Total hours which the catalyst has been contacted with oil at reaction temperature.
b. Percent of sulfur, nitrogen in liquid product.
c. % Removal = 100 x (fraction in feed less fraction in product)/(fraction in feed).
d. Volume of aqueous phase in product sample.

TABLE VII

RESULTS FROM RUN TME 6 WITH SHELL 324 CATALYST FEEDSTOCK:
SRC LIGHT OIL + 100 PPM TITANIUM
(AS TITANOCENE DICHLORIDE)

Sample Number	Hrs[a] On Oil	Wt%[b] S	%S[c] Removal	Wt%[b] N	%N[c] Removal	ppm Ti	%Ti[c] Removal	H/C Atom Ratio	Aqueous[d] Phase (ml)
TME 6-1	6	0.07	81.6	0.014	96.3	0	100	1.836	14.0
TME 6-2	12	0.02	94.8	0.025	93.4	0	100	1.898	17.5
TME 6-3	18	0.09	78.0	0.030	93.1	0	100	1.879	16.5
TME 6-4	24	0.14	63.2	0.020	94.7	0	100	1.877	16.5
TME 6-5	30	0.13	65.8	0.023	93.9	0	100	1.856	16.5
TME 6-6	36	0.00	100	0.051	86.6	0	100	1.880	16.5
TME 6-7	42	0.05	86.8	0.040	89.5	0	100	1.836	16.5
TME 6-8	48	0.03	92.1	0.048	87.4	0	100	1.825	16.0
TME 6-9	54	0.07	81.6	0.042	88.9	0	100	1.828	16.0
TME 6-10	60	0.02	96.8	0.044	88.4	0	100	1.815	16.0
TME 6-11	66	0.15	60.5	0.028	92.6	0	100	1.772	16.0

a. Total hours which the catalyst has been contacted with oil at reaction temperature.
b. Percent of sulfur, nitrogen in liquid product.
c. % Removal = 100 x (fraction in feed less fraction in product)/(fraction in feed).
d. Volume of aqueous phase in product sample.

TABLE VIII

RESULT FROM RUNS TME 7 AND 11 WITH GLASS BEAD PACKINGS FEEDSTOCK FOR TME 7:
SRC LIGHT OIL + 100 PPM TITANIUM (AS TITANOCENE DICHLORIDE)
FEEDSTOCK FOR TME 11 = SRC LIGHT OIL

Sample Number	Hrs[a] On Oil	Wt%[b] S	%S[c] Removal	Wt%[b] N	%N[c] Removal	Wt%[b] H	Wt%[b] C	Wt%[b,d] O
TME 7-1	6	0.08	78.9	0.36	12.2	9.57	81.96	8.03
TME 7-2	12	0.10	73.7	0.31	24.4	9.83	82.75	7.01
TME 7-3	18	0.12	68.4	0.32	22.0	9.84	82.66	7.06
TME 7-4	24	0.12	68.4	0.33	19.5	9.73	82.71	7.11
TME 11-1	6	0.28	26.3	0.35	14.6	9.94	79.35	10.08
TME 11-2	12	0.27	28.9	0.31	24.4	9.86	79.70	9.86
TME 11-3	18	0.28	26.3	0.31	24.4	9.67	79.83	9.91
TME 11-4	24	0.28	26.3	0.32	22.0	9.75	79.80	9.85

a. Total hours which the catalyst has been contacted with oil at reaction temperature.
b. Percent of sulfur, nitrogen, carbon, hydrogen and oxygen in liquid product.
c. % Removal = 100 x (fraction in feed less fraction in product)/(fraction in feed).
d. Wt% O = 100 - Wt% (S + N + C + H).

TABLE IX

RESULTS FROM RUN TME 8 WITH SHELL 324 CATALYST FEEDSTOCK:
SRC LIGHT OIL + 50 PPM TITANIUM
(AS TITANOCENE DICHLORIDE)

Sample Number	Hrs[a] On Oil	Wt%[b] S	%S[c] Removal	Wt%[b] N	%N[c] Removal	ppm[b] Ti	%Ti[c] Removal	H/C Atom Ratio	Aqueous[d] Phase (ml)
TME 8-1	6	0.04	89.5	0.025	93.9	1	98.1	1.853	15.0
TME 8-2	12	0.08	78.9	0.025	93.9	2	96.2	1.855	17.5
TME 8-3	18	0.09	76.3	0.040	90.2	2	96.2	1.831	17.0
TME 8-4	24	0.16	57.9	0.041	90.0	2	96.2	1.796	16.5
TME 8-5	30	0.05	86.8	0.046	88.8	1	98.1	1.806	16.5
TME 8-6	36	0.14	63.2	0.050	87.8	1	98.1	1.804	16.5
TME 8-7	42	0.14	63.2	0.039	90.5	2	96.2	1.814	16.5
TME 8-8	48	0.11	71.1	0.043	89.5	2	96.5	1.809	16.5

a. Total hours which the catalyst has been contacted with oil at reaction temperature.
b. Percent of sulfur, nitrogen and titanium in liquid product.
c. % Removal = 100 x (fraction in feed less fraction in product)/(fraction in feed).
d. Volume of aqueous phase in product sample.

TABLE X

RESULTS FROM RUN TME 9 WITH SHELL 324 CATALYST FEEDSTOCK:
SRC LIGHT OIL + 200 PPM TITANIUM
(AS TITANOCENE DICHLORIDE)

Sample Number	Hrs[a] On Oil	Wt%[b] S	%S[c] Removal	Wt%[b] N	%N[c] Removal	ppm[b] Ti	%Ti[c] Removal	H/C Atom Ratio	Aqueous[d] Phase (ml)
TME 9-1	6	0.01	97.0	0.154	62.4	3	98.4	1.652	8.0
TME 9-2	12	0.00	100.0	0.160	60.9	3	98.4	1.631	9.0
TME 9-3	18	0.01	97.0	0.171	58.5	2	99.0	1.613	8.0
TME 9-4	24	0.02	94.6	0.185	54.9	3	98.4	1.597	8.0
TME 9-5	30	0.05	86.8	0.165	59.8	4	97.9	1.610	7.0
TME 9-6	36	0.07	81.6	0.175	57.3	3	98.4	1.595	7.0
TME 9-7	42	0.03	92.1	0.207	49.5	3	98.4	1.586	6.0
TME 9-8	48	0.06	84.2	0.231	43.7	4	97.9	1.580	6.0
TME 9-9	54	0.06	84.2	0.211	48.5	2	99.0	1.583	6.0
TME 9-10	60	0.05	86.8	0.181	55.9	4	97.9	1.600	6.0
TME 9-11	66	0.07	81.6	0.162	60.5	4	97.9	1.609	6.5

a. Total hours which the catalyst has been contacted with oil at reaction temperature.
b. Percent of sulfur, nitrogen and titanium in liquid product.
c. % Removal = 100 x (fraction in feed less fraction in product)/(fraction in feed).
d. Volume of aqueous phase in product sample.

TABLE XI

RESULTS FROM RUN TME 10 WITH SHELL 324 CATALYST FEEDSTOCK:
SRC LIGHT OIL + 100 PPM TITANIUM
(AS TITANOCENE DICHLORIDE)

Sample Number	Hrs[a] On Oil	Wt%[b] S	%S[c] Removal	Wt%[b] N	%N[c] Removal	ppm[b] Ti	%Ti[c] Removal	H/C Atom Ratio	Aqueous[d] Phase (ml)
TME 10-1	6	0.07	81.6	0.034	91.7	1	99.0	1.845	15.0
TME 10-2	12	0.04	89.5	0.046	88.8	2	98.1	1.844	17.5
TME 10-3	18	0.05	86.8	0.035	91.5	2	98.1	1.872	17.0
TME 10-4	24	0.05	86.8	0.036	91.2	1	99.0	1.853	16.5
TME 10-5	30	0.03	92.1	0.040	90.2	2	98.1	1.834	16.5
TME 10-6	36	0.04	89.5	0.035	91.5	1	99.0	1.837	16.5
TME 10-7	42	0.06	84.2	0.044	89.3	2	98.1	1.831	16.5
TME 10-8	48	0.06	84.2	0.039	90.5	2	98.1	1.822	16.0
TME 10-9	54	0.05	86.8	0.034	90.7	2	98.1	1.827	16.0
TME 10-10	60	0.07	81.6	0.046	88.8	1	99.0	1.820	16.0
TME 10-11	66	0.07	81.6	0.062	84.9	1	99.0	1.792	16.0

a. Total hours which the catalyst has been contacted with oil at reaction temperature.
b. Percent of sulfur, nitrogen and titanium in liquid product.
c. % Removal = 100 x (fraction in feed less fraction in product)/(fraction in feed).
d. Volume of aqueous phase in product sample.

TABLE XII

RESULTS FROM RUN TME 12 WITH SHELL 324 CATALYST FEEDSTOCK:
SRC LIGHT OIL + 200 PPM TITANIUM
(AS TITANOCENE DICHLORIDE)

Sample Number	Hrs[a] On Oil	Wt%[b] S	%S[c] Removal	Wt%[b] N	%N[c] Removal	ppm[b] Ti	%Ti[c] Removal	H/C Atom Ratio	Aqueous[d] Phase (ml)
TME 12-1	6	0.02	94.7	0.046	88.8	2	99.0	1.846	15.0
TME 12-2	12	0.05	86.8	0.020	95.1	2	99.0	1.899	17.5
TME 12-3	18	0.02	94.7	0.033	91.9	2	99.0	1.886	17.0
TME 12-4	24	0.07	81.6	0.030	92.7	2	99.0	1.871	17.0
TME 12-5	30	0.06	84.2	0.033	91.9	3	98.5	1.866	16.5
TME 12-6	36	0.07	81.6	0.037	91.0	2	99.0	1.848	16.5
TME 12-7	42	0.05	86.8	0.040	90.2	3	98.4	1.843	16.5
TME 12-8	48	0.05	86.8	0.050	87.8	2	99.0	1.812	15.5
TME 12-9	54	0.06	84.2	0.040	90.2	2	99.0	1.839	16.0
TME 12-10	60	0.04	89.5	0.042	89.8	2	99.0	1.830	16.0
TME 12-11	66	0.08	79.9	0.043	89.5	1	99.5	1.816	16.0

a. Total hours which the catalyst has been contacted with oil at reaction temperature.
b. Percent of Sulfur, nitrogen and titanium in liquid product.
c. % Removal = 100 x (fraction in feed less fraction in product)/(fraction in feed).
d. Volume of aqueous phase in product sample.

TABLE XIII

ANALYSIS OF SPENT CATALYST

Sample Number	Zone in Catalyst Bed	Surface Area 10^{3} M^2/Kg	Pore Volume 10^{-3} M^2/Kg	Ti[a] (Wt%)	Coke Content (Wt%)
TME 2	Top	110	0.219	0.056	*
	Middle	110	0.190	0.004	*
	Bottom	115	0.196	0.000	*
TME 3	Top	115	0.260	2.560	*
	Middle	119	0.202	0.060	*
	Bottom	139	0.209	0.000	*
TME 4	Top	141	0.268	1.640	11.84
	Middle	131	0.236	0.460	4.70
	Bottom	115	0.210	0.070	0.78
TME 5	Top	138	0.221	0.000	11.40
	Middle	119	0.287	0.000	11.90
	Bottom	135	0.363	0.000	6.46
TME 6	Top	*	*	*	*
	Middle	112	0.342	0.040	7.70
	Bottom	127	0.268	0.000	5.30
TME 8	Top	*	*	*	*
	Middle	125.10	0.320	0.070	6.80
	Bottom	139.70	0.313	0.000	6.20
TME 9	Top	103.64	0.298	0.010	11.70
	Middle	130.29	0.344	0.360	8.30
	Bottom	128.25	0.316	0.090	7.00
TME 10	Top	120.92	0.286	0.750	11.50
	Middle	134.02	0.305	0.040	7.80
	Bottom	118.58	0.291	0.000	5.60
TME 12	Top	130.13	0.285	1.060	11.00
	Middle	125.12	0.315	0.480	7.90
	Bottom	134.02	0.364	0.110	3.40

a. Ti concentration is analyzed by Phillips X-ray Spectrometer PW1410/70 equipped with XRG-300 generator.

*. Measurement not available.

TABLE XIV

TITANIUM CONCENTRATION IN AQUEOUS PHASES[a]

Sample Number	TME 8 (ppm)	TME 9 (ppm)	TME 10 (ppm)	TME 12 (ppm)
1	3	4	2	5
2	4	4	3	5
3	4	4	3	4
4	5	5	2	4
5	3	4	2	3
6	3	3	3	5
7	4	4	3	6
8	4	5	3	4
9		4	3	4
10		4	2	5
11		4	3	3

a. Determined by Atomic Absorption Spectrometer.

TABLE XV

TITANIUM CONCENTRATION IN FEED OILS

Run Number	Nomial Concentration	Measured Concentration[a]
TME 4	400 ppm	387 ppm
TME 6	100 ppm	87 ppm
TME 7	100 ppm	93 ppm
TME 8	50 ppm	52 ppm
TME 9	200 ppm	192 ppm
TME 10	100 ppm	104 ppm
TME 12	200 ppm	206 ppm

a. Determined by Atomic Absorption Spectrometer.

TABLE XVI

TITANIUM CONTENT IN CARBONACEOUS DEPOSITED MATERIALS

Run Number	Titanium wt%[a]	Run Number	Titanium wt%[a]
TME 4	3.63	TME 9	3.23
TME 6	3.43	TME 10	3.15
TME 8	3.71	TME 12	3.52

a. By X-ray spectrometer

TABLE XVII

CHEMICAL COMPOSITION OF CARBONACEOUS DEPOSITED MATERIALS

Sample Number	Ti[a] Wt%	C Wt%	H Wt%	N Wt%
TME 2	3.02	66.0	7.70	4.86
TME 4	3.63	61.6	3.87	3.75

a. By X-ray spectrometer.
Note: The numbers do not add up to 100%. The balance may contain oxygen, sulfur, or chloride which were not analyzed directly.

TABLE XVIII

DISTILLATION DATA

Vol %	TME 4 Sample #3		TME 5 Sample #3		TME 6 Sample #3	
	C	F	C	F	C	F
IBP	96	205	75	167	92	197
10	107	224	82	180	102	216
20	114	238	140	284	106	223
30	118	245	167	333	116	241
40	158	316	174	346	144	292
50	174	345	178	353	174	345
60	181	358	181	358	184	363
70	187	369	184	364	188	371
80	194	381	189	373	193	380
90	204	399	197	386	207	405
END POINT	211	412	208	407	214	418
Recovery	98		98		98	
Residue	1		1		1	
Loss	1		1		1	

TABLE XVIII (Continued)

Vol%	TME 7 Sample #3		TME 8 Sample #3		TME 9 Sample #3	
	C	F	C	F	C	F
IBP	89	193	95	203	73	163
10	169	336	109	217	85	185
20	174	345	110	230	115	240
30	179	354	117	243	165	329
40	181	358	125	257	173	343
50	183	361	154	309	179	354
60	185	365	180	356	183	361
70	187	369	188	370	189	372
80	189	372	195	383	192	377
90	192	378	203	397	194	381
END POINT	199	390	205	401	208	407
Recovery	98		98		98	
Residue	1		1		1	
Loss	1		1		1	

TABLE XVIII (Continued)

Vol%	TME 10 Sample #3		TME 11 Sample #3		TME 12 Sample #3	
	C	F	C	F	C	F
IBP	88	190	60	140	88	190
10	95	203	79	175	101	214
20	105	221	135	275	109	228
30	117	243	174	345	114	237
40	129	264	179	354	120	248
50	157	315	182	360	150	302
60	179	354	184	363	178	352
70	190	374	187	369	187	369
80	197	387	189	372	194	381
90	206	403	193	379	203	397
END POINT	215	419	202	396	212	414
Recovery	98		98		98	
Residue	1		1		1	
Loss	1		1		1	

hydrodeoxygenation, coke content, titanium deposition, surface area, pore volume, titanium removal and ASTM distillation. Due to the different reactor packings and reactor clogging problems in TME #2 and #3, these two runs will not be included in the data analysis.

Hydrogenation Activity

In the hydrotreatment process, the unsaturated compounds are hydrogenated resulting in an increase in the hydrogen content of the oil, which may also be observed as an increase in the hydrogen-to-carbon ratio of the oil.

For runs TME #7 and #11, the variations of the hydrogen contents as a function of time on oil is given in Figure 5. It indicates that in the absence of the Shell 324 catalyst, the galss beads show no significant hydrogenation activity. Also, it can be concluded that the addition of titanocene dichloride to the feedstock did not affect the hydrogen content.

To determine the effects of titanocene dichloride on catalytic hydrotreatment, the hydrogen-to-carbon atom ratio of product oil samples from sample #3 of runs TME #4, #5, #6, #8, #10 and #12 are plotted against the concentrations of titanocene dichloride in feed oils. Figure 6 shows this plot. It shows that the addition of titanocene dichloride improves the hydrogenation activities of the catalyst. The best hydrogenation is achieved when the titanium concentration in the feedstock is between 100 and 200 ppm.

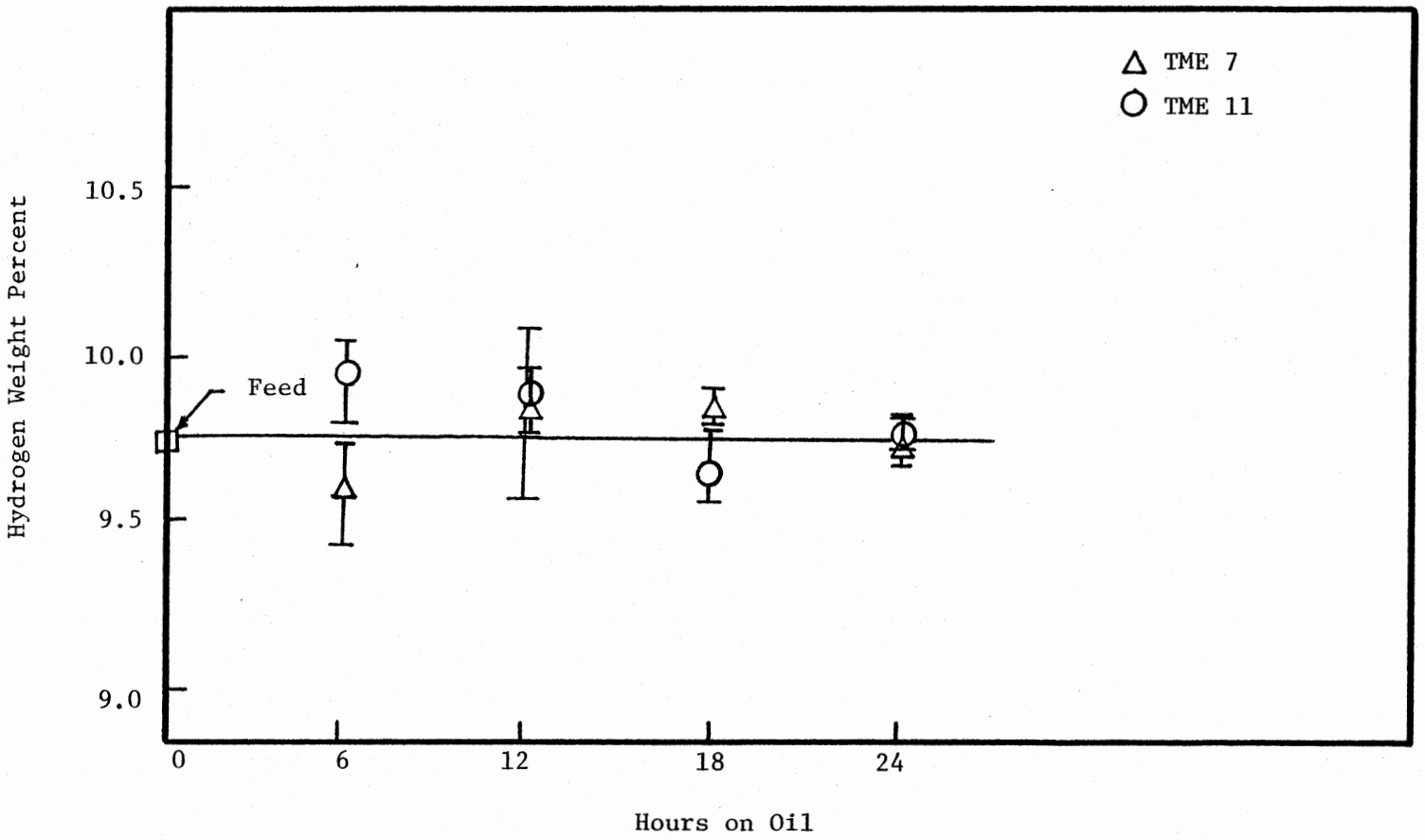

Figure 5. Hydrogen Weight Percent as a Function of Hours on Oil for Runs TME 7 & 11

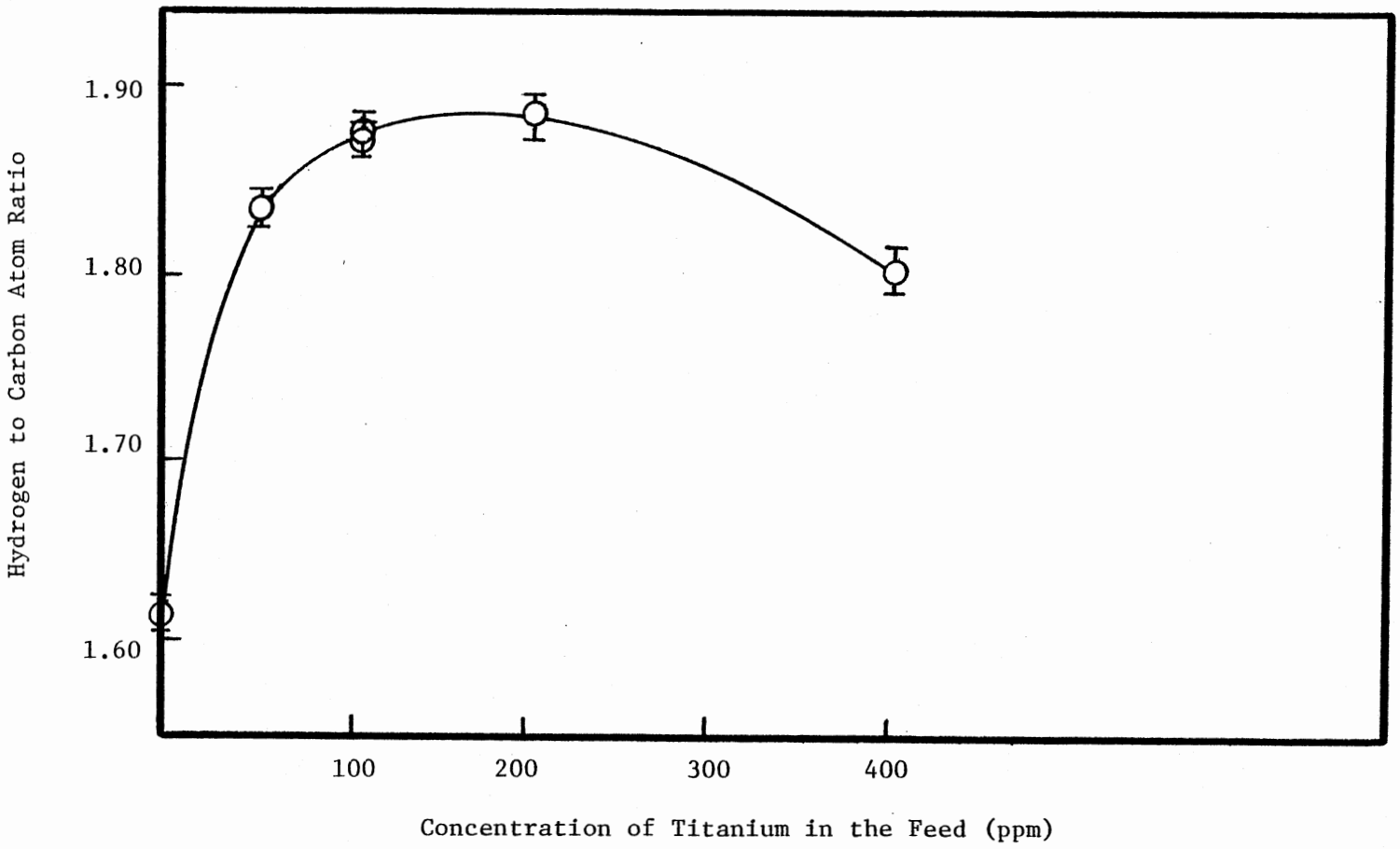

Figure 6. Hydrogenation Activity as a Function of Concentration of Titanium in the Feed (Hours on Oil = 18)

Hydrodesulfurization Activity

Figure 7 shows that the sulfur weight percent in product oils for TME #7 and #11 versus the time on oil. There are about 0.30 wt% of sulfur remaining in the product oils of the TME #11. In other words, partial removal of sulfur can be achieved even in the absence of catalyst. Figure 7 also indicates that an enhanced removal of sulfur is achieved if titanocene dichloride was added to the feedstock.

The sulfur content data for the catalytic hydrotreatment runs are somewhat scattering but a general trend of improved sulfur removal with an increase of titanium addition can be observed. A plot of weight percent sulfur removal versus the titanium concentrations in feed oils is given in Figure 8. Again, only the sample #3 of runs TME #4, #5, #6, #8, #10, #12 are included in this plot.

Hydrodeoxygenation Activity

The aqueous phase produced in the hydrotreated product oils is a good indicator of hydrodeoxygentaion. Figure 9 is a plot of the volume of aqueous phase versus the titanium concentration in the feedstocks. It shows that the hydrodeoxygenation activity is enhanced by the addition of titanocene dichloride. The highest activity is also found around 200 ppm of titanium.

The hydrodeoxygenation activity can also be estimated by the oxygen contents in the product oils. The oxygen content is calculated from the balance of weight percent of C, H, N and S in the oils. No aqueous phase was observed in runs TME #7 and #11. A plot of the variations of the oxygen contents as a function of time on oil for these two runs

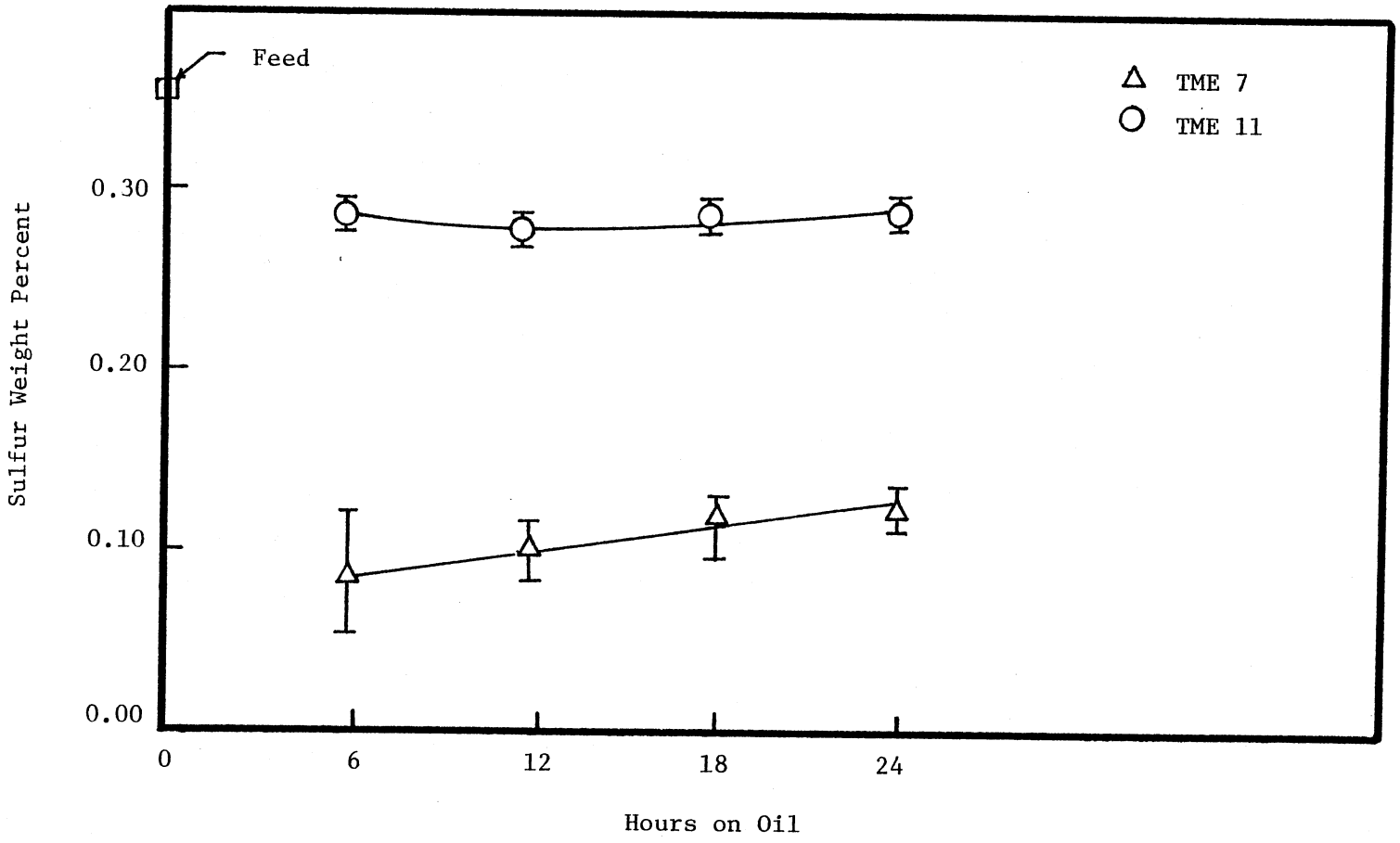

Figure 7. Sulfur Weight Percent as a Function of Hour on Oil for Runs TME 7 & 11

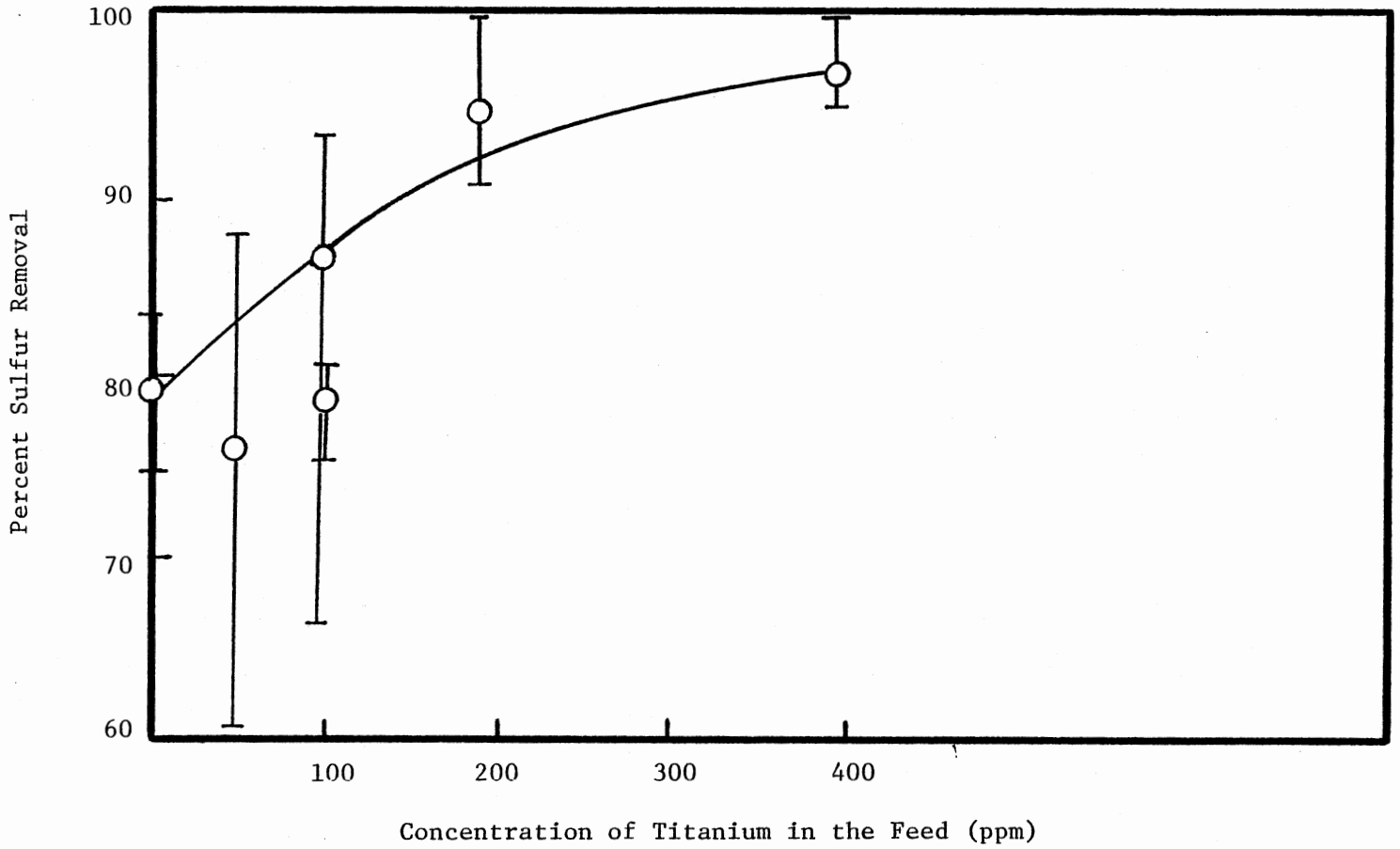

Figure 8. Hydrodesulfurization Activity as a Function of Concentration of Titanium in the Feed (Hours on Oil = 18)

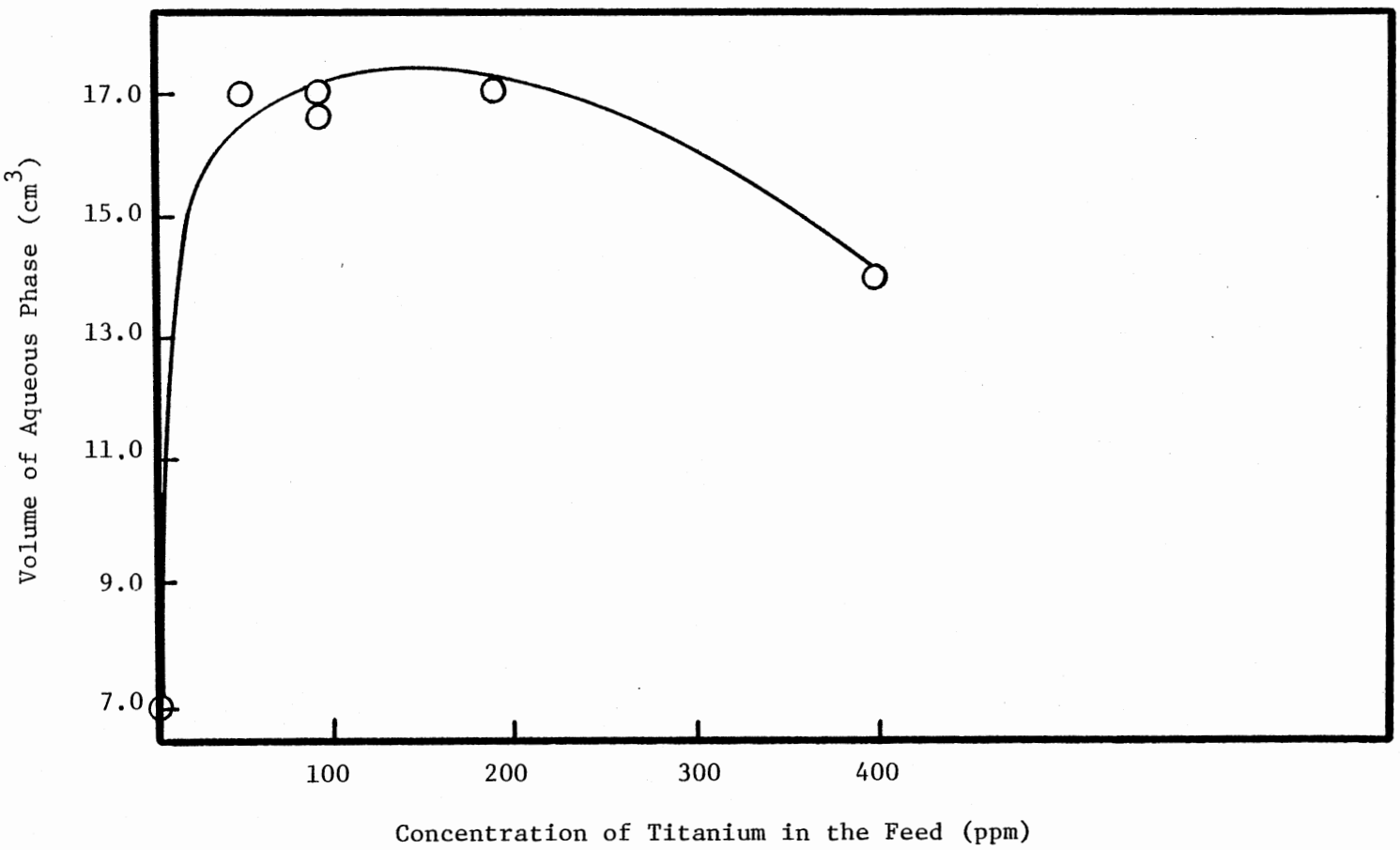

Figure 9. Volume of Aqueous Phase as a Function of Concentration of Titanium in the Feed (Hours on Oil = 18)

is given in Figure 10. Obviously, the oxygen contents in product oils of run TME #7, which used titanocene dichloride doctored feedstock, are lower than that of run TME #11.

In non-catalytic hydrotreatment, some hydrocarbons might be hydrotreated into light hydrocarbon gases and removed with effluent gases. This results in a decrease in the total weight of liquid product oil. Consequently, if the heteroatom containing compounds stay unreacted, their weight percent will appear to have increased. This explains the apparent increase in the oxygen contents of product oils in run TME #11.

Hydrodenitrogenation Activity

The nitrogen weight percent in product oils versus time on oil for runs TME #7 and #11 are shown in Figure 11. Comparable nitrogen removals are observed for these two runs. Obviously, in the absence of catalyst the titanocene dichloride did not enhance the nitrogen removal.

In catalytic hydrotreatments, the titanocene dichloride is shown to improve the hydrodenitrogenation activity significantly. The plot of percent nitrogen removal versus the titanium concentrations in the feed oils is given in Figure 12. The hydrodenitrogenation activity is more or less following the same trend as hydrogenation and hydrodeoxygenation activities.

Titanium Removal and Deposition

The precise titanium concentrations in the oils are measured by Atomic Absorption Spectroscopy. The nominal titanium concentrations

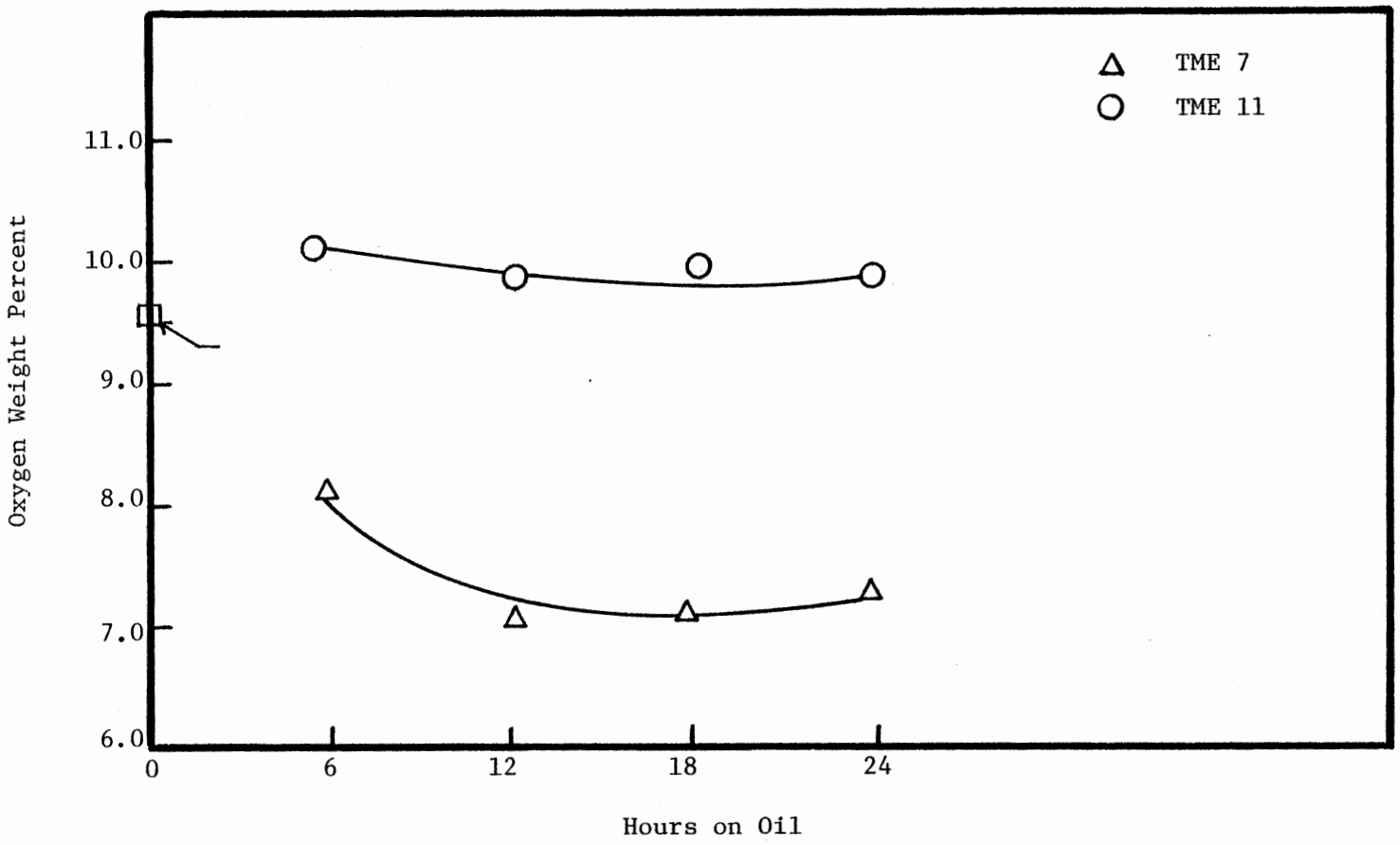

Figure 10. Oxygen Weight Percent as a Function of Hours on Oil for Runs TME 7 & 11

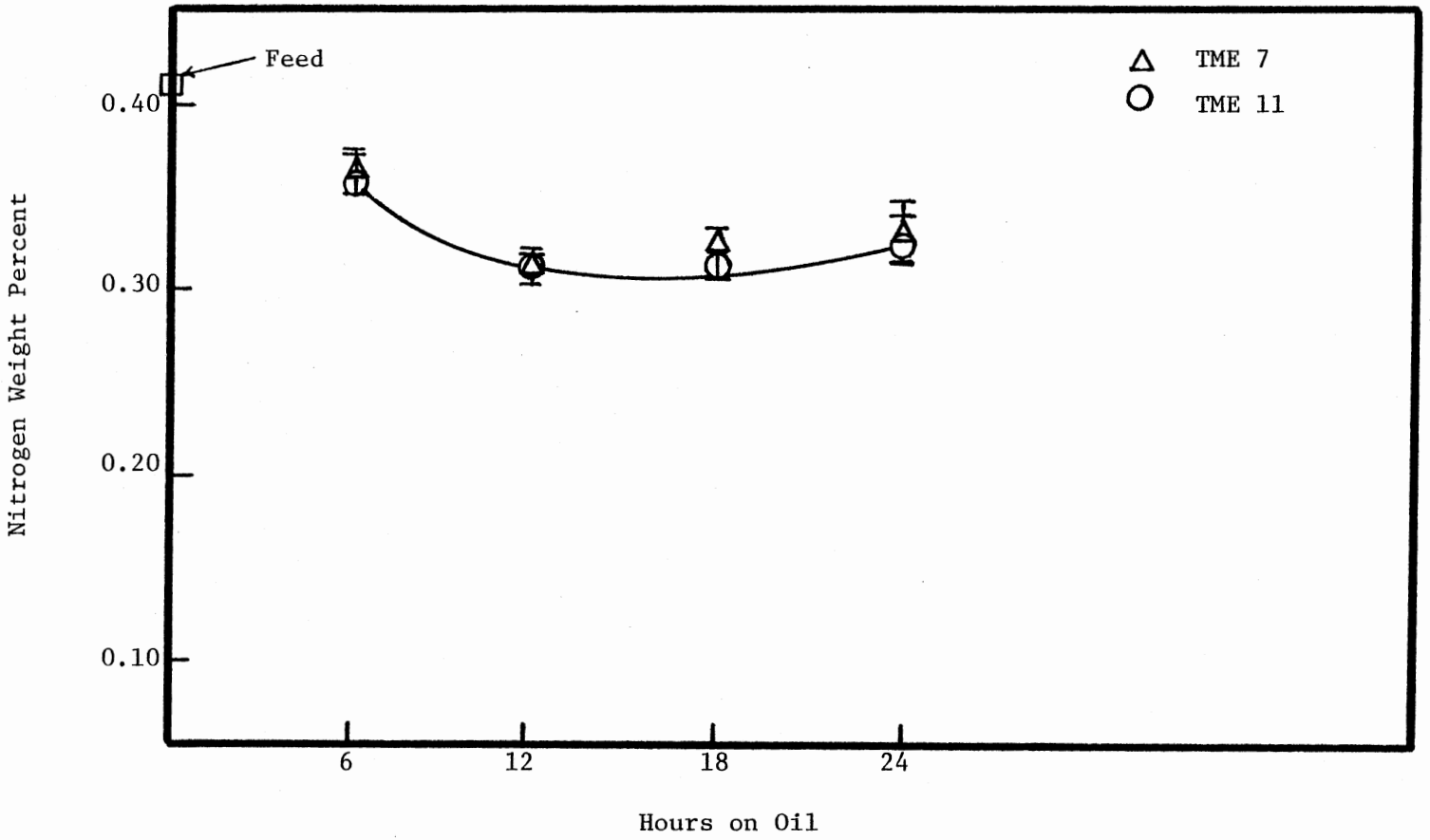

Figure 11. Nitrogen Weight Percent as a Function of Hours on Oil for Runs TME 7 & 11

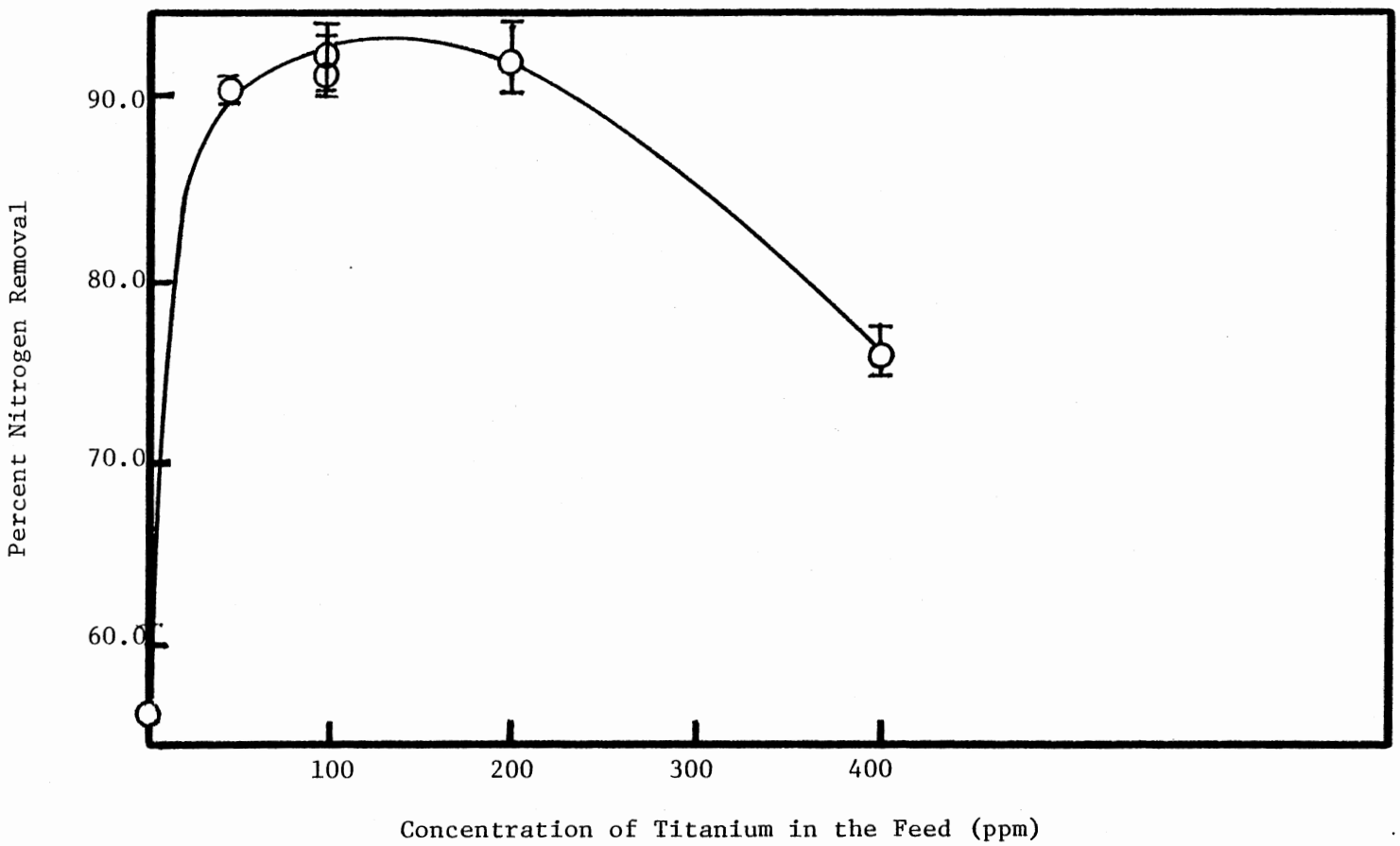

Figure 12. Nitrogen Removal as a Function of Concentration of Titanium in the Feed (Hours on Oil = 18)

used throughout this work and the measured titanium concentrations are listed in Table XV.

The carbonaceous black deposits accumulated above the catalyst bed are analyzed for their titanium contents by X-ray Spectrometer. The results are shown in Table XIII. These granular black materials contain comparable amounts of titanium, regardless of different titanium concentrations in the feedstocks.

Titanium concentrations in the product oils and some of the aqueous phases are analyzed and tabulated in Table IV through XII and XIV. It is observed that the amount of titanium remaining in the oil products and aqueous phases are negligible compared with the titanium concentrations in the feed oils.

The hydrodemetallation reaction occurring inside the catalyst bed results in the removal of titanium and its deposition on the catalyst. Figure 13 shows the titanium deposition profiles along the length of the reactor. The titanium deposition appears to decrease from the top section to the bottom section of the reactor.

X-ray diffraction measurement and Auger Microprobe analysis are used to determine the chemical nature of the deposited titanium on catalyst, and its distribution profile on the catalyst pellets. Researchers at Pittburgh Energy Technology Center found the hydrogenation of model titanium containing organic compounds results in the quantitive yeild of TiO_2 anatase. Our analysis did not obtain the evidence for the existance of TiO_2 anatase on the spent catalysts. This may have been due to the inability of x-ray diffraction techniques to analyze very thin layers of microcrystalline particles.

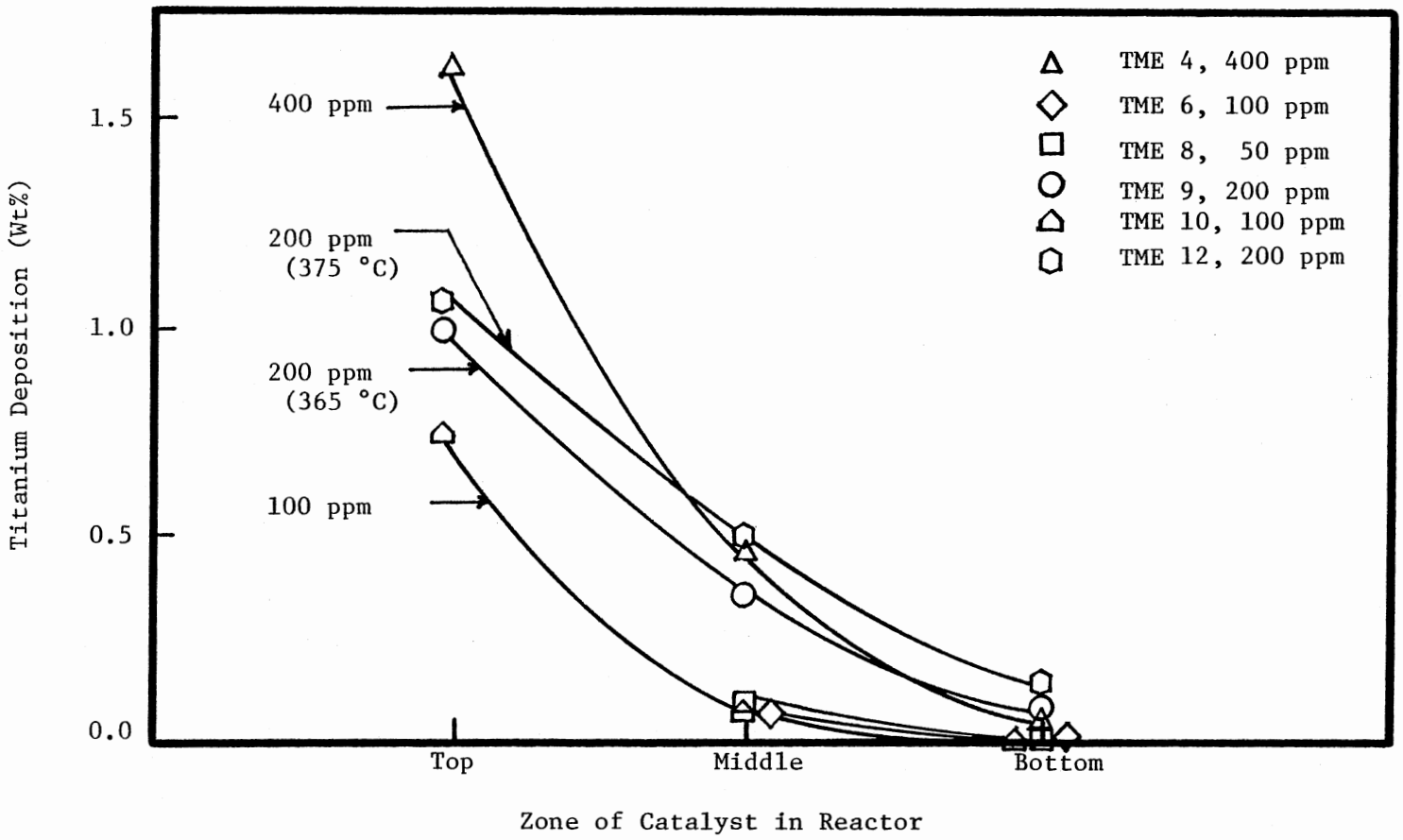

Figure 13. Titanium Deposition as a Function of Reactor Zone

TABLE XIX

AUGER MICROPROBE ANALYSIS

Sample No.	Description of Sample
1	TME #12 (Top Section)
2	TME #12 (Top Section)
3	TME #12 (Top Section)
4	TME #12 (Middle Section)
5	TME #12 (Bottom Section)
6	TME #10 (Top Section)
7	TME #4 (Top Section)
8	TME #5 (Top Section)
9	TME #4 (Middle Section)

Sample No.	Relative Number of Atoms Detected (01s = 100)					
	Al	C	Mo	O	S	Ti
1, Edge	72	--	14	100	15	16
1, 0.01mm from Edge	102	--	9	100	8	7
1, 0.02mm from Edge	92	--	8	100	5	2
1, 0.04mm from Edge	99	--	7	100	3	--
1, Center	84	--	6	100	--	--
2, Edge	86	--	6	100	3	1
2, 0.02mm from Edge	84	--	6	100	3	--
2, Center	95	--	6	100	--	--
3, Edge	100	--	7	100	--	--
3, .01mm from Edge	92	--	12	100	5	--
3, .05mm from Edge	100	--	22	100	--	--
3, Center	86	--	4	100	--	--
4, Edge	87	20	8	100	--	--
4, .02mm from Edge	95	8	4	100	--	--
4, .05mm from Edge	81	3	6	100	--	--
4, .10mm from Edge	82	--	6	100	--	--
4, Center	82	--	6	100	--	--
5, Edge	95	8	10	100	--	--
5, 0.2mm from Edge	90	--	6	100	--	--
5, 0.5mm from Edge	92	--	7	100	--	--
5, Center	97	--	4	100	--	--

TABLE XIX (Continued)

Sample No.	Relative Number of Atoms Detected (01s = 100)					
	Al	C	Mo	O	S	Ti
6, Edge	88	--	4	100	2	--
6, .02mm from Edge	87	--	3	100	1	--
6, .05mm from Edge	88	--	3	100	1	--
6, Center	88	--	3	100	--	--
7, Edge	94	--	8	100	5	--
7, .02mm from Edge	85	--	5	100	6	--
7, .06mm from Edge	87	--	5	100	6	--
7, .15mm from Edge	87	--	5	100	6	--
7, .20mm from Edge	89	--	5	100	6	--
7, .25mm from Edge	88	--	5	100	6	--
7, .30mm from Edge	85	--	5	100	--	--
7, Center	94	--	5	100	--	--
8, Edge	86	--	5	100	1	--
8, Center	90	--	5	100	--	--
9, Edge	85	--	10	100	3	--
9, .05mm from Edge	90	--	8	100	--	--
9, Center	90	--	8	100	--	--

Beam diameter = 10μ meter

Pellets cleaved and analyses performed on ID surface

However, titanium on the spent catalyst may have also been in amorphous phase.

Nine regenerated catalyst pellets were analyzed by SCR Laboratory, Houston, Texas, for the distribution of titanium. The maximum concentration of titanium is observed to be at the edge of catalyst surface. A shallow penetration of titanium into the catalyst pores is also observed.

Coke Content

Figure 14 shows the profiles of coke content inside the reactor. The coke content is shown to have decreased from top to bottom of the reactor.

In the catalytic hydrotreatment runs, the coke content of top sections in all runs have comparable amounts of coke. However, the coke contents in the middle and bottom sections are generally reduced by the addition of titanocene dichloride in the feed oils.

Poisoning on the catalyst by metal deposition has been reported to increase the coke formation (81). To relate the interaction between the coke formation and the titanium deposition on the spent catalysts the coke content is plotted versus the titanium deposition, as shown in Figure 15. From this figure it appears that the coke formation and titanium deposition occurred simultaneously.

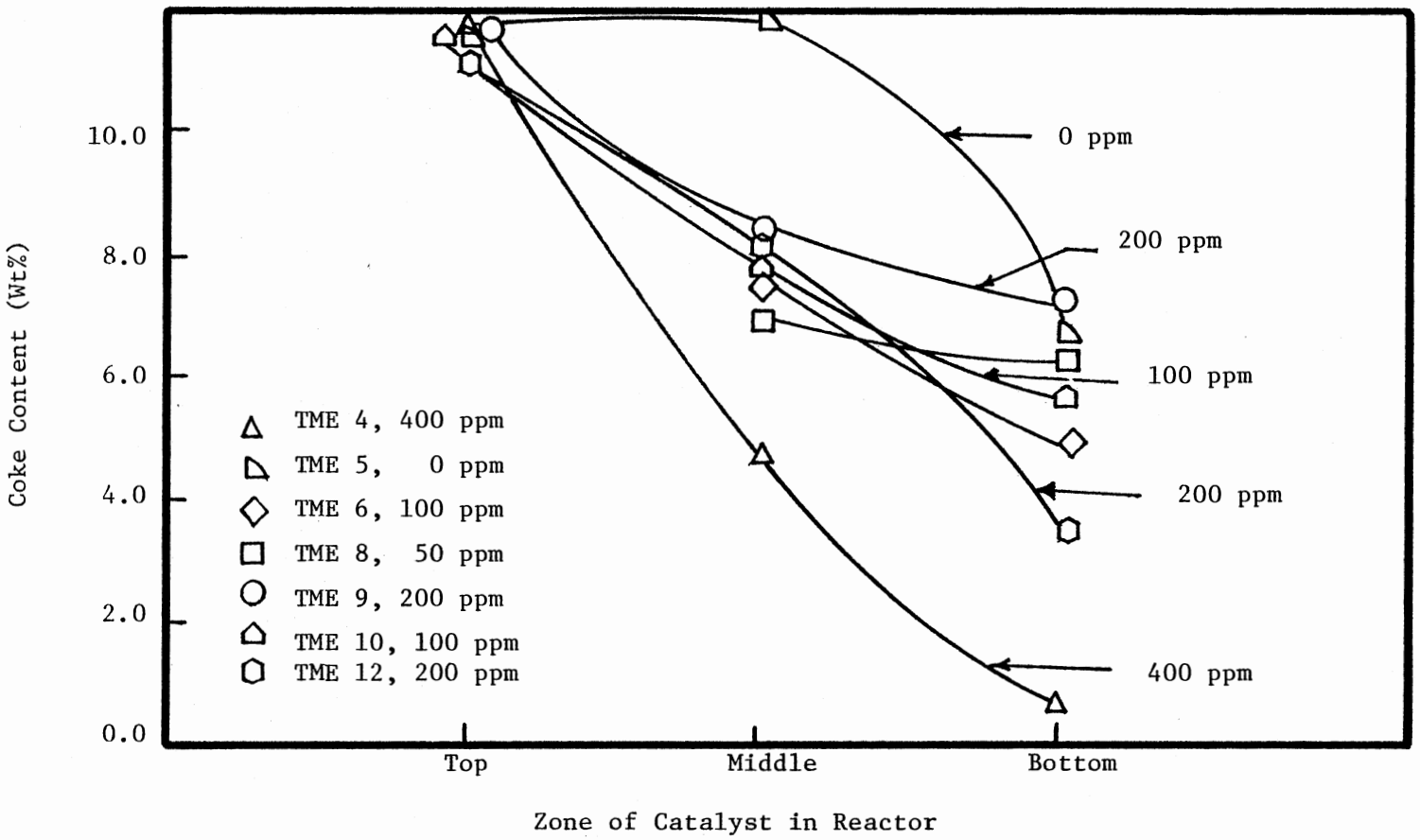

Figure 14. Coke Content as a Function of Reactor Zone

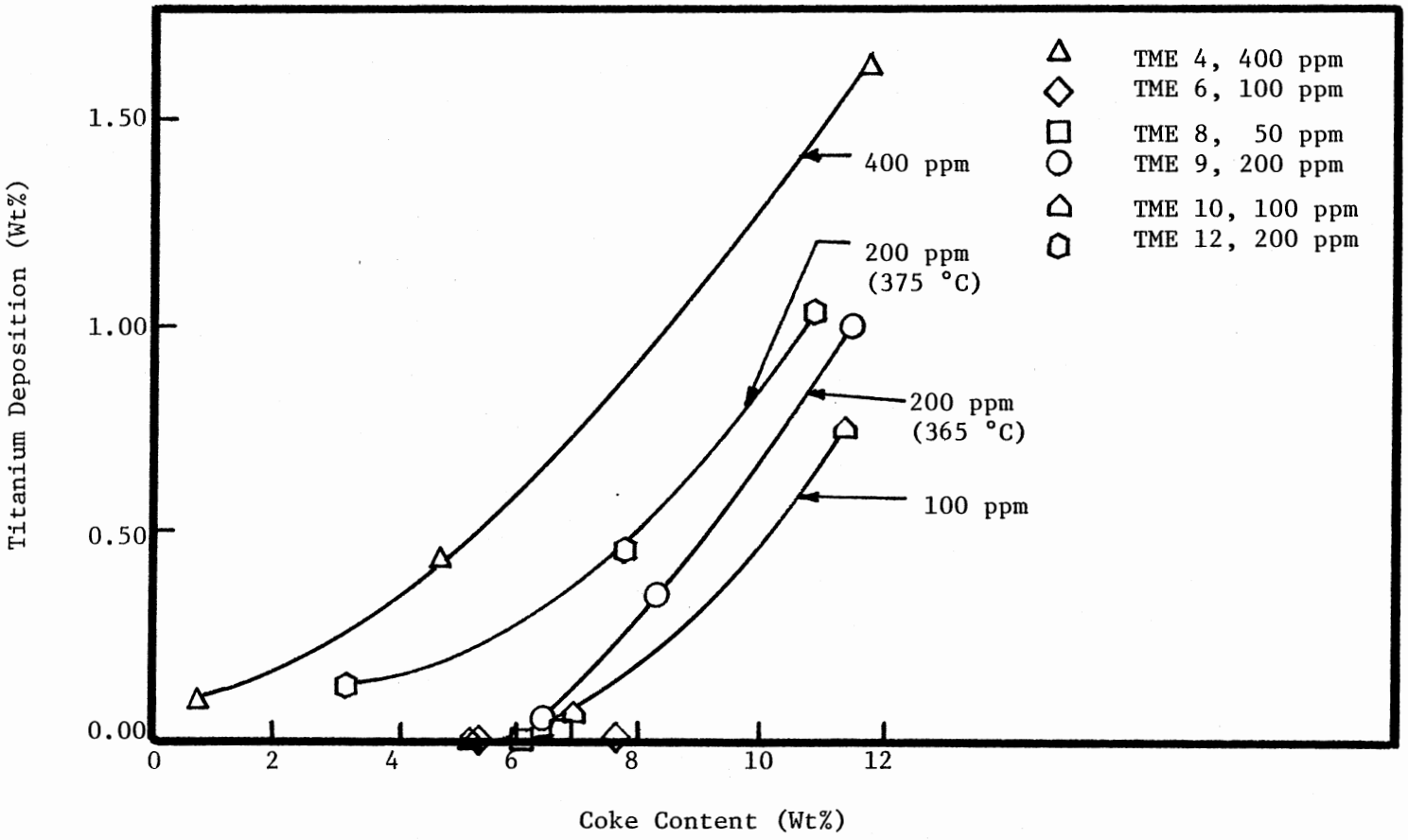

Figure 15. Titanium Deposition versus Coke Content

Surface Area and Pore Volume

The surface areas of spent catalysts are expected to change due to the coke formation and metal deposition. Comparing with the fresh catalyst, the surface areas of spent catalysts are reduced to different extents. The plots for surface area versus pore volume, surface area versus coke content and surface area versus titanium deposition are given in Figures 16, 17 and 18. No good correlations between surface area and other parameters are observed.

The pore volumes of the spent catalysts are also less than the fresh catalyst. The decrease of pore volume is mainly by coke formation which blocks the pores of the catalyst. As the coke content increases, the pore volume decreases. The metals deposition may also have had some effects on the pore volume.

Data obtained in this study show that in the run TME #5 and #12, an increasing trend of pore volume from the top to bottom of reactor can be observed. However, the same trend does not exist in other runs.

Figure 19 gives the pore volume versus coke content for spent catalysts obtained form catalytic hydrotreatment runs. Comparatively, the coke content surpasses the titanium deposition on the spent catalyst. The effect of titanium deposition on pore volume is also not clear. Figure 20 shows the plot of pore volumes versus the titanium deposition, no conclusion can be drawn from this figure either.

Figures 21 and 22 show the plots of the ratio of surface area to pore volume versus coke content and titanium deposition resepctively. Again, no major correlation can be drawn. However, it is observed that the spent catalysts have larger surface area to pore volume

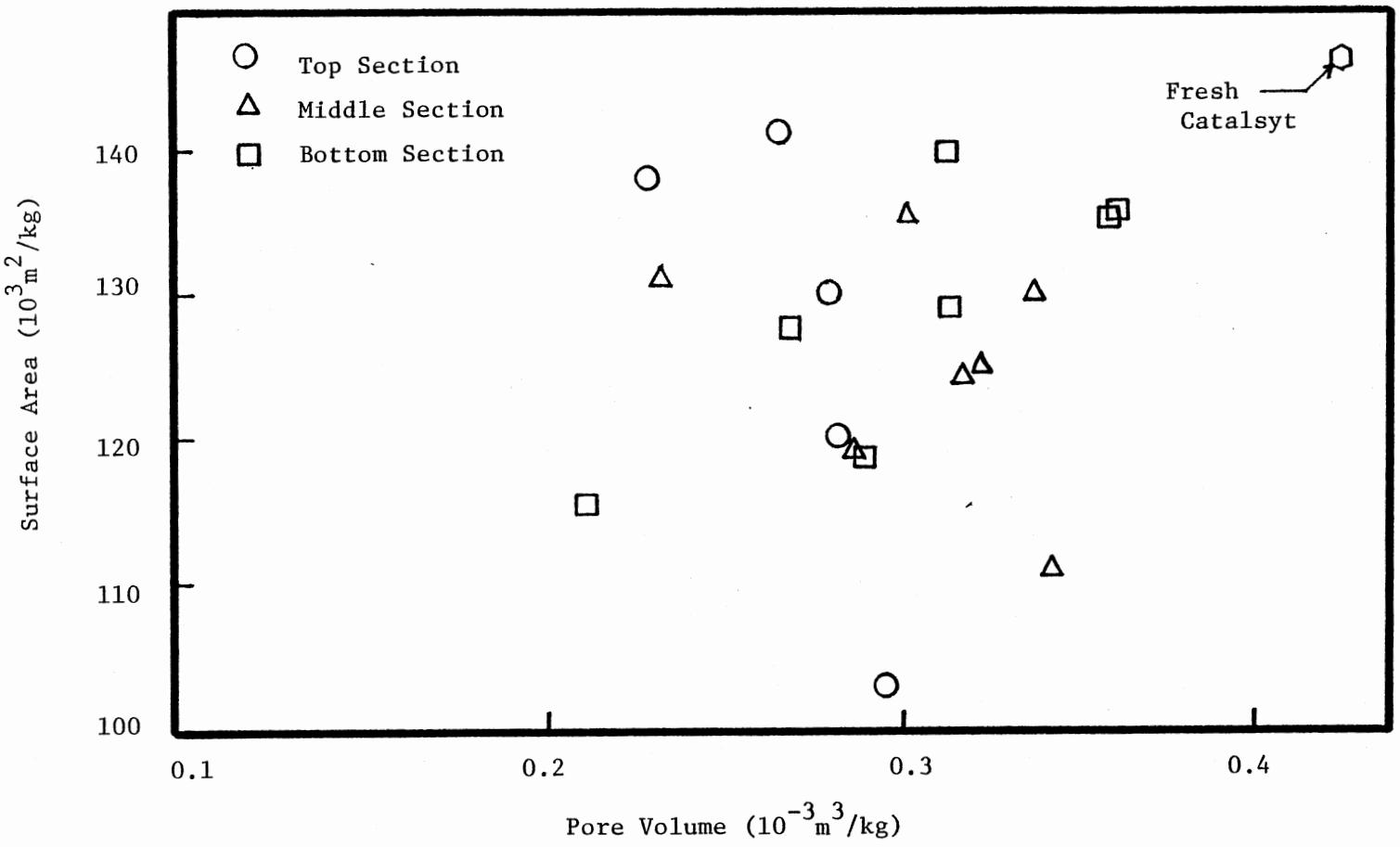

Figure 16. Surface Area versus Pore Volume

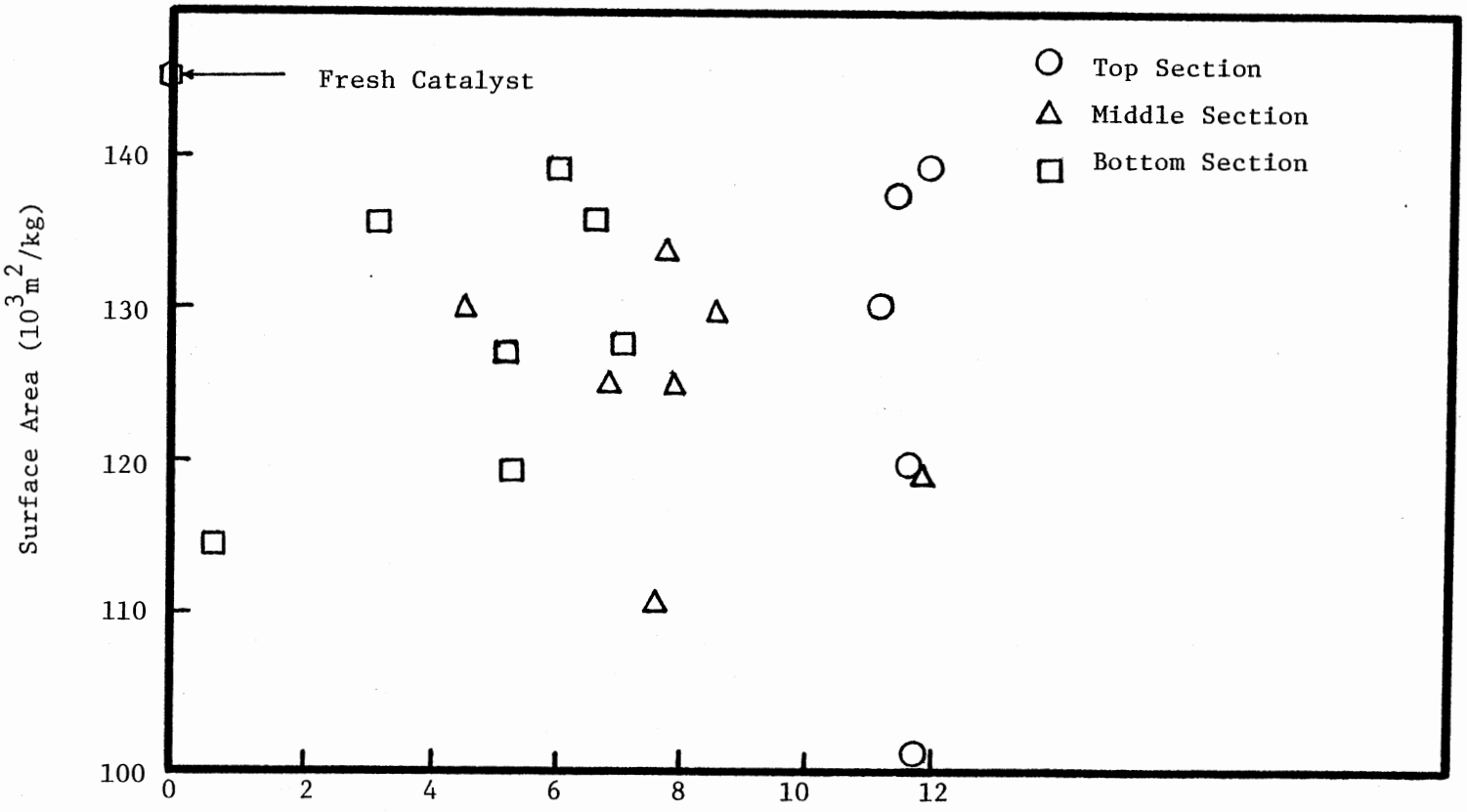

Figure 17. Surface Area versus Coke Content

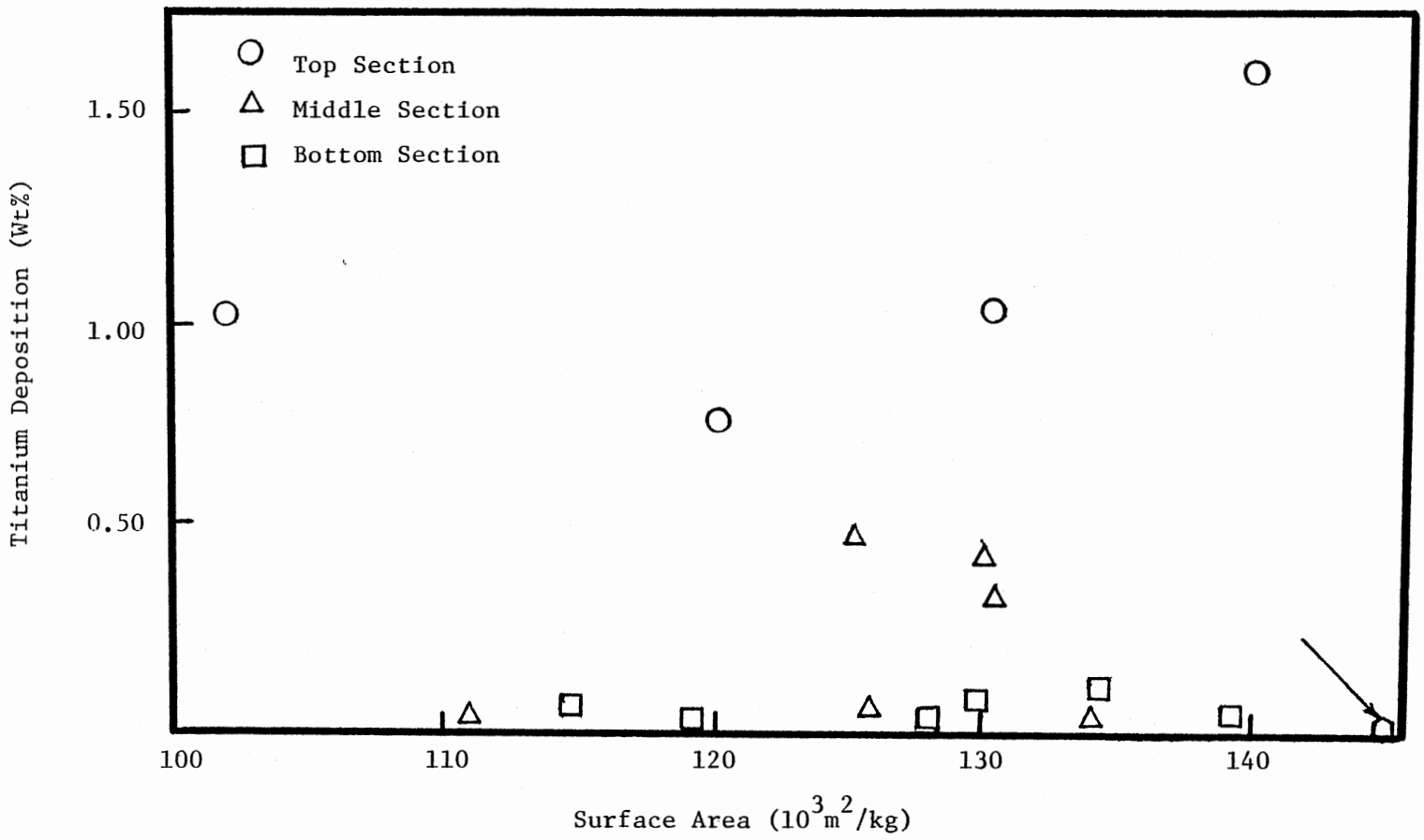

Figure 18. Titanium Deposition versus Surface Area

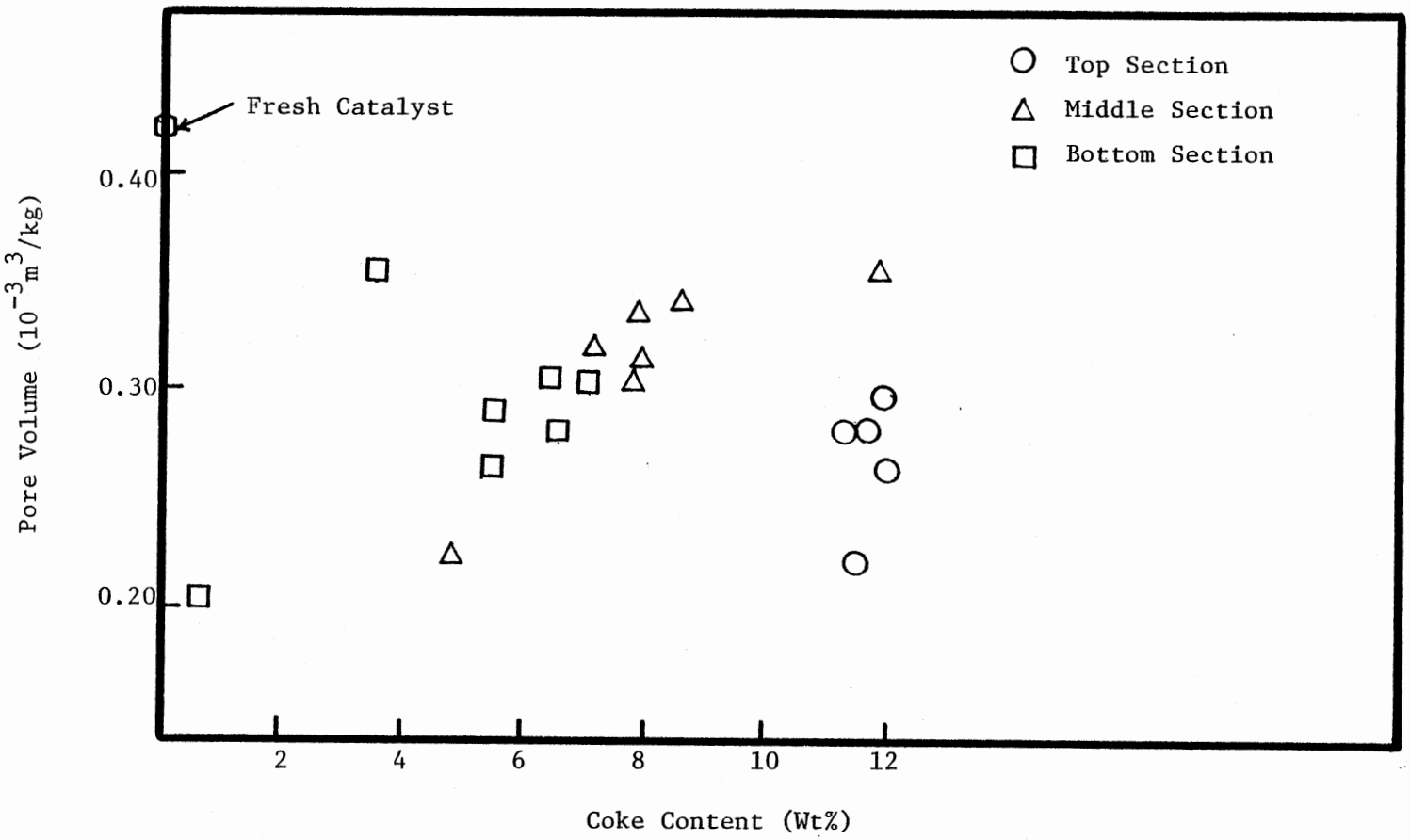

Figure 19. Pore Volume versus Coke Content

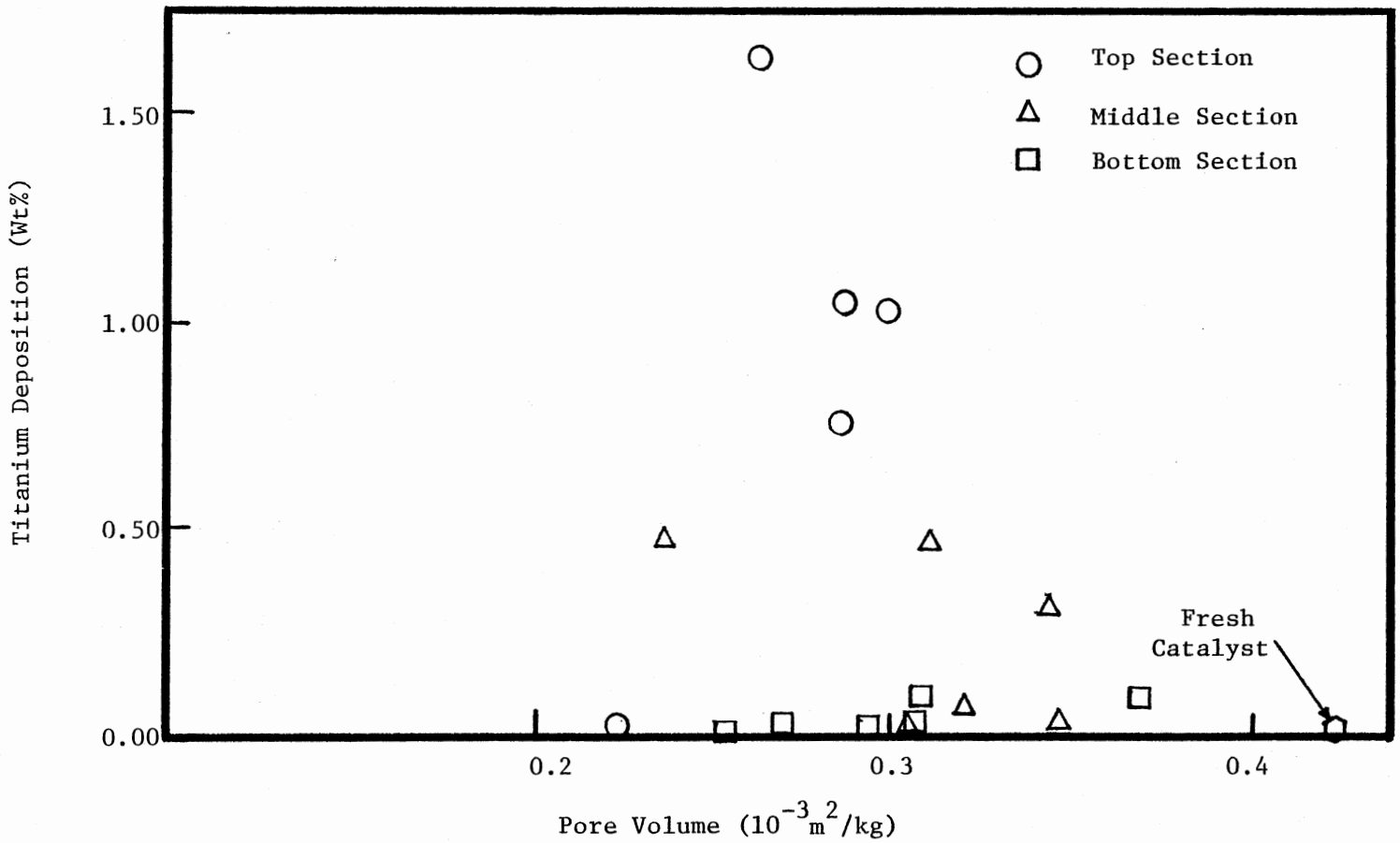

Figure 20. Titanium Deposition versus Pore Volume

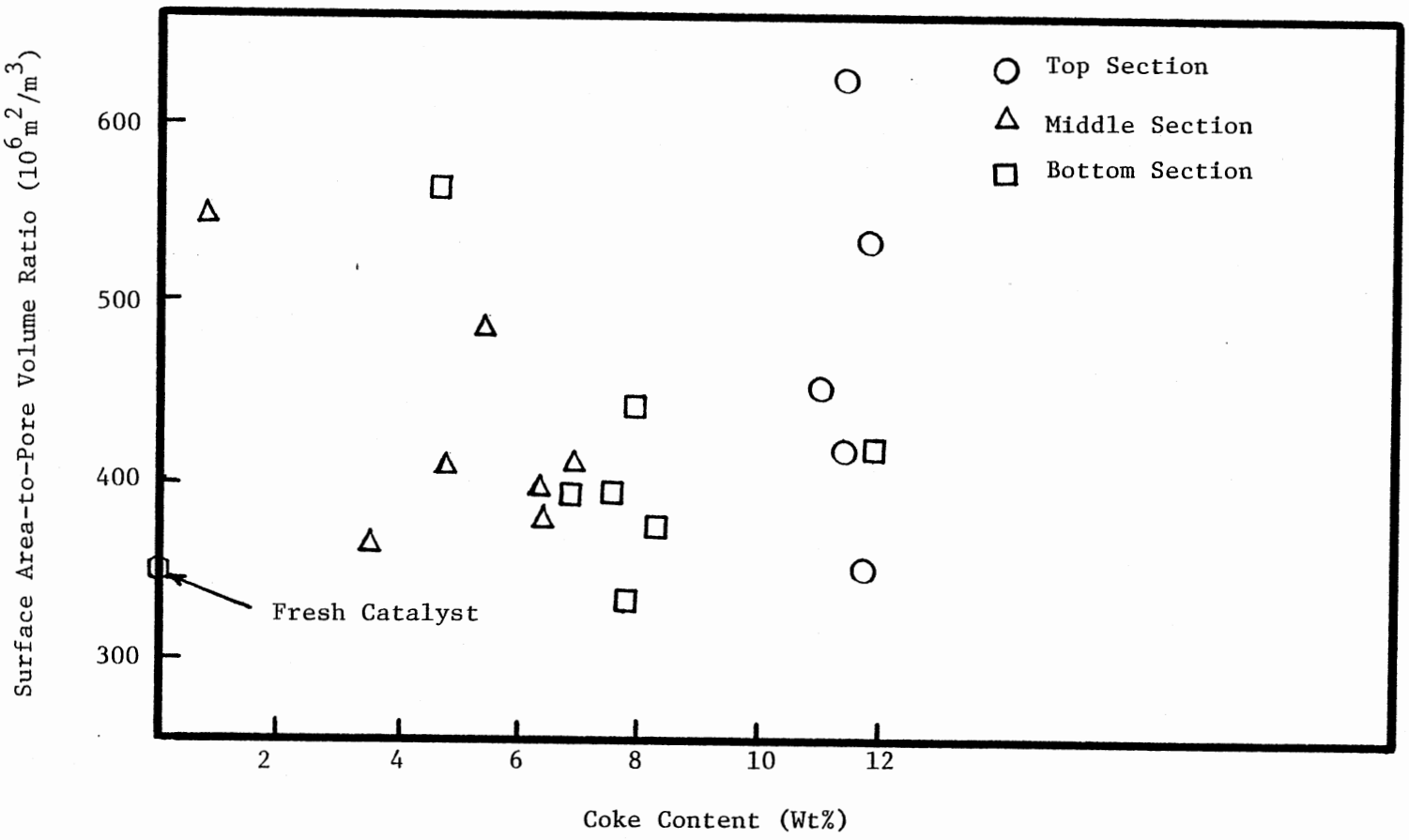

Figure 21. Surface Area-to-Pore Volume Ratio versus Coke Content

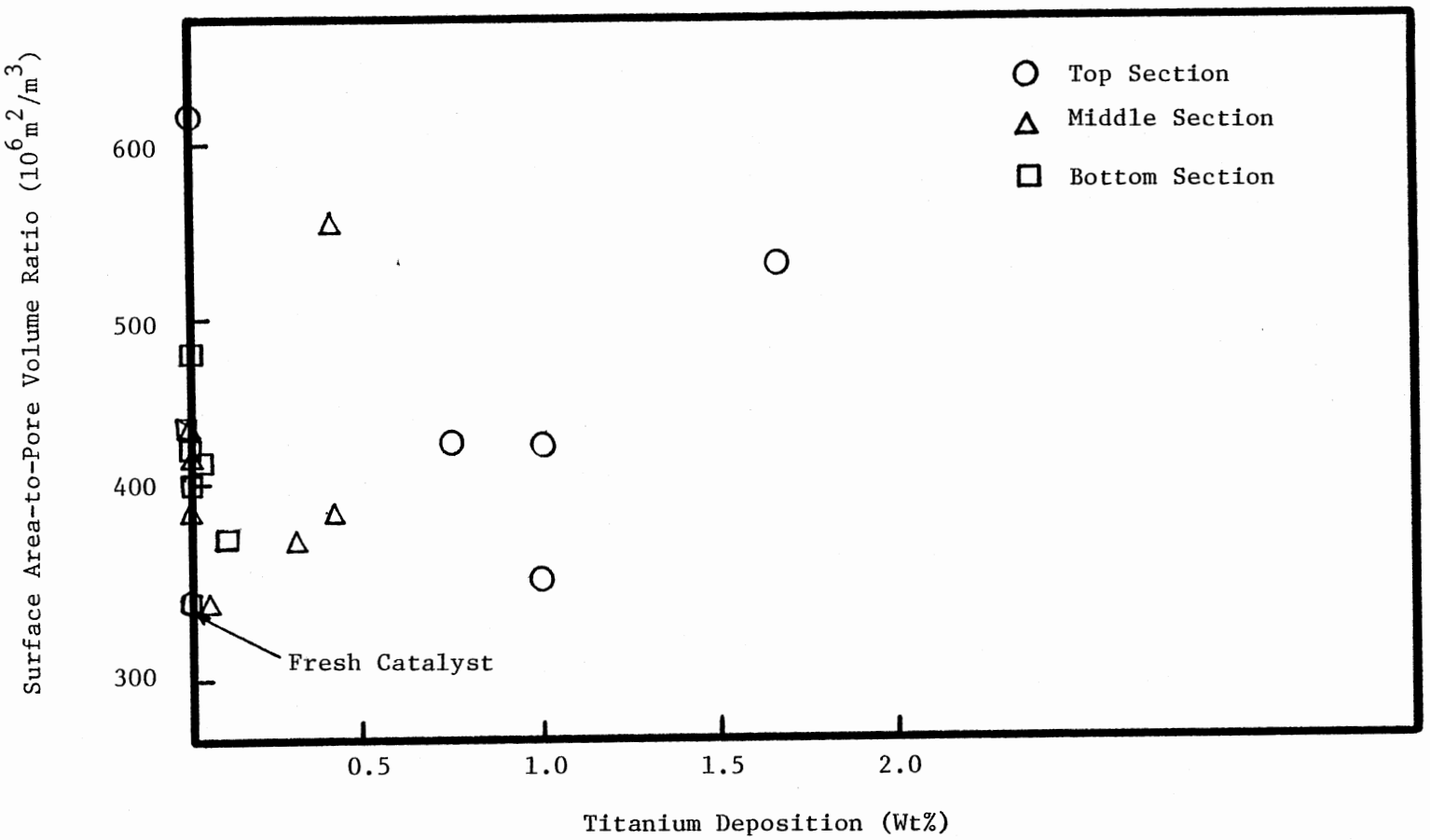

Figure 22. Surface Area-to-Pore Volume Ratio versus Titanium Deposition

ratios than fresh catalyst.

ASTM Distillation Data

The feed and selective samples from sample #3 of each run were fractionated following the ASTM D1160 procedure. All fractionations were done at atmospheric pressure. All distillation data are tabulated in Table XVIII. The distillation data of SRC light oil show that 90% of the oil boils between 176 C (349 F) and 199 C (130 F).

Figure 23 presents the distillation curves of the feed oil and a representative product oil sample from sample #3 of TME #6. The cracking and hydrogenation reactions both can shift the product oil to lower boiling range. By contrast, the reforming and polymerization reactions can produce higher boiling point compounds. In Figure 23, both kinds of shifts can be observed.

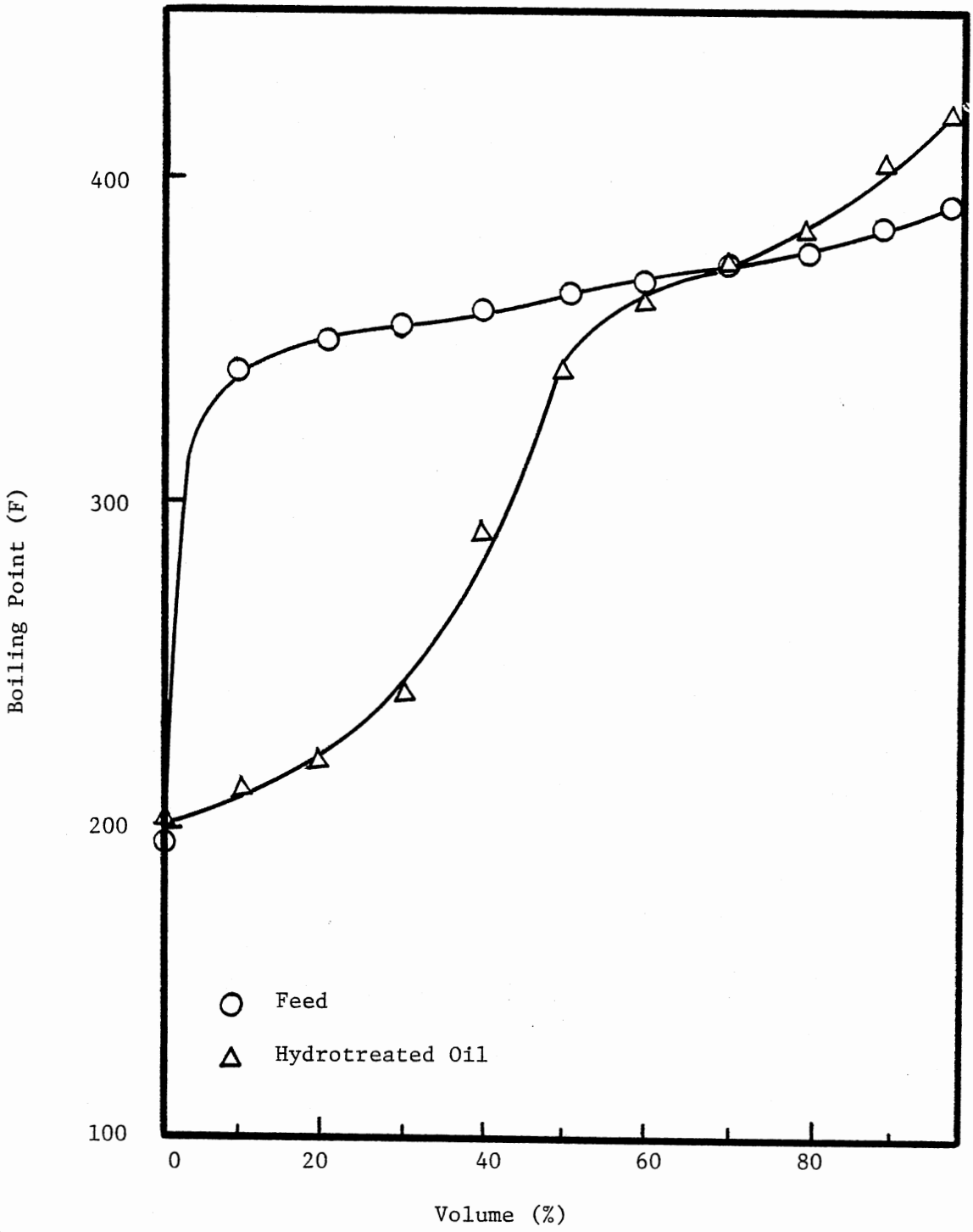

Figure 23. Distillation Curves of Feed and Hydrotreated Oil

CHAPTER V

DISCUSSION

In this chapter the experimental results will be discussed under the following categories:

1. Reactor clogging.
2. Distillation data.
3. Effects of titanocene dichloride on hydrotreatment.
4. Fate of titanocene dichloride during hydrotreatment.
5. Temperature effects on hydrotreatment.
6. Properties of spent catalyst.
7. Reproducibility and precision of data.

The trickle bed reactor used in this study has also been used by previous researchers in Oklahoma State University. The performance of the trickle bed reactor has been discussed by these investigators (2, 16, 18, 19). No serious non-ideal behaviors have been observed. Therefore, the discussion on the performance of the trickle bed reactor will not be given here. However, the temperature profile inside the reactor should be mentioned. The exothermal nature of hydroprocessing reactions causes the deviation of temperature inside the catalyst bed from uniformity. Soni (93) in his hydrotreatment studies of Synthoil-I liquid and raw anthracene oil observed a temperature variation over the length of reactor within 2 F from the desired value. Similar observations were also made by Sooter (19)

and Satchell (18).

The chemical nature of feedstocks and the extent of hydrotreating operations both affect the temperature profile inside the reactor. In this study a highly active catalyst, Shell 324, and a low boiling point feedstock SRC light oil were used. The highly exothermal reactions give a parabolic temperature profile, in the catalyst bed, with the highest temperature appearing between 2 and 4 inches from the top of the bed. A variation of $\pm$ 15 C from the normal temperature was noticed over the entire catalyst bed. The hot spot region of the catalyst bed has profound effects on the hydrotreatment. In this study, the heating rate was controlled to achieve the same hot spot temperature and the closest possible temperature profiles throughout the bed for different runs. Recently two other researchers at Oklahoma State University, using Shell 324 as catalyst, also observed significant temperature differences inside the catalyst bed (94, 95).

Reactor Clogging

The reactor plugging in TME #2, #3 and #4 caused the premature shutdown of runs TME #2 and #3, and a hydrogen flow restriction in run TME #4.

DeRosset et al. (80) had a plug developed in the lower part of their reactor in the hydrotreatment of a filtered Synthoil. Their analyses showed that the ammonium chloride present in the oil was responsible for the plugging of the reactor. The water wash of feed oils removed the ammonium chloride from the oils and resolved their reactor clogging problem. In our laboratory Chang (96) encountered

the reactor plugging in the lower part of his reactor. The analysis of the plugging material suggested that $(NH_4)HS$ formed from the reaction of H_2S and NH_3 was responsible for the clogging. The solidification of this compound plugged on the cold outlet tubing of the reactor caused the clogging. Application of heat to the clogged portion resolved the problem.

Another worker in our laboratory also had a reactor plugging problem. Wilkinson (94) used acid wash technique to remove the basic heteroatom containing compounds from SRC distillate. The remaining chloride from HCl solution was suspected to clog the lower part of the reactor. Analysis of clogging materials showed the presence of chloride. Ahmed (16) also encountered several reactor pluggings. He related the reactor clogging to the coke formation. As the coke content on spent catalyst increases, it restricts the flow of oil through the reactor and finally results in complete plugging of the reactor.

Runnion (97) reported plugging of trickle bed reactor in his hydrotreatment studies of Synthoil. The build-up of the product around the orifice of the back pressure valve was held responsible for the plugging. However, no specific information about the product build-up was reported. They reasoned that the plugging problem was because the lighter fractions from Synthoil feed were easily driven off and hydrotreated, meanwhile some of the heavier fraction were also cracked and hydrotreated, but the tar residue was left unreacted which formed a thick viscous material. A similar arguement has also been given to the plugging problems in the processing of heavy crude oils. The phase separations due to severe hydrocracking may also happen. The heavier

fractions become concentrated in the heavier oil phase and precipitate after some of the lighter oil is hydrotreated to form the lighter oil phase (98).

From the study of the reported reactor plugging cases, one conclusion that can be drawn is that most reactor plugging happened in the lower part of the reactor, inside the catalyst bed and in the downstream tubes or valve of the reactor. In our case, the reactor plugging occurred in the inlet of the reactor and above the catalyst bed. None of the above mentioned explanation are applicable to our case.

Analysis of the plugging materials in this project showed the existence of both titanium and nitrogen in them. The percentages of titanium was found to be independent from the titanocene dichloride concentration of the feed oils. Polymerization of unsaturated hydrocarbons catalyzed by titanium compounds in the preheating zone can be suspected to be responsible for the plugging problem. In the preheating zone, the thermal cracking of oil may surpass the hydrogenation reactions. Thus the free radicals generated by thermal cracking will be polymerized under the catalytic effects of titanium compounds. Titanium has been known to be the main component of Ziegler-Natta catalyst, used for the polymerization of ethylene and propylene.

Inside the catalyst bed, the hydrogenation of free radicals catalyzed by the hydrotreating catalyst will dominate the reaction system thus preventing polymerization. Also, the depletion of titanium in the entrance zone of the catalyst bed will reduce the

possibility of polymerization in the lower parts of the bed and prevent the catalyst bed clogging.

Distillation Data

Fractionation data obtained by standard ASTM D1160 procedure is another method to assess the changes in the quality of the oil during hydrotreatment. All fractionations were done at atmospheric pressure.

The distillation data of feed, SRC light oil, shows a low and narrow boiling range. It has an initial boiling point and an end point of 88 C (190 F) and 199 C (390 F) respectively. 90% oil boils between 172 C (340 F) and 199 C (390 F).

The distillation data of product oils indicates a shift in the boiling range depending on the hydroprocessing performance. This in turn can be indicative of hydrogenation and hydrocracking reactions. The cracking of large molecules and the hydrogenation of unsaturated compounds both can shift boiling points to lower range. In the catalytic hydrotreatment runs of this study a shift to lower boiling point was observed. However, near the end point a shift to higher boiling points was also observed. This can be explained by the polymerization and reforming reactions. During hydrotreatment free radicals are generated from the cracking of high molecular weight compounds. The polymerization reactions and hydrogenation reactions of free radicals compete with each other, therefore the shift of boiling point to lower and high boiling point ranges could result.

Some typical reactions of the heteroatom containing compounds under hydrogenation conditions are discussed by Kobe and Mcketta (99). Most of the hetero-compounds will proceed with the ring saturation before the removal of heteroatoms to produce lower molecular weight

hydrocarbons. The hydrogenation of phenols is different from other heteroatom compounds. Two phenolic rings might couple to generate higher molecular weight compounds. Figure 24 shows the typical hydrogenation reactions of phenols (99).

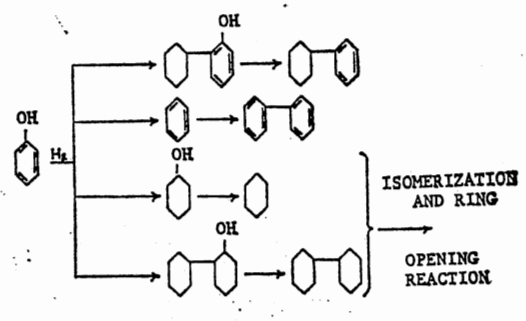

Figure 24. Typical Hydrogenation Reactions of Phenols

The possible presence of phenols in SRC light oil might be one of the explanations to the shift in the boiling points near the end points.

Figure 25 shows the distillation curves for non-catalytic hydrotreatment runs TME #7 and #11. In run TME #11, which used SRC light oil as feedstock, the boiling points of the product was observed to shift lower boiling ranges. However, the hydrogen content of product oil shows negligible change when compared with that of feed oil. Thermal cracking can be an explanation to the shift of distillation curve.

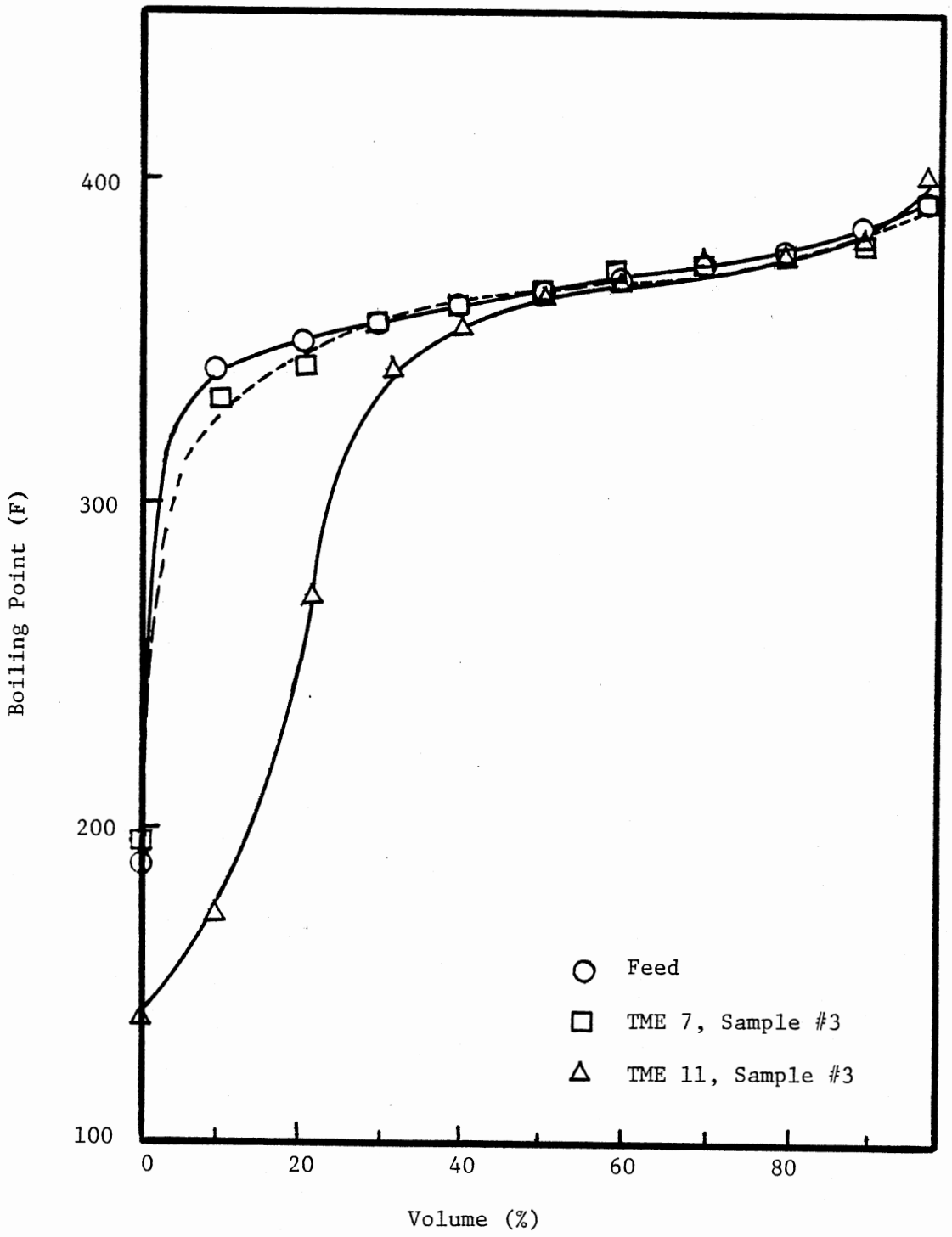

Figure 25. Distillation Curves of Feed and Product Oils of Runs TME 7 & 11

In run TME #7, which was doctored with titanocene dichloride, the distillation curve is close to that of the feed oil. Apparently, titanocene dichloride had some cracking as well as some HDS and HDO effects.

Effects of Titanocene Dichloride On Hydrotreatment

It was shown in this project that the addition of titanocene dichloride to the feed oil improves the hydrotreatment activity. Hydrogenation, hydrodenitrogenation and hydrodeoxygenation were enhanced significantly. The improvement in desulfurization was not very profound, primarily because the desulfurization rate has been quite high even in the absence of titanocene dichloride. The improved performance due to the addition of titanocene dichloride may be explained by the following reasons.

1. Homogenous catalysis of titanocene dichloride.
2. Effects of titanium deposit on the catalyst.
3. Effects of chloride ion on the catalyst.
4. Removal of coke precursors by titanocene dichloride.

Homogeneous Catalysis of Titanocene Dichloride

Titanocene chlorides were reported to have hydrogeneation activity, even though their activity was lower than the polymer supported titanocene chlorides (100). In our research we believe that the carbonaceous material formed in the preheating zone also contained polymerized titanium compounds. But these compounds probably had different chemical compositions than the polymer supported titanocene chlorides. The

catalytic effects of polymer supported titanocene chlorides on the olefin isomerization, oligomerization and hydroformylation have been discussed by many researchers (100, 101).

The data presented in preceeding chapter shows that in the absence of catalyst, titanocene dichloride does not increase the hydrogen content, which also indicates that neither the titanocene dichloride nor the polymerized titanium compounds have noticeable hydrogenation ability in the hydrotreating conditions. However, the presence of titanium compounds, as discussed earlier, did have some effects on hydrotreatment which caused the difference in the pattern of the distillation curves.

Comparison of TME #7 and #11 indicates that titanocene dichloride enhances the removal of oxygen and sulfur. Eisch (102) in his research on the homogeneous desulfurization by organometallics tested the desulfurization activity of bis(1,5-cyclooctadiene) 3-cyclooctenyl cobalt, nickel, iron and titanium and found that organometallic titanium does have some desulfurization activity towards dibenzothiophene, but the activity is lower than that of cobalt or nickel compounds. Similarity of chemical behavior between sulfur and oxygen containing compounds leads to suggest that the organotitanium compounds might have deoxygenation activity.

Effects of Titanium Deposit on the Catalyst

The role of titanium as catalyst supports has also been studied. Massoth (83) evaluated the effect of catalyst support. Alumina was indicated to be the best support, showing high activity for

hydrodesulfurization and hydrogenation, and moderate to high activity for hydrocracking. Titania as a support shows high hydrocracking but low hydrogenation and hydrodesulfurization activities. However, Gates et al. (35) indicated that sulfided NiMo/TiO_2 was almost twice as active per unit surface for quinoline HDN as a comparably prepared NiMo/gamma alumina catalyst.

The effects of titanium impregnation or deposition on catalyst have also been studied. Beuther et al. (82) claimed that NiMo/alumina catalyst when impregnated with titanium tetrachloride showed improved sulfur removal over NiMo/alumina catalyst. Wilson et al. (103) claimed that in the preparation of NiMo/alumina with titanium impregnation, the replacement of titanium tetrachloride by non-acidic solutions of titanium compounds, such as organometallic titanium compounds, would improve the catalyst performance through the increasing physical strength of the catalyst.

Kovach et al. (78) deposited titanium dioxide on CoMo/alumina catalyst and tested its hydrogenation activity. The activity of titanium impregnated catalyst remained at 99% of the activity of the unimpregnated catalyst up to 8% of titanium dioxide impregnation. In the same research, the impregnation of other oxides, like SiO_2, MgO, Fe_2O_3, CaO and Na_2O, all showed higher degree of deactivation than uninpregnated catalyst.

In this study, the amount of titanium deposition on the spent catlysts varied in the range of 0.0-1.7 wt%. In order to evaluate the effects of titanium deposition the catalyst activities for HDS, HDN, HDO and hydrogenation reactions and the coke formation were tested.

Effects of Chloride Ion on the Catalyst

Research on the hydrocracking catalysts has shown that halogen can increase the Lewis acidity of alumina, and improve the activity of catalyst (104, 105). The presence of halogen in CoMo/alumina, NiMo/alumina, or NiW/alumina catalysts was reported to improve the activity of catalytic hydrodenitrogenation (106, 107).

Gates et al. (35) showed that the incorporation of acid sites into alumina by addition of flouride to sulfided NiMo/alumina catalyst increases the rate of nitrogen removal by 40%. Massoth (83) disclosed that the HCl treated CoMo/alumina catalyst had improved catalytic activities.

In this study, the chloride of titanocene dichloride is likely to have been converted to HCl during hydrotreatment. The analyses proved the existence of chloride in the aqueous phase. This chloride could have contributed to the improved catalyst activity observed in this study.

The improved catalytic activity may also be due to the less coke content observed with titanium deposited catalysts. However, a definite conclusion can not be drawn unless further information is obtained. A systematic study on the effects of halogen on various hydroprocessing reactions and coke content should be conducted. By decoupling the effects of titanium and halogen, it can be determined whether titanium or halogen or both contribute to the improved catalytic performance.

Removal of Coke Precursors by
Titanocene Dichloride

The basic nitrogen-containing compounds can be adsorbed on the active acid sites of the catalyst and increase the tendency for coke formation. Also, the oxygen-containing compounds like phenols were suggested to be coke precursor (39).

Results of TME #7 and #11 show that titanocene dichloride enhances the removal of oxygen and sulfur in non-catalytic hydrotreatment runs. The analyses of the black granular carbonaceous deposits accumulated in the preheating zone show that in addition to titanium they contain high contents of nitrogen. All these results show that the nitrogen and oxygen containing compounds can be removed by titanocene dichloride before they contact the hydrotreating catalyst.

Although there is no direct evidence that nitrogen and oxygen containing compounds are coke precursors, the decreased coke contents for runs with titanocene dichloride doctored feeds could possibly support this idea.

From the four possible mechanisms for the improved catalytic activities, the homogeneous catalysis of titanocene dichloride appears to be less important. The promotional effect of titanium deposits and chloride ion, and the removal of coke precursors by titanocene dichloride are all important for the enhanced activities of the catalyst.

Kovach et al. (78) studied the effects of titanium deposits from titanocene dichloride on the hydrogenation activity of CoMo/alumina catalyst under coal liquefaction conditions. The catalyst maintained

its activity at the same level as the fresh catalyst up to a processing of about 24 kgs equivalent coal per kg of catalyst. After that, the activity dropped sharply. They concluded that the titanium deposit had no deactivation effect as long as the weight percent of titanium was low. At higher percentages of deposit, the catalyst loses its activity sharply.

In our study, the percent of titanium deposit on the catalyst is quite low, moreover, the feedstock for our study is different from those used by Kovach et al. (78). They first allowed the titanium to deposit on the catalyst then tested the activity of the catalyst. Whereas in our experiments it is the interaction of titanocene dichloride with the catalyst and SRC light oil that is studied. This might be the reason for the difference in the observations obtained in our study.

The catalyst activity improvement depends on the concentration of titanocene dichloride. Titanium concentrations of 100-200 ppm appear to promote the catalyst most, but higher concentrations show lower activities.

Figures 26 through 28 show the variation of catalytic activity as a function of time on oil for all catalytic hydrotreatment runs. The runs TME #6, #8, #10 and #12, with titanium concentrations of 50-200 ppm in the feed oils, show negligible catalyst deactivation in the duration of experimental runs. Reference run TME #5 shows a slight deactivation in catalytic activities. The run TME #4, with 400 ppm of titanium in feed oil, shows the highest degree of catalyst deactivation. After 60 hours of operation, the hydrotreating performance of TME #4 decreased to the level of the reference run TME #5.

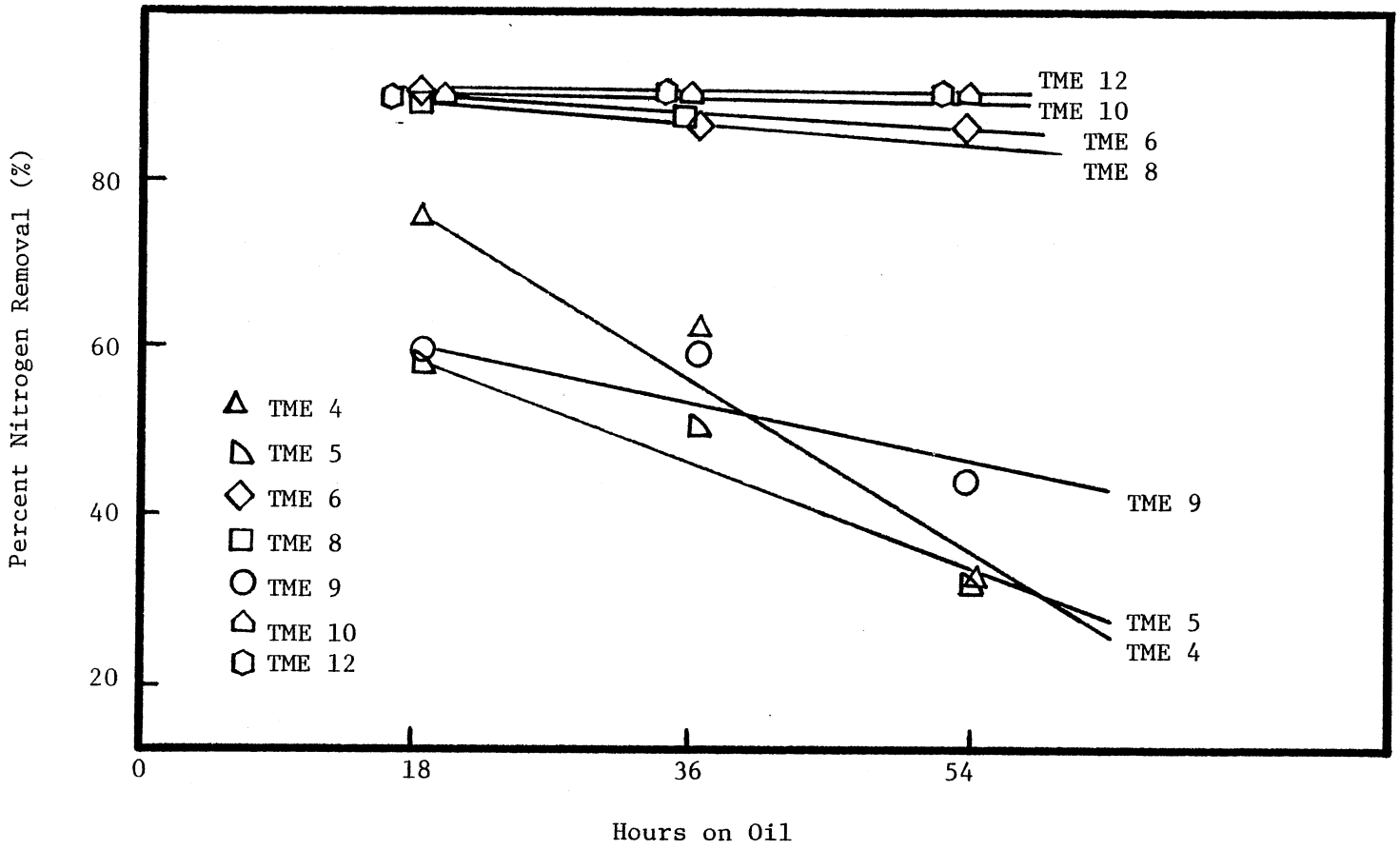

Figure 26. Percent Nitrogen Removal as a Function of Hours on Oil

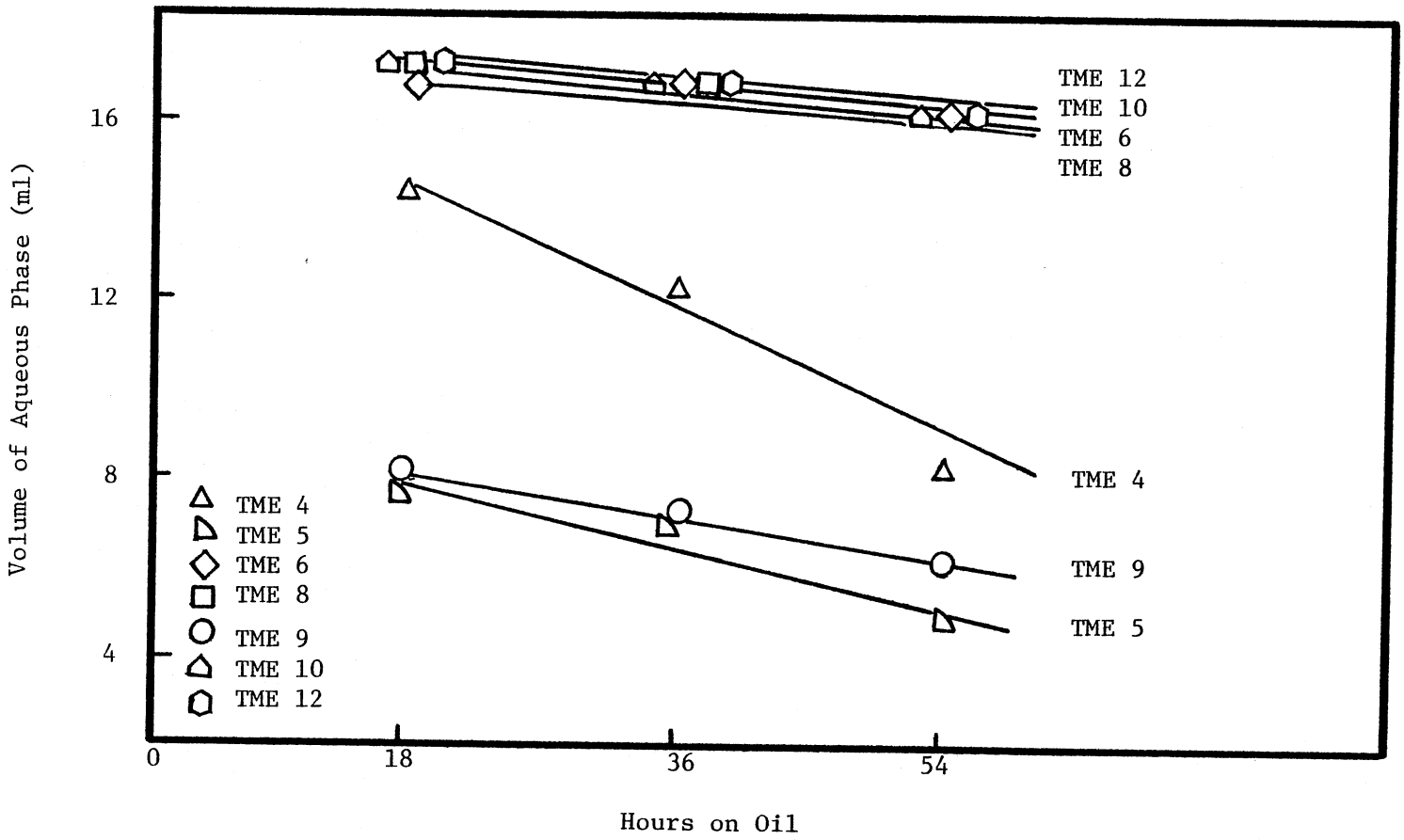

Figure 27. Volume of Aqueous Phase as a Function of Hours on Oil

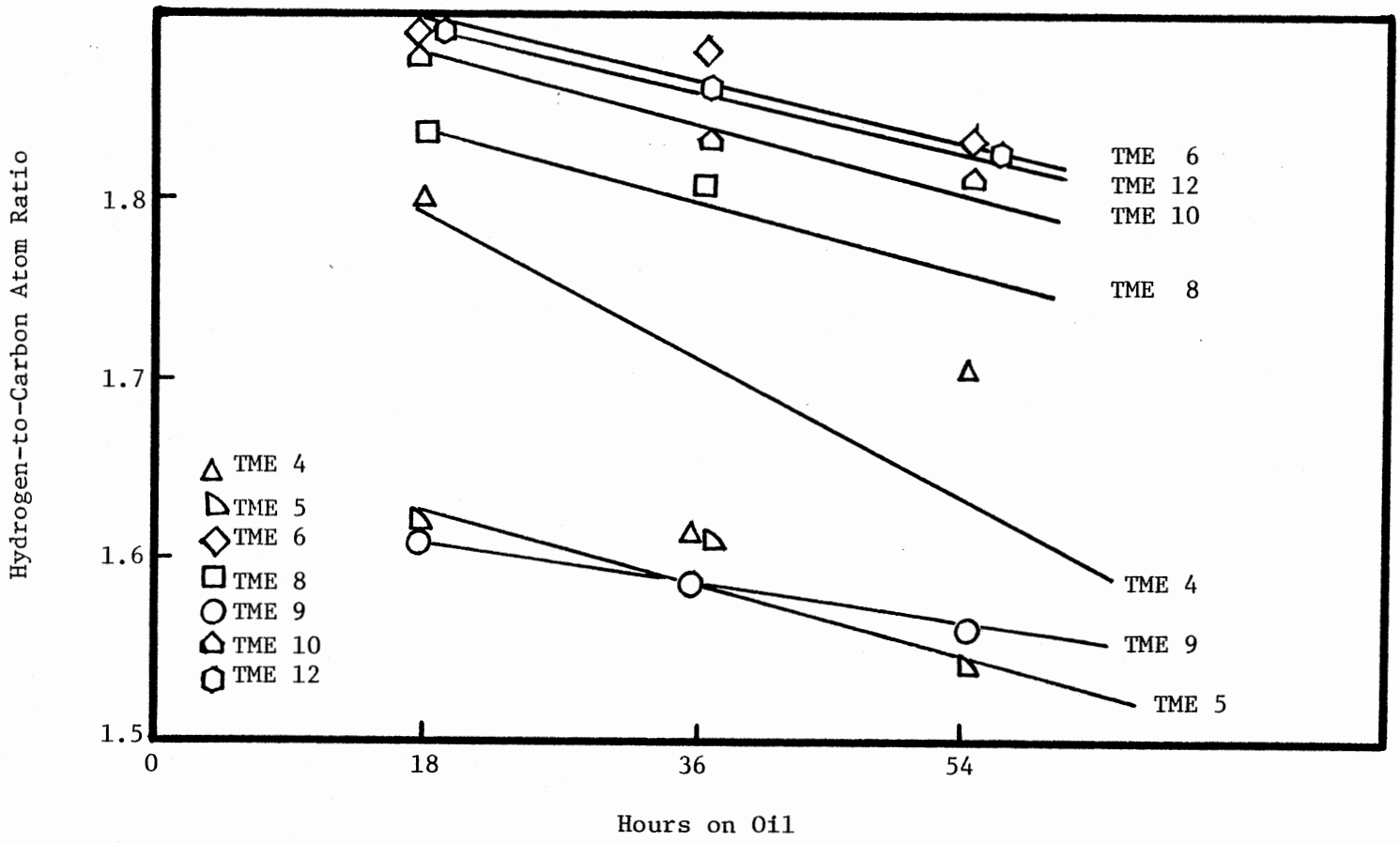

Figure 28. Hydrogenation Activity as a Function of Hours on Oil

Fate of Titanocene Dichloride During Hydrotreatment

After the hydrotreatment experiments, titanium was found to be present in the black granular carbonaceous materials accumulated in the preheating zones, on the spent catalysts, and in the products including the oil and aqueous phases.

The titanium left in the oil and present in the aqueous phase are negligible in comparison with the titanium concentrations added into the feedstocks. Hydrodemetallation of titanocene dichloride seems to be an easy process.

The granular black carbonaceous materials accumulated above the catalyst bed are analyzed to contain 3-4 wt% of titanium. The titanium content in these granular materials is independent of the titanium concentrations added into the feed oils. These titanium containing compounds caused the reactor cloggings in runs TME #2 and #3, and restriction of hydrogen flow in TME #4. Free radical polymerization catalyzed by titanium compounds was suggested to be responsible for the formation of the carbonaceous clogging materials. A portion of titanium added into the feed is used by the polymerization reaction. The fact that the titanium percentage in the carbonaceous deposit is independent of the titanocene concentration in the feed indicates that it must be formed by polymerization and it must have a fixed composition.

The spent catalysts were found to have titanium deposits. The hydrodemetallation reaction occurring inside the catalyst bed results in the removal of the titanium from the oils and the deposition of titanium on the catalysts. Qualitative analysis for chloride was done on the aqueous phases, the precipitate of silver chloride confirmed

the existence of chloride in the aqueous phases. The chloride from titanocene dichloride was probably converted into hydrogen chloride during hydrotreatment and dissolved in the aqueous phases.

Based on the material balance the fate of titanocene dichloride can be described as follows. About 60-70 wt% of the titanocene dichloride is consumed by the polymerization reactions in the preheating zone which accumulates in the carbonaceous deposits there. About 20 wt% of titanium dichloride is subjected to hydrodemetallation and deposits on the catalyst. Only 1-3 wt% of titanium is left in the oil and aqueous phases.

In the material balance of titanium, about 10-20 wt% of titanium is lost. The incomplete collection of granular carbonaceous materials from the reactor and the error in the determination of its weight may be responsible for these unaccounted titanium.

Temperature Effects on Hydrotreatment

In order to assess the temperature effects on hydrotreatment, two runs TME #9 and #12 were conducted under the same run conditions except that the temperature of run TME # 9 was 10 C lower than that of TME #12. The comparisons of the HDN, HDO, hydrogenation activity and the coke content and titanium deposition on spent catalyst were made between runs TME #9, #12 and the reference run, TME #5.

Figures 26 through 28, presented earlier in this chapter, also show these comparisons. The temperature was shown to have considerable effects on the HDN, HDO and hydrogenation reactions when comparing

TME #9 and #12. A higher degree of HDN, HDO and hydrogenation reaction was observed for the run with a higher temperature.

The effects of titanocene dichloride on hydrotreatment were confirmed again when the runs TME #9 and #5 are compared. The improved catalytic activities through the addition of titanocene dichloride offsets the temperature difference in these two runs, and gives comparable performance.

The temperature can also affect the titanium deposit and coke content on spent catalyst. Comparatively, a higher titanium deposition and lower coke content was observed for the experimental run with higher temperature. Comparisons between TME #9 and #12 confirmed this conclusion. A higher temperature can have higher catalytic hydrodemetallation, resulting in a higher titanium deposition on spent catalyst, which in turn lowers the coke content on spent catalyst. This observation once more confirms that titanocene dichloride acts as an inhibitor to the coke formation.

Properties of Spent Catalyst

The coke formation affects the surface area and pore volume of the spent catalyst. Ramser and Hill (76), and Hollaway and Nelson (73) observed significant changes in the surface area. Ahmed (16) also observed same results. However, Ozawa and Bischoff (75) reported no changes in the surface area due to coke formation. Chang (95) observed an increased surface area in the spent catalyst. In this study, the surface areas of spent catalysts were lower than the fresh catalyst.

As to the correlation between surface area and coke content, Hollaway and Nelson (73) observed that the surface areas decreased with an increase of carbon deposition. Ahmed (16) reported similar observation for coke contents on both NiMo/alumina and CoMo/alumina catalysts. But in his three runs with same operating conditions but different space time, the surface area in one run was reduced significantly when compared with the other runs. He speculated that possibly a different kind of surface existed for the nitrogen adsorption. Chang (95) attributed the increased surface area to the porous nature of the coke deposited on the catalyst.

In this study, the plot of surface area versus coke content is given in Figure 17 (page 97). No correlation is found between the surface area and the coke content. It seems that besides the coke content which affects the surface area, the coke structure also influences the surface area. This is based on the fact that the spent catalysts with comparable coke contents show significant differences in their surface areas.

The pretreatment methods used in the analyses of the spent catalysts have been different for various research works. Some of the solvent used for the removal of the oil is left on the catalyst. Moreover the drying temperature and vacuum may also play an important role in the determination of surface area. A strong solvent like pyridine not only removes the unreacted oil from the catalyst, but also it can dissolve some of the carbonaceous coke deposit. A systematic study of various methods for pretreatment is necessary in order to establish a standard method for coke determination.

In this study, the pore volumes of the spent catalysts have been less than the fresh catalyst. The decrease of pore volume is mainly due to coke formation which blocks the pores of the catalyst. Data obtained in this study shows that the pore volumes of the catalysts from reactor top sections, which have high coke contents, are less than the other two sections. A good correlation of coke content and pore volume is found in TME #5 and #12. But a similar correlation does not exist in the other runs, especially for the middle and bottom sections. Again, the structure of coke might have had some effects on the pore volume when the coke contents are comparable.

The coke formation has been related to the metal poisoning. Habibs et al. (81) observed a large increase in the coke due to the metals poisoning of the catalyst. In this study, the profile of titanium deposition and coke content in the reactor both show a decrease from the top section to the bottom section. It may be misleading to jump into the conclusion that metal deposition causes the heavier coke formation on the catalysts, if we ignore the coke contents data obtained from TME #5. The data show that the coke content of the top section in TME #5, which has no titanium deposition on the catalyst, is comparable with those of the top section catalysts with titanium depositions, and even a higher content in the middle section.

Ahmed (16) observed that NiMo/alumina catalyst has a superior HDN activity over CoMo/alumina, while the coke content on NiMo/alumina is found to be less than that on CoMo/alumina catalyst. Chang (108) reported that the dependence of hydrogenation and HDN activity on the reactor coke content is stronger than linear. In this study the

addition of titanocene dichloride improved the catalytic activities and reduced the coke contents on the middle and bottom sections. It appears that the coke formation has a profound relation with the catalyst activity. If the deposition of metals cause the deactivation of catalyst, then the coke content will be expected to increase. On the other hand, the coke content is expected to be reduced as the catalytic activity increases, due to the hydrogenation of free radicals and minimization of coke formation.

Froment and Bischoff (109), and Beeckman and Froment (110) developed a mathematical model to predict the conversion and coke formation profile in a fixed bed reactor by assuming several relationships between the activity and the bulk coke content in the catalyst pellets. Their results show that coke deposition decreases toward the reactor exit for the parallel fouling, but increases toward reactor exit for series fouling, Crynes (74) in his coke study using a mixture of 30% SRC and 70% solvent as feed observed that the profile of coke content in the reactor follows the parallel fouling model, but when Exxon Donor Solvent is used as the feed, a series fouling was observed. Hollaway and Nelson (73) observed that the coke accumulation profile built from the reactor bottom toward the top in a Synthoil process. DeRosset et al. (80) observed a higher carbon deposition at middle sections of the reactor.

In this study, the coke content was observed to decrease from top to bottom of the reactor. The mechanism of coke formation is quite complex and is not under the scope of this study. However, it can be

speculated that the concentration of coke precursors, the metal deposit, and the temperature profiles inside the reactor can possibly affect the coke formation profile.

The metal deposition inside the reactor have been reported to decrease from reactor top toward reactor exit. Tamm et al.(44) in their catalyst aging study in the hydroprocessing of petroleum residuum, found that the metal deposits from organometallics followed this pattern. DeRosset et al. (80) also found that titanium in Synthoil had a similar deposition pattern. In this study, the titanium deposition from titanocene dichloride followes the same profile as observed for organometallics in petroleum and for titanium in Synthoil.

The chemical nature of the deposited metals and their distribution profiles over a single catalyst pellet have been studied in the case of hydrotreatment of petroleum feedstocks. The hydrodemetallation of organometallic nickel and vanadium compounds results in the formation of metals which are later converted to metal sulfides in the presence of H_2S. Therefore, the metals deposited on the catalysts are always found in the form of sulfides (34, 44).

Tamm et al. (44), and Hardin et al. (11) studied the deposition of nickel and vanadium from their organometallic compounds in petroleum feedstocks. They observed that the maximum concentration of metals occur inside the edge of the catalyst pellets. Argawal and Wei (112) observed the same results when hydrotreating model organometallic vanadium and nickel compounds.

The nature of deposited metals and their distribution for coal liquefaction and upgrading of coal derived liquids have received less

attention than the petroleum feedstocks. Researchers at Pittsburgh Energy Technology Center (53) have found that titanium accumulated on the catalyst has a unique form of TiO_2 polymorph, anatase, while the predominate polymorph of TiO_2 found in coals is rutile, not anatase. They also found that the hydrogenation of model titanium containing organic compounds generate anatase.

Stanulonis (113) examined aged catalysts obtained from H-coal process by scanning electron microscopy and electron microprobe. Titanium was found to have a maximum concentration inside the edge of catalyst, and only a negligible amount on the outer crest of the catalyst. Sivasubramanian et al. (114) analyzed the aged NiMo/alumina catalyst, which was generated from the hydroprocessing of a mixture of raw anthracene oil and Synthoil oil. The results show that the exterior crust contains an intermediate amount of titanium, while the inner crust is seen to produce a very high titanium signal. The shallow crates and cracks in the catalyst interior were also decorated with titanium.

Two spent catalyst samples obtained from the top section of catalyst bed were analyzed for the chemical natures of the deposited titanium using X-ray diffraction techniques. The analysis did not show any anatase. The low titanium concentration on the spent catalysts and the carbonaceous coke deposits both added to the difficulties of the analyses. It may be concluded that the titanium compounds have amorphour structure. However, it may have been due to the inability of X-ray diffraction to analyze very thin layers of microcrystalline particles.

The regenerated catalyst pellets obtained in this project were analyzed using Auger Microprobe analysis service provided by SCR Laboratories, Inc. Because most of the samples contain less than 1.0% titanium, the inherent limitations of the technique made it difficult to measure the titanium. Consequently, only one of the samples showed a distribution pattern for titanium. The data show that the maximum titanium deposition is at the edge of catalyst. The penetration of titanium into the pores of catalyst appears to be less significant.

Reproducibility and Precision of Data

Two runs, TME #6 and #10 were conducted under the same operating conditions and approximately the same titanium concentration to test the reproducibility of experimental results. Figure 29 through 33 compare the distillation data, hydrogenation, HDN, HDS and HDO activities as shown by the volume of aqueous phase formed from hydrodeoxygenation. In general, acceptable agreements are observed in these two runs, except that the data for HDS are somewhat scattered. This might be due to the instrumental limitations in determining the low levels of sulfur.

In the characterization of spent catalyst, the coke content, pore volume, surface area and titanium deposition were measured. Due to the limited quantity of catalysts available from each section of the reactor, most of the spent catalyst samples were subjected to one measurement only. However, the weight of sample used in these measurements was in the range of 0.5 to 1.5 grams which reduces the possibility of bad sampling.

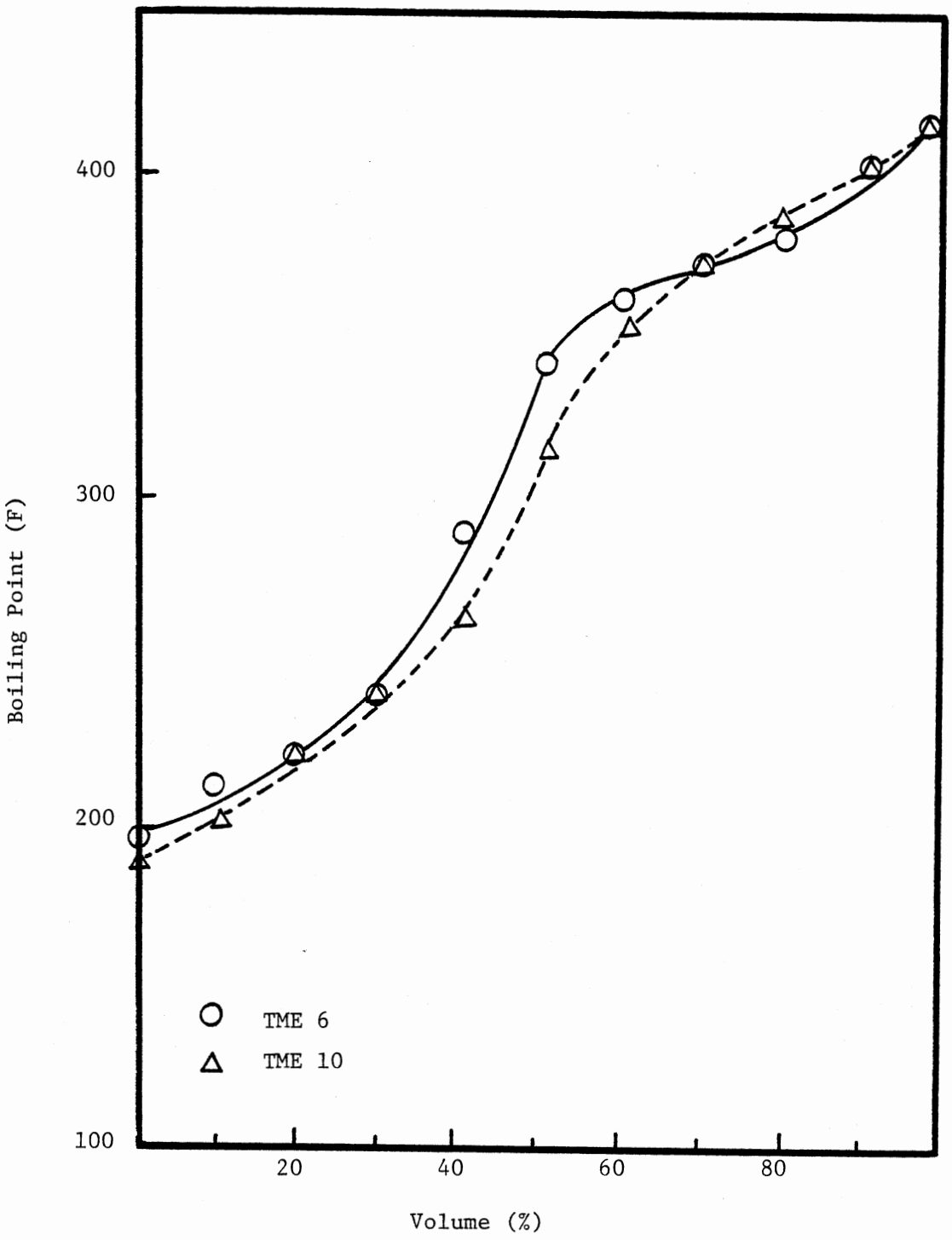

Figure 29. Reproducibility of Distillation Data of Runs TME 6 & 10

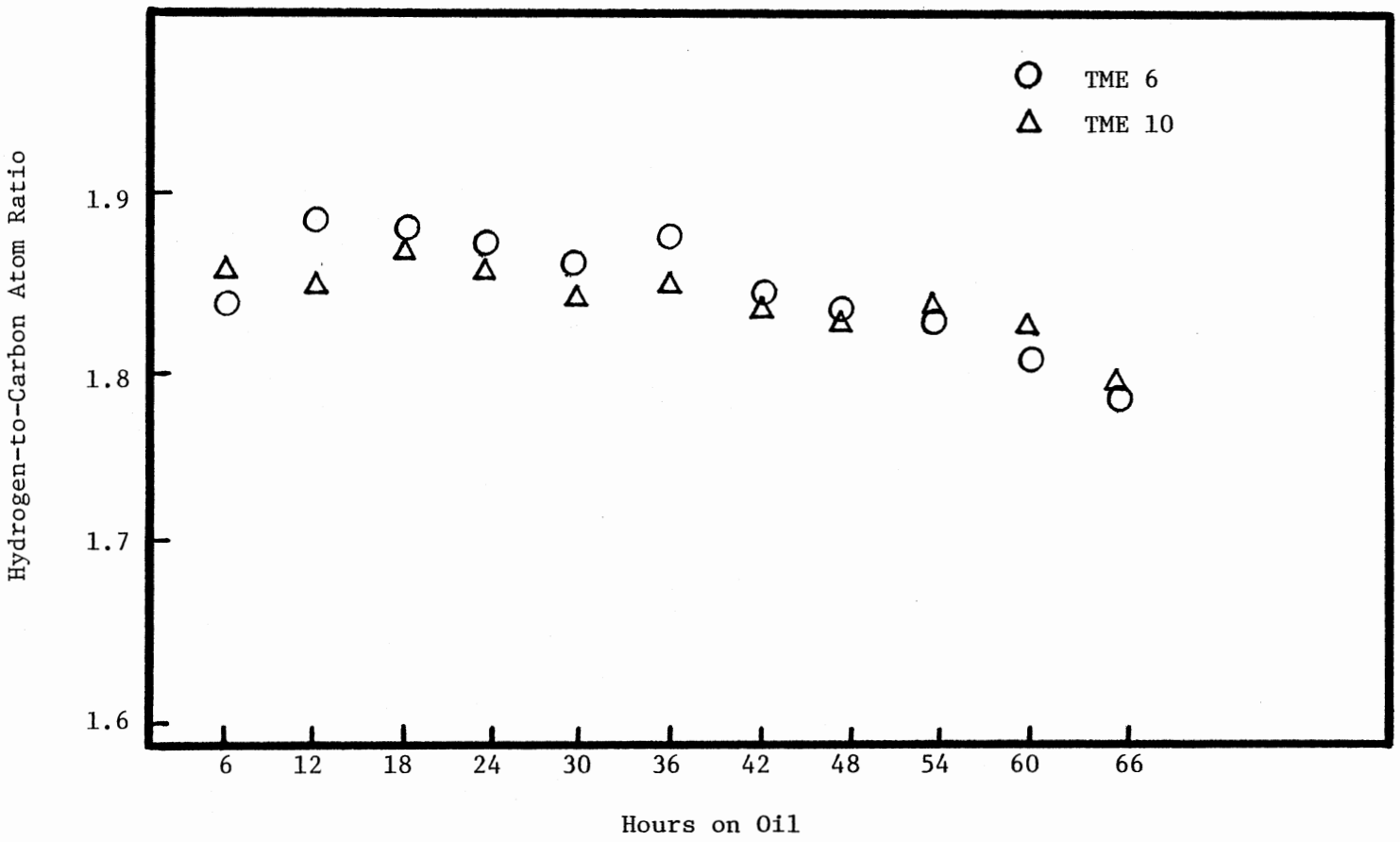

Figure 30. Reproducibility of Hydrogenation Activity of Runs TME 6 & 10

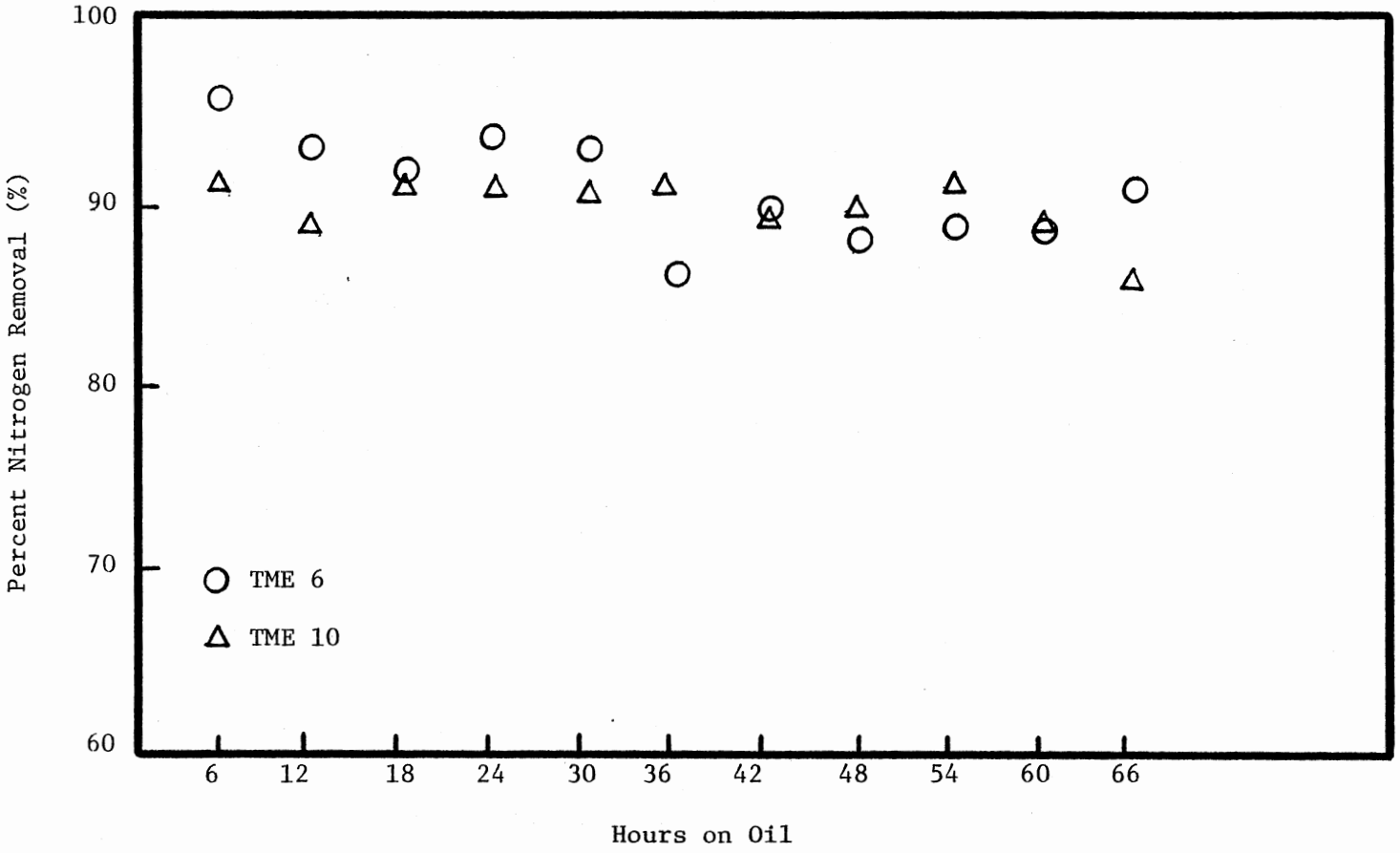

Figure 31. Reproducibility of Nitrogen Removal of Runs TME 6 & 10

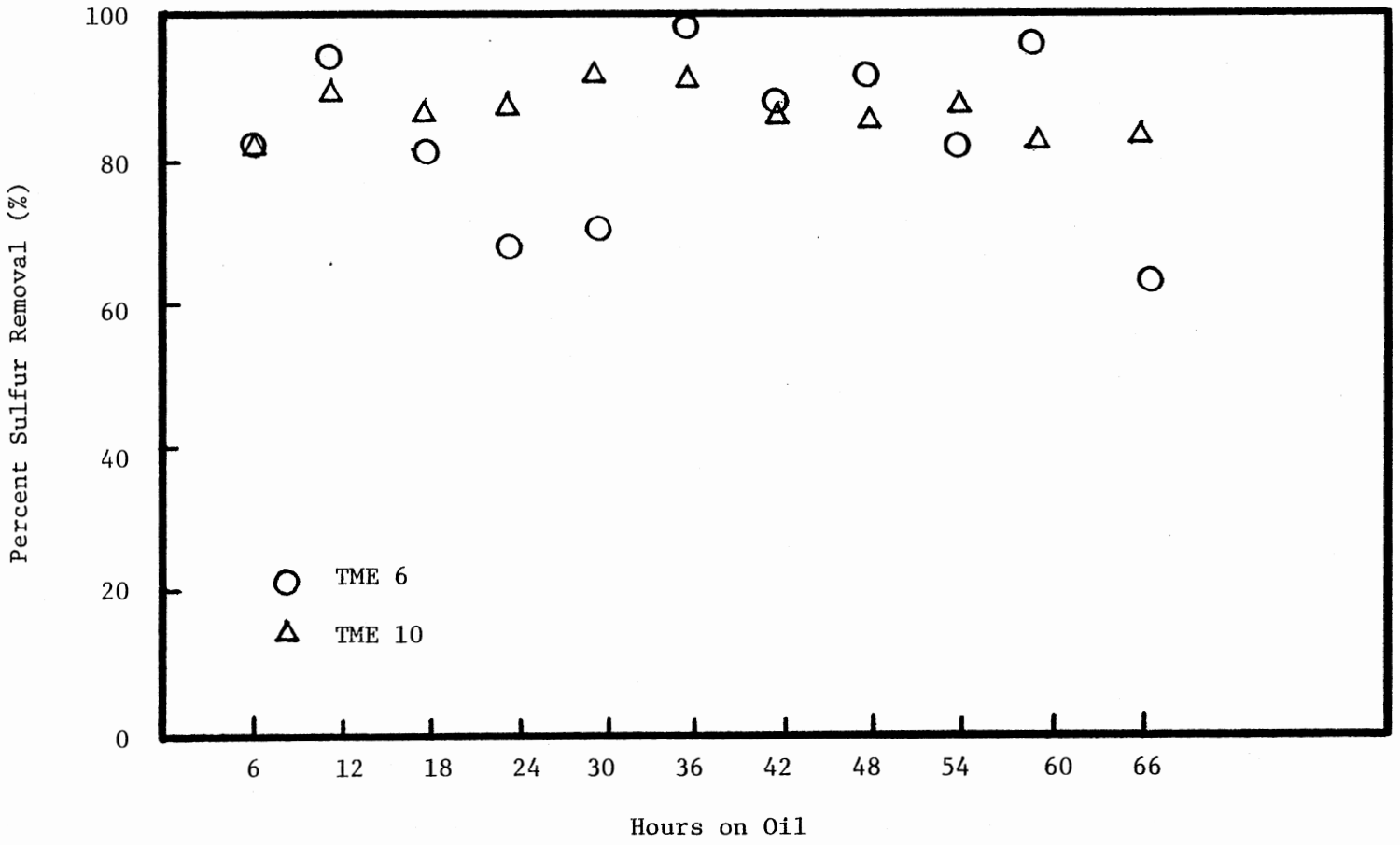

Figure 32. Reproducibility of Sulfur Removal of Runs TME 6 & 10

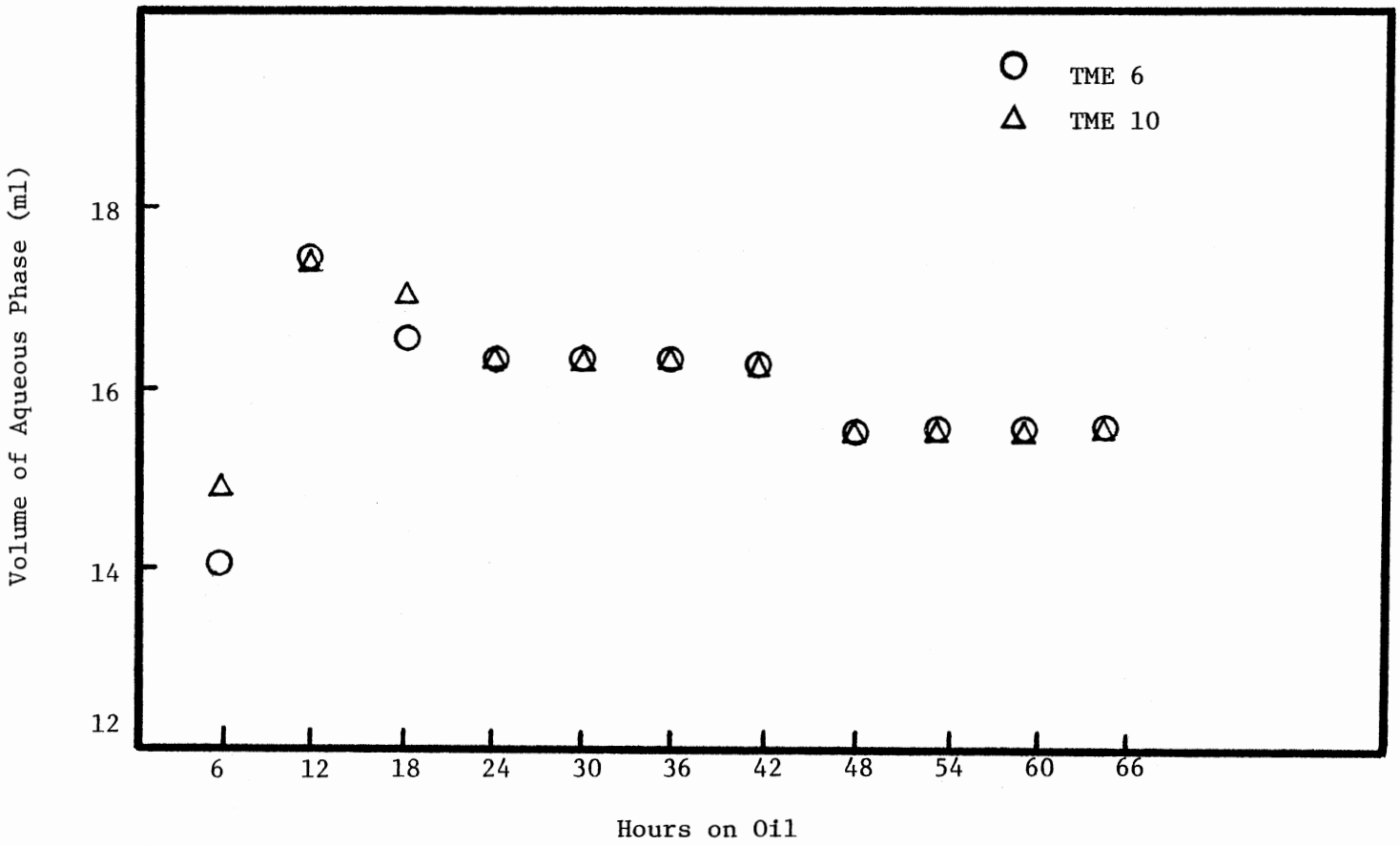

Figure 33. Reproducibility of Oxygen Removal of Runs TME 6 & 10

The methods used in the characterization of the feed oil and the hydrotreated products include distillation, elemental analysis of nitrogen, sulfur, carbon, hydrogen and titanium. The distillations were conducted at atmospheric pressure. Some selected samples were distillated twice. The results show excellent agreement.

The sulfur analyzer employed in this study has been used by previous investigators. Sooter (19) and Ahmed (16) studied the analytical precision of the sulfur analysis in FMC feed and product oils. A higher deviation was reported for the samples with lower sulfur content. The SRC light oil used as feedstock in this study was analyzed for 36 times, the average sulfur concentrations was 0.36 wt% with a standard deviation of 2.03 %. The hydrotreated products were analyzed three times for each sample. Since the sulfur contents were mostly in the range of 0-0.1 wt% the data show some scattering for the same run.

The precision of the Perkin-Elmer Model 240 Elemental Analyzer has been double checked with standards and with the feed before analyzing the hydrotreated samples. The elemental analysis of the feedstock was conducted for 36 times, the nitrogen content had an average value of 0.41 wt% with a standard deviation of 0.08 %. The hydrotreated oil samples have been analyzed at least three times for each sample.

Direct measurement of organometallics in petroleum and lubricating oils are becoming more common. The direct method is fast and free from the preparation errors of wet ashing. In this study the oil was diluted in methyl isobutyl ketone and analyzed by the atomic absorption

spectrometer to determine the titanium concentration. The titanium concentrations in the feeds calculated from the quantities of titanium added into the feedstock are in good agreement with the concentrations determined by atomic absorption spectrometer shown in Table XV.

CHAPTER VI

CONCLUSIONS AND RECOMMENDATIONS

The following conclusions can be drawn based on the results of this study:

1. Titanocene dichloride added to the SRC light oil feed enhances the clogging in the preheating zone where no catalyst is present. This is probably due to some polymerization reactions initiated by titanocene dichloride.

2. The carbonaceous deposit in the preheating zone contains both nitrogen and titanium in addition to carbon and hydrogen.

3. Addition of titanocene dichloride promotes the HDS and HDO of the oil on the glass beads but has no effects on the hydrogenation or HDN of the oil.

4. Titanocene dichloride is easily hydrodemetalized by hydrotreatment in the presence of NiMo/alumina catalyst, and deposits on the catalyst.

5. Coke formation on the catalyst is suppressed by the addition of titanocene dichloride. This is especially true for the middle and bottom sections of the catalyst bed. However, the coke content of the top sections are independent from the concentrations of titanocene dichloride in the feedstock.

6. The addition of titanocene dichloride in the SRC light oil feed improves the HDS, HDN, HDO and hydrogenation activity of the catalyst.

7. The catalyst activity improvement depends on the concentration of titanocene dichloride. Titanium concentration of 100 ppm to 200 ppm appear to promote the catalyst best, but further increase of concentration shows lower activity.

8. In distillation data a shift of boiling point of hydrotreated oils to lower point ranges with respect to the feedstock was observed.

Recommendations

1. To assess the effects of titanium deposits on the catalyst, catalysts impregnated with inorganic and other organometallic titanium compounds should be subjected to hydrotreatment tests in batch and/or trickle bed reactors. The effects on the HDS, HDN, HDO, hydrogenation and coke formation should be studied systematically. The determination of the optimal impregnation will be of industrial value.

2. Similarly, the effects of halogen should be studied too.

3. In the recommended studies both the complex feed oils and single model compounds should be used. The latter feed will give the evidence of the effects on every single hydrotreating reaction; while the former can provide the information valuable for the upgrading technology and catalyst development.

BIBLIOGRAPHY

1. Filby, R. H., et al., Department of Energy Report FE/496-T17 (1976).

2. Ahmed, M. M., "An Investigation of the Activity of Two Cobalt-Molybdenum-Alumina Catalysts for Hydrodesulfurization of FMC Oil, a Coal-Derived Liquid," M.S. Thesis, Oklahoma State University, Stillwater, Oklahoma (1973).

3. Seapan, M. and B. L. Crynes, "Kinetics of Hydrogenation of Alternative Crude Oils," First Annual Report submitted to DOE Bartlesville Energy Technology Center (1981).

4. Schwartz, J. G. and G. W. Roberts, "Analysis of Trickle Bed Reactors: Liquid Backmixing and Liquid-Solid Contacting," 74th National Meeting of A.I.Ch.E., New Orleans (1973).

5. Docksey, P. and R. J. H. Gilbert, Seventh World Petroleum Congress, Mexico City (1967).

6. Schwartz, C. E. and J. M. Smith, Ind. Eng. Chem., 45 (6), 1209 (1953).

7. Schlesser, W. E. and L. Lapidus, AIChE. J., 7, 163 (1961).

8. Satterfield, C. N., AIChE. J., 21 (2), 209 (1975).

9. Ross, L. D., Chem. Engr. Progr., 61 (10), 77 (1965).

10. Henry, H. C. and J. B. Gilbert, Ind. Eng. Chem., Process Des. Develop., 12, 328 (1973).

11. Satterfield, C. N. and P. E. Way, AIChE. J., 18 (2) (1972).

12. Mears,D. E., Am. Chem. Soc., Adv. in Chem. Ser., 133, 218 (1974).

13. Satterfield, C. N. and F. A. Ozel, AIChE. J., 19 (6) 1259 (1973).

14. Mears, D. E., Chem. Eng. Sci., 26, 1361 (1971).

15. Shah, Y. T. and J. A. Paraskos, CES., 30, 1169 (1975).

16. Ahmed, M. M., "Coal Derived Liquids Hydrotreatment Catalyst Deactivation Study," Ph.D. Thesis, Oklahoma State University, Stillwater, Oklahoma (1979).

17. Satterfield, C. N., et al., AIChE. J., 15, 226 (1969).

18. Satchell, D. P., "Hydrodenitrogenation of a Coal Derived Liquid," Ph.D. Thesis, Oklahoma State University, Stillwater, Oklahoma (1974).

19. Sooter, M. C., "Effect of Catalyst Pore Size on Hydrodesulfurization of Coal Derived Liquids," Ph.D. Thesis, Oklahoma State University, Stillwater, Oklahoma (1974).

20. Van Deemter, J. J., Third Eur. Symp. Chem. Reaction Eng., 215 (1974).

21. Addlington, D. and E. Thompson, Third Eur. Symp. Chem. Reaction Eng., 203 (1964).

22. Van Zoonen, D. and C. T. Douwes, J. Inst. Petrol., 49, 383 (1963).

23. Jones, J. J. and J. F. Jones, Preprint, Div. of Fuel Chem., ACS, 1, 26 (1972).

24. Jones, J. F. and L. D. Friedman, "Char Oil Energy Development Final Report," Office of Coal Research Report No. 56, 25 (1970).

25. Mckinley, J. B., Catalysis, Emmett ed. Volume V, 405 (1957).

26. Schuman, S. C. and H. Shalit, Catal. Rev., 4, 245 (1970).

27. Wan, K. T., "Establishment of Equipment and its Operations for Hydrotreating of a Coal-Derived Liquid," M.S. Thesis, Oklahoma State University, Stillwater, Oklahoma (1973).

28. Qader, S. H., et al., Ind. Eng. Chem., Process Design Develop., 7, 390 (1968).

29. Crynes, B. L., Chapter in Chemistry of Coal Utilization (1979).

30. Stein, T. R., et al., "Upgrading of Coal Liquids for Use as Power Generation Fuel," EPRI Report AF-444 (1977).

31. Satterfield, C. N., et al., AIChE. J., 1100 (1975).

32. Satterfield, C. N. and Shan Hsi, "Abstracts and Research Accomplishments of AR & TD Coal Liquefaction Projects and Advanced Coal Research Projects," Pittsburgh Energy Technology Center (1980).

33. Weekman, V. W., Ind. Eng. Chem., Process Res. Develop., Vol. 7, 90 (1968).

34. Katzer, J. R. and R. Sivasubramanian, Catal. Rev., Sci. Eng., 20 (2) 155-208 (1979).

35. Gates, B. C. and J. R. Katzer, "Abstracts and Research Accomplishments of AR & TD Coal Liquefaction Project and Advanced Coal Research Projects," Pittsburgh Energy Technology Center (1980).

36. Flinn, R. A., et al., Hydrocarbon Processing, 42 (9), 129 (1963).

37. Sarbak Z., et al., Unpublished Results, quoted from Catal Rev., Sci. Eng., 20 (2) 155-208 (1979).

38. Moschopedis, S. E. and Speight, J. G., Fuel, 55, 187 (1976).

39. Furimsky, E., Fuel, 57, 494 (1978).

40. Howard, J. A., Adv. Free Rad. Chem., 4, 49 (1972).

41. Rollmann, L. D. J., Catalysis, 46, 243 (1977).

42. Massoth, F. E., Adv. in Catalysis, Vol. 27 (1978).

43. Riley, K. L., et al., US Patent 3,720, 602 (1973).

44. Tamm, P. W., et al., Ind. Eng. Chem., Process Des. Develop., 20, 262-273 (1981).

45. Beuther, H. and B. K. Schmid., Paper presented in Sixth World Petrol. Cong., Sec. III. (1963).

46. Oleck, S. M. and H. S. Sherry, Ind. Eng. Chem., Process Des. Develop., 16 (4), 525 (1977).

47. Larson, O. A. and H. Beuther, Preprint, Div. of Petrol. Chem., ACS, 11 (2), 1395 (1966).

48. Chang, C. D. and A. J. Silvestri, Ind. Eng. Chem., Process Des. Develop., 15 (1), 161 (1976).

49. Riley, K. L., Preprint, Div. of Petrol. Chem., ACS, 23 (1), 81 (1978).

50. Cecil, R. P., et al., Paper presented at Am. Inst. Chem. Engr. Meeting, Los Angeles (1968).

51. Van Dongen, R. H., Chemical Engineering of Gas-Liquid-Solid Catalyst Reactions, CHBEDOC, Liege, Belgium (1979).

52. Levy, A. L. and E. E. Peterson, Department of Energy Report LBL-12933 (1981).

53. Pittsburgh Energy Technology Center, Informal Information.

54. Mitchell, T. O., Coal Process Technology, Vol. 1, American Institute of Chemical Engineers (1980).

55. Beuther, H., et al., Ind. Eng. Chem., Prod. Res. Dev., 9, 272 (1970).

56. Sultanov, A. S., et al., Kint. Catal. (USSR) 13, 1207 (1972).

57. Mone, R., Preparation of Catalysts, Elsevier, Amsterdam (1976).

58. Chevron Research Compnay, Dutch Patent 123, 195 (1973).

59. Kiviat, F. E. and L. Petrakis., J. Phys. Chem., 77, 1232 (1973).

60. Mone, R. and L. Moscou., Preprint, Div. of Petrol. Chem., ACS, 20 (2), 564 (1975).

61. Tantarov, M. A., et al., Ind. Chem. Eng., 12 (1), 85 (1972).

62. Brewer, M. B. and T. H. Cheavens., Hydrocarbon Processing, 45, 203 (1966).

63. Schuit, G. C. A., et al., J. Catal., 15, 179 (1969).

64. Wakabayashi, K., Seiyu Gakkai Shi, 16, 651 (1973).

65. Massoth, F. E. and C. L. Kibby., J. Catal., 47, 300 (1977).

66. Madison, J. J. and R. M. Roberts, Ind. Eng. Chem., 50, 237 (1958).

67. Appleby, W. G., et al., Ind. Eng. Chem., Process Des. Dev., 1, 102 (1962).

68. Voorhies, A., Jr., Ind. Eng. Chem., 37,318 (1945).

69. Rudershausen, C. G. and C. C. Watson, CES, 3, 110 (1954).

70. Lipovich, V. G., et al., Ind. Chem. Eng., 18 (1), 98 (1978).

71. Nitta, H., et al., 86th National AIChE Meeting, Houston, Texas (1979).

72. Ternan, M., et al., Fuel Processing Technology, 2, 45-55 (1979).

73. Hollaway, P. H. and G. C. Nelson, Preprint, Div. of Petrol. Chem., ACS, 22 (4), 1352 (1977).

74. Crynes, B. L., Department of Energy Report DOE/ET/14700-6 (1980).

75. Ozawa, Y. and K. B. Bischoff, Ind. Eng. Chem., Process Des. Dev., 7, 72 (1968).

76. Ramser, J. N. and P. B. Hill, Ind. Eng. Chem., 50, 117 (1958).

77. Prasher, B. D., et al., Ind. Eng. Chem., Process Des. Dev., 17, 266 (1978).

78. Kovach, S. M., et al., Ind. Eng. Chem., Prod. Res. Develop., 17, 62 (1978).

79. Chiou, M. T. and J. H. Olson, Catal. Rev., Sci. Eng., 2012, 155-208 (1979).

80. DeRosset, A. J., et al., Department of Energy Report FE-2010-09 (1977).

81. Habil, E. T., et al., Ind. Eng. Chem., Prod. Res. Dev., 4, 16 (1977).

82. Beuther, H., et al., US Patent 3,840,473 (1963).

83. Massoth, F. E., et al., Department of Energy Report DOE/ET/14700-5 (1980).

84. Gluskoter, H. J., Trace Elements in Fuel, ACS, Washington, D.C. (1975).

85. Finkeman, R. B., Ph.D. Dissertation, University of Maryland (1980).

86. Eskenazy, Gr., Fuel, 51, 221 (1972).

87. Miller, R. N. and P. H. Given, Department of Energy Report FE02494-TR-1 (1978).

88. Yen, T. F., The Role of Trace Metal in Petroleum, Ann Arbor Science Publishers Inc., Michigan (1975).

89. Mcginnis, E. L., Preprint, Div. of Petrol. Chem., ACS, 23 (3), 1340 (1978).

90. Weiss, C. S., Department of Energy Report DOE/ET/10104-T6 (1980).

91. Godnev, I. N. and A. V. Pamfilov, J. Gen. Chem., USSR, 7,1264 (1937), Chem. Abstr., 31, 6088 (1937).

92. Cotton, F. A. and G. Wilkinson, Advanced Inorganic Chemistry, 3rd ed., Interscience Publishers, N.Y. (1972).

93. Soni, D. S., "A Comparison of the Desulfurization and Denitrogenation Activities of Monolith Alumina Inpregnated with Cobalt and Molybdenum and Nalcomo C74 Catalyst," M.S. Thesis, Oklahoma State University, Stillwater, Oklahoma (1977).

94. Wilkinson, S., unpublished work.

95. Chang, H. J., unpublished work.

96. Chang. H. J., Department of Energy Report DE-14876-5 (1980).

97. Runnion, K. N., Energy Research and Development Administration Report FE-2034-3 (1976).

98. Sosnowski, J., et al., CEP, Feb. (1981).

99. Kobe, K. A. and J. J. McKetta, Advan. Petrol. Chem. Refining, 3, Chap. 5 (1960).

100. Chandrasekaran, E. S., et al., J. Organometallic Chemistry, 120, 49-63 (1976).

101. Bond, W. D., et al., J. Am. Chem. Soc., 97, 2128 (1975).

102. Eisch, J. J., Department of Energy Report DE-AC01-79 ET14879 (1981).

103. Wilson, G. R., U.S. Patent 4,018,714 (1975).

104. Webb, A. N., Ind. Eng. Chem., 49, 261 (1957).

105. Peri, J. B., J. Phys. Chem., 70, 1482 (1966).

106. Wadkour, M., et al., J. Indian Chem. Soc., 46,720 (1969).

107. McCandless, F. P. and L. Berg, Ind. Eng. Chem., Process Des. Dev., 9, 110 (1970).

108. Chang, H. J., Department of Energy Report DE-14876-8 (1981).

109. Froment, G. F. and K. B. Bischoff, Chem. Eng. Sci., 16, 189 (1961).

110. Beeckman, J. W. and G. F. Froment, Ind. Eng. Chem., Fund, 18, No. 3, 245 (1979).

111. Hardin, A. H., et al., Preprint, Div. of Petrol. Chem., ACS, 23 (4), 1450 (1978).

112. Agrawal, R. and J. Wei, Paper presented at 73rd AIChE Annual Meeting, Chicago, Illinois (1980).

113. Stanulonis, J. J., et al., J. AIChE., 22, 576 (1976).

114. Sivasubramanian, R., et al., Preprint, Div. of Fuel Chem., ACS, 25 (1), 84-148 (1980).

VITA

Wu Shan Chan

Candidate for the Degree of

Master of Science

Thesis: EFFECTS OF TITANOCENE DICHLORIDE ON THE HYDROTREATMENT OF COAL LIQUIDS

Major Field: Chemical Engineering

Biographical:

Personal Data: Born in Chang-Hwa, Taiwan, April 14, 1953, the son of Chi Kwang Chen and Yih Shaun Liang.

Education: Graduated from Chang-Hwa High School, Chang Hwa, Taiwan, in June, 1971; received Bachelor of Science in Engineering degree from National Taiwan University in 1975; completed requirements for the Master of Science degree at Oklahoma State University in July, 1982.

Professional Experience: Staff officer, Material Service of Combined Service Force, 1975-1977; Chemical Engineer, Chemical Division of Mitsubishi Corporation, Taipei Branch, 1977-1980.